BIOENGINEERED COLLAGEN GRAFT FOR URETHRAL RECONSTRUCTION IN ANIMAL MODELS

GANESH VYTHILINGAM

FACULTY OF MEDICINE
UNIVERSITY OF MALAYA
KUALA LUMPUR

2018

BIOENGINEERED COLLAGEN GRAFT FOR URETHRAL RECONSTRUCTION IN ANIMAL MODELS

GANESH VYTHILINGAM

THESIS SUBMITTED IN FULFILMENT OF THE REQUIREMENTS FOR THE DEGREE OF DOCTOR OF PHILOSOPHY

FACULTY OF MEDICINE
UNIVERSITY OF MALAYA
KUALA LUMPUR

2018

UNIVERSITY OF MALAYA

ORIGINAL LITERARY WORK DECLARATION

Name of Candidate: Ganesh Vythilingam

Matric No: MHA 140007

Name of Degree: Doctor of Philosophy

Title of Thesis: Bioengineered collagen graft for urethral reconstruction in animal models

Field of Study: Surgery

I do solemnly and sincerely declare that:

(1) I am the sole author/writer of this Work;
(2) This Work is original;
(3) Any use of any work in which copyright exists was done by way of fair dealing and for permitted purposes and any excerpt or extract from, or reference to or reproduction of any copyright work has been disclosed expressly and sufficiently and the title of the Work and its authorship have been acknowledged in this Work;
(4) I do not have any actual knowledge nor do I ought reasonably to know that the making of this work constitutes an infringement of any copyright work;
(5) I hereby assign all and every rights in the copyright to this Work to the University of Malaya ("UM"), who henceforth shall be owner of the copyright in this Work and that any reproduction or use in any form or by any means whatsoever is prohibited without the written consent of UM having been first had and obtained;
(6) I am fully aware that if in the course of making this Work I have infringed any copyright whether intentionally or otherwise, I may be subject to legal action or any other action as may be determined by UM.

Candidate's Signature Date:

Subscribed and solemnly declared before,

Witness's Signature Date:

Name:

Designation:

BIOENGINEERED COLLAGEN GRAFT FOR URETHRAL RECONSTRUCTION IN ANIMAL MODELS

ABSTRACT

With the increase incidence of hypospadias and urethral stricture, the need for a surgically efficient and cost effective graft to reconstruct the urethra has become paramount, especially in view of the complications arising from presently used technologies. Current available surgical techniques require harvesting of grafts from autologous sites resulting in complications. In addition, lack of tissue availability and added patient discomfort further limits present surgical options. Cell based approaches have shown progress in this area. However, these have been associated with high costs and regulatory hurdles. An acellular graft using relatively inexpensive materials that has been previously approved by regulatory bodies and possesses good regenerative potential is thus more likely to be used in clinical practice. In this thesis we examined and reengineered four tubular collagen grafts of different densities over a period of 3 years using initially rat tail collagen and subsequently bovine collagen, which has been previously approved by FDA. This effort has resulted in the development of a relatively easy to fabricate acellular bovine collagen graft with the desired mechanical property that allows better surgical and regenerative performance of damaged urethra. Grafts were analytical and empirical mechanical tested prior to the *in-vivo* study. 2 cm of the urethra was resected in each of the 65 (N=65) male New Zealand rabbits and replaced with the grafts. Rabbits were evaluated at 1, 3, 6, 9 and 11 months using visual examination and contrast voiding cysto-urethrography. Biopsies of repaired sites from euthanized rabbits were then subjected to histological examination and immunohistochemistry. The outcome of the four different types of engineered acellular collagen grafts were compared. This multi-centric study revealed from the contrast voiding cysto-urethrography that the initial produced acellular collagen tube had a 40% failure rate as compared to the final version, with a 10% failure

rate. The variation in density between the engineered four grafts appeared to influence the functional outcome. It was noted on histology that urothelial cells favored higher density grafts compared to smooth muscle cells. Smooth muscle cells preferred grafts with less density. The adequate smooth muscle cells remodeling of the engineered graft influenced by density modification of its matrix is a finding that has not been described yet. Improved smooth muscle regeneration is an advantage, as the primary pathology in urethral stricture is due to muscular fibrosis. Furthermore, spontaneous urothelial coverage of the grafts and smooth muscle cell migration in the implanted graft could be demonstrated by standard histology and immunohistochemistry. The final graft subjected to X-Ray sterilization according to ISO-11137 standards, (N=4 rabbits), showed similar graft function as compared to non-sterilized grafts. Preliminary results of a pilot dog study with 3 animals implanted with a 4cm tubular graft also demonstrated the functional potential of the engineered grafts in a clinically relevant length of urethral defect. The final acellular graft developed may have the potential to be an off the shelf product; is easy for the surgeon to work with, regenerative efficient and safe for urethroplasty.

Keywords: Urethra, tissue engineering, collagen, cell free, graft

BIOENGINEERED COLLAGEN GRAFT FOR URETHRAL RECONSTRUCTION IN ANIMAL MODELS

ABSTRAK

Dengan peningkatan kes hipospadia dan pengetatan uretra, keperluan untuk pembedahan yang berkesan dengan kos graf berefektif untuk membina semula uretra menjadi amatlah penting, terutamanya memandangkan komplikasi yang tertimbul daripada teknologi yang digunakan sekarang. Teknik pembedahan sedia ada semasa memerlukan penuaian graf dari tapak autolog yang menyebabkan komplikasi. Di samping itu, kekurangan ketersediaan tisu dan pernambahan ketidakselesaan pesakit selanjutnya membataskan pilihan pembedahan yang ada sekarang. Kaedah berasaskan sel telah menunjukkan kemajuan dalam bidang ini. Walau bagaimanapun, ini telah dikaitkan dengan kos tinggi dan halangan dari pengawalseliaan. Satu graf tanpa sel menggunakan biomaterial yang agak murah dan telah diluluskan sebelum ini oleh badan pengawalseliaan dan juga mempunyai potensi penjanaan yang baik adalah lebih cenderung untuk digunakan dalam amalan klinikal.Di dalam tesis ini, kami telah mengkaji dan menjana semula empat tiup graf kolagen dengan ketumpatan yang berlainan dalam tempoh 3 tahun dengan menggunakan kolagen lembu, yang telah diluluskan sebelum ini oleh FDA. Usaha ini telah menghasilkan pembangunan yang agak mudah untuk menghasilkan graf kolagen lembu tanpa sel dengan mekanikal yang diingini bagi membolehkan prestasi pembedahan dan regeneratif yang lebih baik terhadap uretra yang rosak. Graf adalah diuji secara analitikal, empirical dan mekanikal sebelum kajian *in-vivo*. 2 cm daripada uretra telah dikeluarkan dari setiap 65 ekor (N = 65) arnab jantan New Zealand dan digantikan dengan graf tiub. Arnab diperiksa pada 1, 3, 6, 9 dan 11 bulan menggunakan pemeriksaan visual dan "kontras voiding cysto-urethrography". Biopsi tapak yang diambil daripada arnab yang telah dieuthaniskan kemudiannya tertakluk kepada pemeriksaan histologi dan pewarnaan-imuno. Hasil daripada 4 jenis graf kolagen tanpa sel berlainan yang

dijuruterakan telah dibandingkan.Kajian multi-centric ini menunjukkan daripada "kontras voiding cysto-urethrography" bahawa tiub kolagen tanpa sel yang awalnya dihasilkan mempunyai kadar kegagalan 40% berbanding dengan versi terakhir, dengan kadar kegagalan 10%. Variasi ketumpatan antara empat graf yang dijuruterakan kelihatan dapatnya mempengaruhi kefungsiannya. Ia diperhatikan pada histologi bahawa sel-sel urothelial cenderung terhadap ketumpatan graf yang lebih tinggi berbanding dengan sel otot licin. Sel-sel otot licin pula lebih cenderung terhadap graf yang kurang tumpat. Pembentukan semula sel-sel otot licin yang mencukupi daripada graf dijuruterakan dipengaruhi oleh pengubahsuaian ketumpatan matriksnya adalah satu penemuan yang belum diterangkan lagi. Penambahbaikan penjanaan semula otot licin adalah satu kelebihan, sebab patologi utama dalam penyekatan uretra adalah disebabkan oleh fibrosis otot. Tambahan pula, liputan urothelial spontan untuk graf dan penghijrahan sel otot licin ke dalam graf yang diimplan boleh ditunjukkan dengan histologi dan imunohistokimia piawai. Graf terakhir ditaklukkan kepada pensterilan x-ray mengikuti piawaian ISO-11137, (N = 4 arnab), menunjukkan fungsi graf yang serupa berbanding dengan graf yang tidak disterilkan. Keputusan awal dalam sebuah kajian perintis atas anjing dengan 3 ekor haiwan yang diimplankan dengan graf tiub 4cm juga menunjukkan potensi kefungsian graf yang dijuruterakan dalam jangka masa berkait secara klinikal dengan kecacatan uretra. Graf tanpa sel terakhir yang dihasilkan mungkin mempunyai potensi untuk menjadi produk rak; adalah mudah untuk pakar bedah untuk mengguna, berkesan secara regeneratif, dan selamat untuk pembedahan urethroplasty.

Kata kunci: Uretra, kejuruteraan tisu, kolagen, tanpa sel, graf

ACKNOWLEDGEMENTS

First I would like to thank my thesis supervisors Prof C.R Thambidorai and Prof Tunku Kamarul for their guidance and support. Prof Peter Frey my external supervisor, who had given an opportunity to a pediatric surgeon from Malaysia to work with his team in Switzerland. I will be forever indebted to him. Thank you Prof Jeffrey Hubbell for allowing me to be part of the LMRP family for 2 years. A special thank you to Hans Mattias Larsson, my scientific teacher, bench mate, office mate and house mate. I appreciate all the scientific discussions and conversations we had in the lab, metro and at home. To the rest of Peter's Experimental Pediatric Urology Group, Elif Vardar and Eva Maria Balet thank you for being such great colleagues at work and great friends outside work. Thank you Kalitha Pinnagoda my fellow clinician in the group for convincing me that I didn't need to learn French in a class but could do it in" Satellite". Thank you to all the core facilities at EPFL especially Bio imaging and Histo-facility where I had spent countless hours. I would like acknowledge The Faculty of Medicine University Malaya and especially Prof T.M Ramanujam for supporting my decision to do a PhD. To my collaborators at the AEU, Faculty of Medicine University Malaya and University Putra Malaysia Dr Haryanti Azura,Dr Nurul Hayah, Dr Chen Hui Meng, Dr Mark Liew and Dr Rozanaliza thank you for assisting with the animal models used in this thesis. Dato Dr Selvalingam, I greatly appreciate the time you took from your busy schedule to assist in the *in-vivo* experiments and advise on urethral surgery. To my EPFL coffee mates Jean Phillip Gaudry and Priscilla Briquez, thank you for being there to share a cuppa and a good conversation with. I wish to thank all members of the colocation in Lausanne who came and went: Marco, Cara, Andrea, Lorenzo, Saurabh, Vinay, Sylvia and Vicky for making the "coloc" a fantastic place to live in. Special thanks to Valentina for being a great housemate and tolerating me stealing Mattias for all the experiments and other activities we got up too. I wish to thank all the friends I met in Lausanne, you guys know

who you are. Thank you for the memories. To my parents Ponniah Vythilingam and Rajeswary Kathiravelu, you always instilled in me the need to succeed academically and this PhD is me completing that dream for you. To my father in law Dato Dr Selvaprahasam, thank you for being a part time neurosurgeon and a full time grandfather for my kids when I was away. My 4 darling children Arjay, Raeya, Arhan and Anura, Papa was away from your lives for 2 years and I promise never to go anywhere without you guys again. Finally, my wife Vanthini, you are the foundation of this family. You were both mother and father for the children when I was busy pursuing my dream of being a "surgeon scientist". This thesis could not have been done without your support. Thank you for being you and making my life so wonderful.

TABLE OF CONTENTS

LIST OF FIGURES

LIST OF TABLES

LIST OF SYMBOLS AND ABBREVIATIONS

AAMI	:	Association for the Advancement of Medical Instrumentation
ANSI	:	American National Standards Institute
AAP	:	American Academy of Pediatrics
Alpha MEM	:	Alpha modification Minimum essential media
ATMP	:	Advanced Therapy Medicinal Products
AUA	:	American Urological Association
BAMG	:	Bladder Acellular Matrix Graft
BDMP	:	Birth Defects Monitoring Program
CBER	:	Center for Biologics Evaluation and Research
CFC	:	Collagen-fibrin-Collagen
CHUV	:	Centre Hospitalier Universitaire Vaudois
CPD	:	Critical point drying
DAPI	:	4',6-diamidino-2-phenylindole
dCGT	:	Double-layered collagen gel tube
DNA	:	Deoxyribonucleic acid
dsDNA	:	Double stranded Deoxyribonucleic acid
EGF	:	Epidermal growth factors
ECM	:	Extracellular matrix
EPFL	:	Swiss Federal Institute of Technology Lausanne
FDA	:	Food And Drug Authority
FGF-2	:	Fibroblast growth factor -2
GFs	:	Growth factors
GFP	:	Green fluorescent protein
GLP	:	Good laboratory practice

HD	:	High Density
HPV	:	Human Papilloma Virus
H&E	:	Hematoxylin & Eosin
LD	:	Low Density
MACDP	:	Metropolitan Atlanta Congenital Defects Program
MDA	:	Medical Device Authority
MT	:	Masson's Trichrome
MyoHC	:	Myosin Heavy Chain
NaOH	:	Sodium hydroxide
PBS	:	Phosphate buffered saline
PFA	:	Paraformaldehyde
PGA	:	Polyglycolic acid
SEM	:	Scanning electron microscope
sCGT	:	Single-layered rat-tail collagen gel tube
SD	:	Standard deviation
SMA	:	Smooth Muscle Actin
SMC	:	Smooth muscle cells
SIS	:	Small intestinal submucosa
TBS	:	Tris-buffered saline
TEBM	:	Tissue Engineered Buccal Mucosa
TEP	:	Tissue Engineered Product
UTS	:	Ultimate tensile strength
UP2	:	Uroplakin 2
VEGF	:	Vascular endothelial growth factor
10x MEM	:	Minimum essential media

CHAPTER 1: GENERAL INTRODUCTION

1.1 Background

The organ to be addressed in this thesis is the urethra. Urethral diseases can be both congenital and acquired of which may represent a severe morbidity in both children and adults. The current gold standard for treating this disease involves the incorporation of autologous tissue such as buccal mucosa for urethral reconstruction. This, however, can lead to complications such as paresthesia at the site of harvesting and unnecessary prolonged surgery. Failure rates after urethral reconstructions are unfortunately still relatively high at 21%, and the urologists are often left with no other tissue for use as a graft to perform a second surgery. Therefor an off the shelf easy to use replacement tissue will aid urologist in their urethral surgeries.

1.2 Objective and Aim of thesis

Tissue engineering has the potential to fulfill this need by providing an alternative bioengineered tissue source to be utilized as a graft for urethral reconstruction. The current available engineered grafts have failed to translate into clinical practice and replace autologous harvested tissue. Therefore, the aim of this thesis is to engineer such a graft. To fulfill the need for a graft that is practical and clinically translatable, the focus will be in designing a urethral graft without the incorporation of cells and bioactive molecules. Animal collagen will be utilized to fabricate the graft improving on an existing method of fabrication. The rabbit animal model will be utilized for all *in-vivo* experiments examining complete urethral defects of 2cm in length. Briefly cellular engineering will be utilized to study cell remodeling of the collagen grafts. The final optimized version of the graft will be examined for long term implantation and compatibility with standard sterilization protocols. This graft will also be test in a larger animal model with a clinically significant urethral defect of 4cm in length.

1.3 Research Questions to be addressed

i. Does a 2cm acellular tubular collagen graft implanted into the urethra induce functional urethral regeneration in rabbit models? The outcome is measured by the patency of the graft after implantation, histology, and immunohistochemistry.

ii. Will cell seeding followed by decellularization of a collagen matrix modify the density of the fabricated collagen graft resulting in increased growth of urothelial cells and smooth muscle cells (SMC)?

iii. Will modifying the density of the engineered acellular collagen graft improve the mechanical property of the graft and increase the ingrowth of urothelial cells and SMC?

1.4 Study Overview

Collagen, an integral component of the human extracellular matrix and a natural biomaterial, was utilized to fabricate the graft. In Chapter 3 a graft was engineered on an existing method developed by the group of Prof. Frey at the Swiss Federal Institute of Technology (EPFL) following modifications and improvements to the initial method described by Prof Robert Brown of University College London. The graft fabrication was further improved to ensure that the rat tail collagen- based graft is mechanically strong enough to be sutured. In Chapter 3, it was examined if an acellular tubular collagen graft can regenerate an iatrogenic complete urethral defect of 2cm. The rabbit animal model was utilized for this purpose and for all subsequent *in-vivo* experiments. (N=69). Apart from several modified native collagen grafts originating from rat and bovine sources, "humanized" collagen grafts were fabricated by cellular engineering. The remodeling of rat or bovine collagen grafts into human collagen grafts by seeded human smooth muscle cells was studied by histology and immunohistochemistry in Chapter 4. Modification in the density and architecture of the collagen by the seeding of human smooth muscle cells was also analyzed. This understanding was utilized to improve graft fabrication to promote increased ingrowth of native urothelial and smooth muscle cells into the engineered urethral graft. Low cost and minimal complexity of fabrication is an integral criterion to ensure the potential translation of such a graft.

Based on information acquired from previous versions of the graft in Chapter 3 and 4, an optimized tubular collagen graft with the best potential for clinical application was developed in Chapter 5.Bovine collagen was utilized to fabricate this graft at is more widely utilized and accepted in clinical practice compared to rat tail collagen to ensure future translation of the engineered graft. This final graft was tested in the same rabbit model as previous grafts engineered in this thesis assessing functional, histological and immunohistochemistry outcomes. This was compared with previous graft versions

developed in Chapter 3 and 4. A pilot study utilizing the dog (N=3), to create a more clinically relevant urethral defect was initiated in Chapter 6 to test the efficacy of the final graft. The ultimate objective of this thesis is to provide the pre-clinical data on which the fabrication of an "off-the-shelf" urethral graft for clinical application will be undertaken.

CHAPTER 2: LITERATURE REVIEW

2.1 Urethral anatomy and pathology

The male urethra is a narrow fibro muscular tube that conducts urine and semen from the bladder and ejaculatory ducts, respectively, to the exterior of the body. The male urethra originates at the bladder neck and terminates at the urethral meatus on the glans penis. It is roughly 15-25 cm long in the adult male. It is divided into 3 segments: the prostatic, the membranous, and the spongy (or penile) urethra (Figure 2.1). The developed female urethra on the other hand is a 4cm tubular, richly vascularized structure that begins at the bladder neck and terminates at the vaginal vestibule. The urethra is subject to both congenital and acquired diseases.

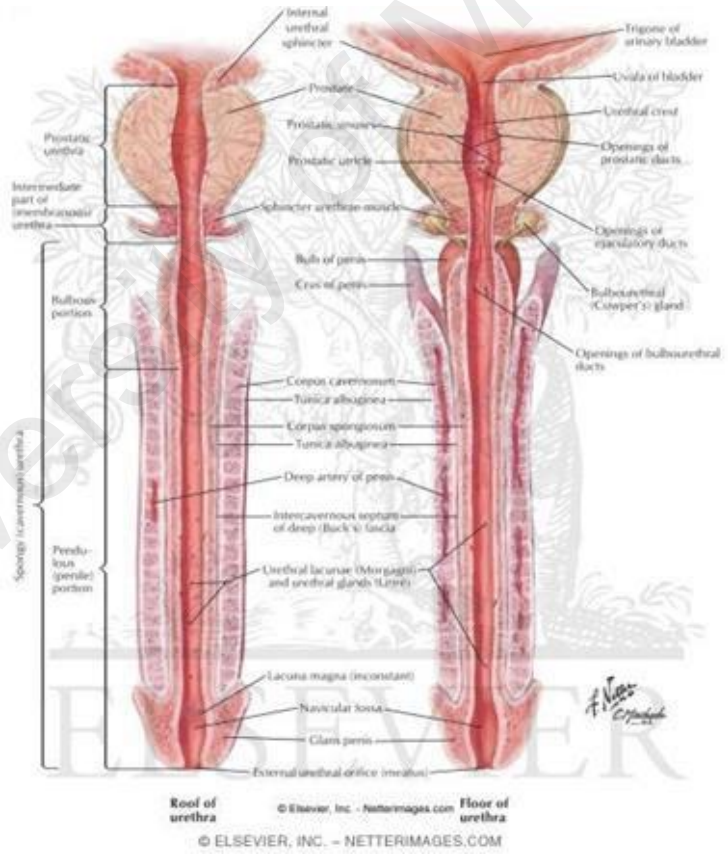

Figure 2.1: Anatomy of the male urethra. (NETTERIMAGES.COM)

The most common congenital urethral malformation is hypospadias. The hallmarks of this anomaly are the non-fused ventral prepuce, the pathological position of the urethral meatus anywhere on the midline between the glans and the scrotum and in severe cases the formation of chordee, fibrous bands in the muscular component of the penile shaft ventrally tilting the glans (Ducket J.W 1996).(Figure 2.2)

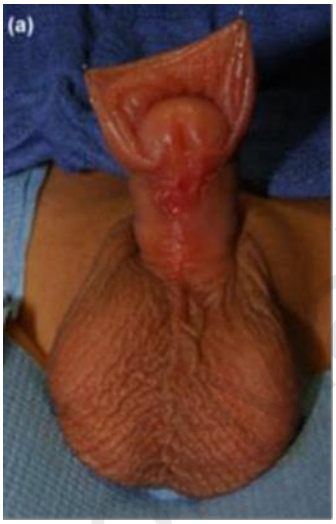

Figure 2.2: Image of a Distal Hypospadias (Stein, 2012)

The incidence of this pathology varies geographically from 0.26 per 1000 live male births in Mexico to 2.11 in Hungary and 2.6 per 1000 live male births in Scandinavia (Källén, 1988). In a recent 2-year prospective study, the rate of hypospadias was found to be 38 in 10 000 live male births in Netherlands, a number six times higher than previously recorded in that nation(Pierik et al., 2002). In 1997, two independent surveillance systems in the United States – the nationwide Birth Defects Monitoring Program (BDMP) and the Metropolitan Atlanta Congenital Defects Program (MACDP) – reported a near doubling of the incidence of hypospadias when compared with immediately preceding decades (Paulozzi et al., 1997). The incidence of all types of hypospadias increased from 20.2 to 39.7 in 10 000 live male births during the period

from 1970–1993; which translates that one in every 250 live male births in the United States suffers from hypospadias.

The exact etiology of hypospadias is still very much debated. Embryonically, it results from partial or complete failure of the urethral folds to develop in normal length or from a failure of the developed distal folds to close ventrally. The extent of the closure determines the position of the urethral orifice. This incomplete developmental anomaly could be attributed to abnormal androgen production by the fetal testis, limited androgen sensitivity in target tissues of the developing genitalia, and premature cessation of androgenic stimulation due to early atrophy of the Leydig cells of the testes (Willis 1948). It has been hypothesized that the disease may have a complex genetic background, with gene expression acting in concert with environmental factors. The familial rate of hypospadiasis is approximately 7%, which reflects a non-familial, sporadic finding in most cases.

Recent studies have identified the role of Mullerian inhibiting substance and fibroblast growth factor 10 in hypospadias development(Baskin, 2000; Teixeira, Maheswaran, & Donahoe, 2001). The contamination of our environment with industrial estrogenic substances may also be a contributing factor to the increase in the global incidence of hypospadias in the last decade (Baskin, 2000). Classification of the disease is done based on the location of the meatus, the urethral opening. In 70-80 % of the patients, the meatus is located distally on the penile shaft and in the glandular region. Another 20-30% will have the meatus located in the middle of the penile shaft or proximal of it (Morey, McAninch, Duckett, & Rogers, 1998).

A normal developed urethra is also not spared from acquiring pathologies that would require surgical intervention. Urethral stricture as it names suggest is characterized by narrowing of the urethra. This can be caused by trauma or chronic

infection/inflammation. A stricture is the result of ischemic spongiofibrosis manifesting as scar tissue in the corpus spongiosum, the spongy erectile tissue in the urethra. Contraction of this scar tissue leads to a decrease in the urethral caliber, which in turn leads to a reduction in flow of urine resulting in compromised voiding(Mangera & Chapple, 2014). Urethral stricture has an incidence of 0.6% in a susceptible population(Hillary, Osman, & Chapple, 2014).

The different causes of urethral strictures can be summarized as follows(C. Chapple et al., 2004):

1) **Congenital**: predominantly seen in the bulbar urethra.

2) **Iatrogenic**: 20 % of urethral stricture are due to traumatic catheterization, failed hypospadias surgery, and post prostatic surgery.

3) **Infection**: Historically one of the main causes of urethral stricture is gonococcal urethritis, which has been in decline since antibiotic treatment was available. However, it is still seen in some under developed parts of the world.

4) **Inflammation**: Lichen Sclerosis is a progressive inflammatory condition thought to have an autoimmune basis, which commonly affects the anterior urethra.

5) **Trauma**: Urethral trauma is relatively rare in Europe and in the US, but fairly common in Malaysia. This is due to the high number of motorcycle accidents leading to pelvic traumas and associated urethral injuries(Abdul Manan & Várhelyi, 2012) Association of urethral injuries in pelvic trauma is explained by the close proximity and attachment of the urethra to the pubic bones and the high velocity nature of the injury(Mathur, Aggarwal, Satsangi, Khan, & Odiya, 2011). It can range from mild contusion with preservation of epithelial continuity to a partial tear of the urethral

epithelium, or full urethral transection. All these pathological conditions can potentially induce urethral strictures.

Urethral injuries in females(Thambi Dorai, Boucaut, & Dewan, 1993) are very rare owing to the short and mobile female urethra having no significant attachments to bone. The male urethra however is anatomically more predisposed. The site of most iatrogenic injuries to the male urethra is at its 90-degree bend where the urethra pierces the perineal membrane and is invested into the corpus spongiosum(Nicolaas Lumen et al., 2009). Urethral strictures lead to urinary tract infection, acute urinary retention, high-pressure voiding leading to secondary bladder thickening and bladder irritability, and even urinary fistula with gangrenous super-infection. The length and severity of the stricture seems to correlate with the increased risk of complications(Fenton, Morey, Aviles, & Garcia, 2005).

2.2 Current treatment options

Hypospadias and urethral strictures require surgical intervention for correction. In 1996, the American Academy of Pediatrics (AAP) suggested that the optimal time for elective hypospadias surgery is between 6 and 12 months(Kass & Kogan, 1996). Based upon consideration of emotional, cognitive, and psychosexual factors, pediatric urologists now recommend that hypospadias surgery should be completed by 15 months the latest(Schultz, Klykylo, & Wacksman, 1983). The goals of the surgery are to provide a straight penis adequate for sexual function and to move the urethral meatus to the tip of the penis to allow the patient to void with a normal urinary stream. A detailed assessment to guarantee the best operative technique is generally done with the patient under anesthesia to examine the level of division of the corpus spongiosum, the quality of the urethral plate, and the length of the urethra that needs to be constructed. The surgeon is then left to decide the surgical technique to employ (i.e. Duplay/TIP, Mathieu Onlay, Koff, Bracka Koyanagi/Hayashi). But the plethora of operations described in literature attests to the difficulties encountered by surgeons to achieve the earlier mentioned goals. The apparent need for additional tissues to reconstruct the neo-urethra and/or resurface the ventral shaft leads to the use of various grafts including genital and extra genital skin flaps, mucosal grafts from the bladder or buccal regions, tunica vaginalis, and peritoneal grafts(Caldamone, Edstrom, Koyle, Rabinowitz, & Hulbert, 1998; Dessanti, Rigamonti, Merulla, Falchetti, & Caccia, 1992; Ehrlich, Reda, Koyle, Kogan, & Levitt, 1989; Koyle & Ehrlich, 1987). The use of non-genital tissues for urethroplasty may be associated with additional procedures for graft retrieval, prolonged surgery time, extended hospitalization periods, and increased morbidity.

Even though many techniques have been described, the outcome is far from perfect. Fistula rates as high as 21% are reported along with other complications such as stricture, meatal stenosis, urethral diverticulum, dehiscence and recurrent penile curvature (W. Snodgrass, MacEdo, Hoebeke, & Mouriquand, 2011; W. T. Snodgrass & Lorenzo, 2002).

A urethral stricture patient is initially assessed with a symptom score such as the American Urological Association (AUA) symptom index and combined with uroflowmetry(Heyns & Marais, 2002; Morey et al., 1998). Retrograde urethrography (RUG) is done to provide information regarding the stricture location, length, and other identifiable pathologies affecting the urethra (i.e., diverticulum, fistula, false passage), which can aid in operative planning (Figure 2.3).

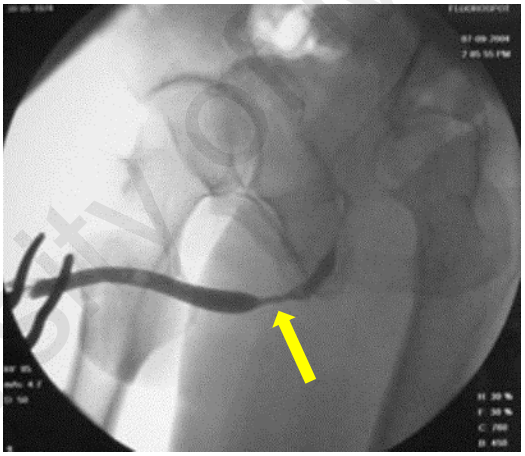

Figure 2.3: Stricture at the distal bulbar and proximal urethra shown by retrograde urethrography (Mundy & Andrich, 2011)

An antegrade urethrogram can be performed when a suprapubic catheter is *in situ*. Flexible or rigid urethroscopy can be helpful in the assessment of the location and degree of urethral stricture and to assess the state of the urethra distal to the stricture (Figure 2.4). Recurrence of the disease is followed up by cystoscopy which is more sensitive to diminishing urethral caliber prior to presence of any significant uroflowmetry results (Y. J. Lee & Kim, 2013).

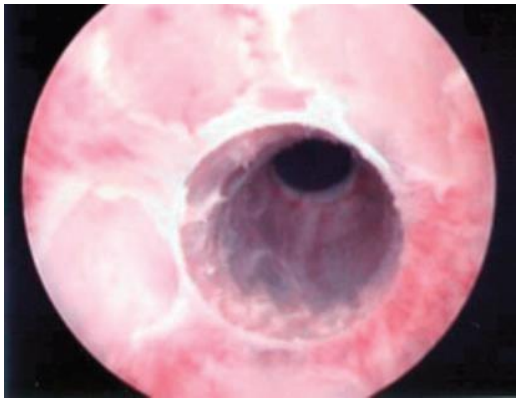

Figure 2.4: Endoscopic image of a developing stricture (Mundy & Andrich, 2011)

Strictures can be managed endoscopically by urethral dilatation and internal urethrotomy. However repeated dilatation of the urethra can exacerbate scar formation; thus, adding length and severity to the stricture. For more pronounced strictures, the gold standard is open urethroplasty. Short strictures (≤2-5 cm) in the bulbar urethra are treated with excision and primary anastomosis. Longer strictures (>2-5 cm) in the bulbar urethra and strictures in the distal location along the penile shaft, require usually a urethral substitution procedure where a graft or a flap are put in place to augment the stenotic segment. The graft used for surgery was previously obtained from the penile skin, scrotal skin, and bladder mucosa, but with not so encouraging results. Buccal mucosa utilized as graft (Figure 2.5) gained popularity in the 1990s and was popularized by pediatric urologists in hypospadias surgery(Andrich & Mundy, 2001; el-Kasaby et al., 1993; Jordan, Eltahawy, & Virasoro, 2007). However, extensive harvesting of buccal mucosa for lengthy strictures has been reported to be associated with donor site morbidity(Jang, Erickson, Medendorp, & Gonzalez, 2005; N. Lumen et al., 2016; Soave et al., 2017) .

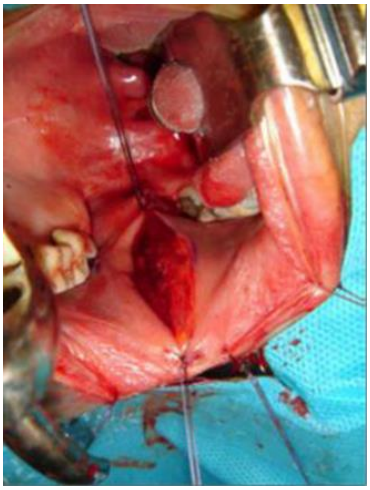

Figure 2.5: Harvesting of buccal mucosal graft (www.urethralcenter.it)

With such varied surgical techniques and the relatively high complication rates, experts in the field recommend that urethral strictures and hypospadias to be treated in specific centers by a team of dedicated surgeons and that the material used to reconstruct the diseased urethra should be improved(Fossati et al., 2016).

2.3 Biomaterials for tissue engineering

Tissue engineering has the potential to fulfill the need for an alternative graft for urethral reconstructive surgery. In a scaffold-based tissue engineering approach, the choice of the biomaterial is crucial to engineer an optimal graft. Numerous biomaterials are available for tissue engineering applications, each with its own advantages and limitations. The decision which material to use is made based upon the intended application; nevertheless, the foundation of the decision will be based on the capability of the biomaterial to support cell attachment, proliferation, and differentiation (Abou et al., 2013).

Biomaterials can be broadly classified as natural or synthetic. The fabrication of synthetic polymers is relatively easy, tunable, and reproducible. Therefore, it is easy to maintain a good quality control. There are, however, concerns regarding its biocompatibility and degradation over time either in respect to the presence of manufacturing residuals or to the release of degradation products (Atala, 2009). Naturally derived biomaterials on the other hand have the advantage of being bioactive, biocompatible, with given degradation and mechanical kinetics, and an intrinsic structural resemblance to the extracellular matrix of native tissue. Upon degradation, they do not release cytotoxic products (Stoppel, Ghezzi, McNamara, III, & Kaplan, 2015). The innate ability of naturally derived biomaterials to promote cell adhesion, proliferation, and differentiation results in excellent tissue regeneration (Renth & Detamore, 2012). The disadvantages of natural biomaterials are their weak mechanical property and the batch-to-batch variability due to their natural origin. This makes it difficult to ensure the reproducibility of the material (Barnes, Pemble, Brand, Simpson, & Bowlin, 2007).

The use of synthetic biomaterials in tissue engineering has several advantages when compared to naturally derived biomaterials. Synthetic biomaterials can be fabricated with a controlled shape, architecture and chemistry to mimic the natural extracellular matrix(B.L. Seala et al., 2001; Lutolf & Hubbell, 2005). Examples of synthetic biomaterials used for tissue regeneration purposes are poly (α-hydroxyacids), which include polylactic acid (PLA), polyglycolic acid (PGA) and their copolymer, poly (lactic-co-glycolicacid) (PLGA)(Okamoto & John, 2013; Pan & Ding, 2012). These biomaterials produce nontoxic degradation products (lactic acid and glycolic acid) which are then cleared away by normal metabolic pathways. The properties of synthetic biomaterials, such as tensile strength, the mechanical modulus and the degradation rate, can be easily customized for target applications by altering the lac-tide/glycolide proportions and polymerization parameters. Due to these features synthetic biomaterials have already been utilized to engineer urethral and bladder grafts (Atala, Bauer, Soker, Yoo, & Retik, 2006; Raya-Rivera et al., 2011a; Ribeiro-Filho & Sievert, 2015). However certain synthetic biomaterials, such as poly (α-hydroxy esters), may produce acidic degradation products which can alter the pH of the surrounding tissues(Lu et al., 2000). This pH change can affect cell behavior and survival and cause adverse tissue and inflammatory reactions(Vacanti et al., 2012). Synthetic biomaterials also lack biologically functional domains. This lack of a peptide side-chain reactivity for the binding of regulatory peptides, growth factors and other biological signals does not allow for the facilitation of cell adhesion or direct phenotypic expression, when compared to a natural biomaterial.

Naturally derived biomaterials can be classified into two groups: Protein-based biomaterials (i.e., collagen, silk fibroin, gelatin, fibronectin, keratin, fibrin, and egg shell membrane) and polysaccharide-based biomaterials (e.g. hyaluronan, cellulose, glucose, alginate, chondroitin, chitin and its derivative, and chitosan). Protein-based biomaterials are obtained from animal and humans sources, whereas polysaccharide based biomaterials are obtained from animals and algae (Chow, Nunalee, Lim, Simnick, & Chilkoti, 2008; Cui, Li, & Ge, 2007; Mano et al., 2007). Another class of natural biomaterials is termed decellularized animal or human tissue-derived biomaterials, which are created by the elimination of all cellular and most nuclear materials from native tissues/organs (i.e.; small intestine submucosa (SIS)).

Polyhydroxyalkanoates (PHAs) is a polysaccharide based biomaterial that is synthesized by bacteria. Microorganisms synthesize them for their intracellular carbon and energy storage(Li, Yang, & Loh, 2016). There are more than 150 monomers identified as constituents of PHAs(Iqbal, Kyazze, Tron, & Keshavarz, 2014a). This offers a broad range of biomaterials with different properties. Some of the most used examples are poly3-hydroxybutyrate, 3-hydroxybutyrate, and 3-hydroxyvaleratecopolymer, poly 4-hydroxybutyrate, 3-hydroxybutyrate and 3-hydroxyhexanoate copolymer, and poly 3-hydroxyoctanoate. However, there are some limitation such as brittleness, tendency to acquire a high degree of crystallinity, poor stiffness, slow degradation rate, and hydrophobic character with regards to the utilization of this biomaterial for tissue engineering applications(Iqbal, Kyazze, Locke, Tron, & Keshavarz, 2015; Iqbal, Kyazze, Tron, & Keshavarz, 2014b; Ozdil & Aydin, 2014).

Alginate is an anionic polysaccharide consisting of beta-d-mannuronic acid and alpha-l-glucuronic acid. Alginate is commonly found in the cell wall of brown seaweed and is produced extracellularly in some bacteria. Its molecular weight, composition, and sequence will vary depending on the source and species that produces the compound(Pawar & Edgar, 2012). Alginate hydrogels resemble the extracellular matrix of the body and can be easily modified into sponges, foams, and fibers, a property that makes it an attractive biomaterial for tissue engineering(Venkatesan, Bhatnagar, Manivasagan, Kang, & Kim, 2014).It is a widely-used because alginate can be easily fabricated into hydrogels in the presence of divalent cations(Ozdil & Aydin, 2014). However, alginate has a poor cell adhesion and poor *in-vivo* degradation

Chitin is a biomaterial derived from the shells of crabs, shrimp, prawn and other crustaceans as well as some insects. It is a linear polysaccharide built from beta-1,4 linked N-acetyl glucosamine units, and it is highly insoluble in common solvents(Ozdil & Aydin, 2014). Chitin is the second most abundant natural biomaterial available, just behind cellulose, and it has a simple derivative called chitosan. Chitosan is obtained from the deacetylation of chitin, and it is a copolymer of N-acetyl glucosamine and d-glucosamine. Unlike chitin, chitosan is soluble, and this property make it easy to handle and utilize for fabrication. Both compounds have been used in tissue engineering for different applications. Besides being a soluble polymer, chitosan has a high bio degradability and biocompatibility, non-antigenicity, good adsorption properties, non-toxicity, and bio-functionality(Babu, O'Connor, & Seeram, 2013). It's limiting property is that, chitosan has poor mechanical strength and is unstable to maintain a predefined shape(Shanmugasundaram et al., 2001).

Many natural protein based biomaterials have also been studied for tissue engineering applications. Each with a distinguishing mechanical, chemical, electrical, electromagnetic, and optical property. Protein based biomaterials are characterized by their long range ordered molecular secondary structures (e.g., beta-pleated sheets, coiled coils, or triple helices) that arise due to the highly repetitive primary amino acid sequences within these proteins. These features promote self-assembly, the formation of structural hierarchy and thus functional roles in nature. These properties make them attractive as building blocks for tissue engineers(Hu, Cebe, Weiss, Omenetto, & Kaplan, 2012).

Elastin proteins are critical in forming elastic fibers in most tissues, such as blood vessels and dermis(Almine et al., 2010). Different elastin protein networks can be isolated from animal tissues such as skin, while recombinant human tropoelastin (full-length 60 kDa), the soluble precursor of elastin, is an alternative source. Resilin proteins on the hand are 'super elastic rubbers' found in the flight and jumping organs of insects where cyclic extension and retraction are needed millions of times over the lifetime of the animals. Cross-linked resilin (via tyrosines) exhibits high resilience up to 95 % under high-frequency motion and has over 300 % elongation before breaking. This biomaterial can be utilized for tissue engineering applications in areas of high frequency elastic motions(Elvin et al., 2005; Qin et al., 2009).

Silk proteins are fibrous proteins synthesized by silkworms and spiders. In the salivary gland of *Bombyx mori* silkworms, silk fibroin exists in a water-soluble form and is spun into fibers while being coated with glue-like sericin proteins. The spinning process leads to the rapid transition from the silk solution state to an insoluble form dominated by anti-parallel beta sheet crystals. Silk fibroins combine high tensile strength with toughness(Hu et al., 2011; Jin & Kaplan, 2003; Omenetto & Kaplan, 2010).

Keratin proteins(Reichl, 2009; Rouse & Van Dyke, 2010) are another broad category of insoluble proteins that form intermediate filaments in the cytoplasmic epithelia and epidermal appendage structures (e.g. hairs, nails, wools, hooves). There are other natural proteins currently being studied for different biomaterial applications, including reflectins for optical devices(Crookes et al., 2004; Kramer, Crookes-Goodson, & Naik, 2007), amyloids for biosensors(Gebbink, Claessen, Bouma, Dijkhuizen, & Wösten, 2005; Shorter & Lindquist, 2004) and many others.

Within this wide available choice of naturally derived biomaterials, collagen was selected, in the frame of this thesis work, for the fabrication of a urethral graft due to the fact that it is the most abundant protein in the extracellular matrix (ECM). Collagen makes up 30% of the ECM and it is the integral component of many human tissues (Mouw, Ou, & Weaver, 2014). Collagen comprises a right-handed bundle of three parallel, left-handed polyproline II-type helices. This protein has an integral role in connecting the entire ECM into a single framework. Along with elastin and keratin it ensures that this network is able to withstand the repetitive and high tensile stress without plastic deformation or rupture (Muiznieks & Keeley, 2013). At the cellular microenvironment, the linkage created by collagen is essential for the adequate transfer of oxygen and nutrient. Due to this collagen has been utilized in numerous biomedical applications such as drug delivery and regenerative medicine (Chattopadhyay & Raines, 2014; Gillette et al., 2008; Pedraza, Marelli, Chicatun, McKee, & Nazhat, 2010).

Collagen can be extracted from any animal source. The common source of collagen for tissue engineering application is bovine skin and tendon, porcine skin, and rat tail. Recombinant human collagen, which is now commercially available is potentially less immunogenic than animal derived collagen. But more importantly there are no batch to batch differentiation and it appears to be the future of collagen based scaffold

engineering(Olsen et al., 2003). However, it is still considerably more expensive than collagen derived from animal sources.

There are more than 20 distinct forms of collagen. Type 1 collagen is the most abundant one, making up approximately 90% of mammalian tissue (Hubbell, 2003; Kim, Choi, Kim, Yoon, et al., 2012). Studies have shown that collagen type 1 plays an important role in the adherence of various cell types to the ECM and in cell division (Kuraitis, Giordano, Ruel, Musarò, & Suuronen, 2012). Moreover, collagen biomaterials are attractive as they can be incorporated with growth factors and other bioactive molecules. Controlled release of growth factors and/or bioactive molecules improves the therapeutic effects of grafts (Mano et al., 2007; Murphy et al., 2014).

Collagen type 1 does not signal mesenchymal stem cell migration on its own, studies have shown that if the cell is stressed upon injury, the release of a protease like substance by the cells interacts with the collagen matrix to recruit stem cells to the damaged area. This shows that collagen type 1 can induce a potent migratory response in the right environment (Mauney, Olsen, & Volloch, 2010; Ode et al., 2010). Though inherently weak, it has been demonstrated that by increasing the density of the collagen construct, while conserving its capacity to induce good cell proliferation when seeded with fibroblast and urothelial cells its mechanical properties can be enhanced (Ghezzi, Marelli, Muja, & Nazhat, 2012).

The focus of this thesis is, to take advantage of the intrinsic property of collagen to induce regeneration without incorporation of *ex-vivo* cultured cells and bioactive agents.

2.4 Preclinical development in urethral tissue engineering

There are two approaches in tissue engineering, one is to utilize an acellular graft to replace the defect and allow cell infiltration to occur *in-vivo* and the other involves the seeding of the graft with the specific cells of the area of interest prior to implantation. Cellular grafts, however, require a longer period to be fabricated and necessitate prior biopsy and cell expansion that makes it far less attractive than acellular grafts. Once the intended graft has been fabricated and the initial mechanical characterization and *in-vitro* examination of the tissue engineered graft has been done, the next step is the *in-vivo* analysis of the graft.

The choice of the animal model for this phase of graft development takes into consideration the intended outcome to be measured and the anatomical similarities between the chosen animal and human's. The rabbit model is the most common animal model used in the *in-vivo* analysis for urethral regeneration. This animal model has been utilized to examine both acellular and cell seeded grafts(Versteegden et al., 2017). The surgical utilized technique for the implanting of the tissue engineered graft varies. Some research groups implant a tubular graft after an excision of a complete segment of the native urethra. Others just apply a patch of biomaterial on the ventral aspect in an attempt to regenerate only a portion of the excised urethra. The later described method is called an on-lay procedure. Both methods are established techniques utilized in clinical practice during urethral surgery.

In 1988, Kropp had utilized porcine small intestinal submucosa (SIS) and implanted it as an on-lay in the rabbit model without the utilization of cells(Kropp et al., 1998). The graft measured 1cm in length and all 8 animals had demonstrated no complications.

Other research groups also had experienced similar favorable outcomes when attempting an on-lay method utilizing different acellular matrices(Chen, Yoo, & Atala, 1999; J. E. Nuininga et al., 2003). Acellular grafts have convincingly demonstrated that they will well regenerate the tissue at the graft site when implanted as an on-lay on a partially excised urethra.

The focus was then shifted to examine if an acellular tubular graft could regenerate as well a complete urethral defect. In 2000, Sievert had decellularized homologous rabbit urethra and implanted it into 30 rabbits to replace a 1.0-1.5cm long urethral defect(K D Sievert & Tanagho, 2000). The results were encouraging with no complications in any of the animals. To investigate the maximum distance that a tubular acellular graft could regenerate, Dorin proceeded to implant tubular decellularized porcine bladder grafts of various lengths (0.5cm, 1cm, 2cm, and 3cm) in the rabbit animal model(Dorin, Pohl, De Filippo, Yoo, & Atala, 2008). His findings concluded that the maximum defect distance that can support normal tissue formation using acellular tubular grafts, which relies on native cells for tissue regeneration, is 0.5 cm. However when tubular, cell seeded matrices were utilized by different research groups, they performed consistently well to repair defects ranging from 1 cm to 1.5 cm in length irrespective of the type of matrix utilized(Feng, Xu, Zhu, Cui, & Chen, 2011; Fu, Deng, Liu, & Cao, 2007; Gu et al., 2012) . The utilization of cell based technology promising with initial good results was still complicated to translate due to the need of a prior biopsy and *ex-vivo* cell proliferation. To circumvent this issue and to improve the regenerative potential of acellular grafts, researchers then explored the benefit of growth factor incorporation into their engineered grafts.

It is known that; multiple growth factors (GFs) are involved in urethral regeneration because different cell populations are needed to restore the defect site. Epidermal GF (EGF) is known to play a key role in urothelial regeneration, whereas fibroblast GF-2 (FGF-2) and vascular endothelial GF (VEGF) are involved in angiogenesis and blood vessel maturation(Daher et al., 2003; Nillesen et al., 2007). Therefore, Nuininga et al developed a tubular collagenous graft containing heparin to increase the binding of growth factor to the matrix and incorporated HB-EGF, FGF-2, and VEGF within the matrix. These growth factor-loaded tubular grafts were implanted in a 1cm long urethral defect and were compared to a heparin-collagen graft without growth factor. The results showed that all animals that were implanted with a graft without growth factors had good functional outcome and that the incorporation of growth factors did not significantly enhance the functional outcome. However, histological examination of the growth factor incorporated graft showed an increase in extracellular matrix deposition and neovascularization. Further, urothelial regeneration was promoted and strong infiltration of granulocytes and fibroblasts could be demonstrated. But the excessive regeneration stimulated by the incorporation of growth factors eventually lead to complications such as urethral stenosis, diverticulum, and fistula formation that were only observed in animals that had received a growth factor- loaded graft. They concluded that the utilization of growth factor incorporation into urethral graft engineering should be done with caution(Jody E. Nuininga et al., 2010).

The FDA suggest that the anatomy and size of the studied area in the animal utilized for applied research be comparable to human. Safety and efficacy should also be demonstrated in 2 different animal models prior to initiating clinical trials(M. H. Lee et al., 2010). The maximum length of the urethra that can be replaced after subtotal urethral excision in the rabbit model is only 2 cm. A larger animal model is required if longer than 2 cm grafts are to be tested for clinical translation.

The commonly utilized large animal model for urethral tissue engineering applied research is the dog. The most distal part of the dog's urethra is protected within a bony structure called the Baculum. However, it is still possible to pass a transurethral catheter into the bladder. Shokeir et al had implanted a decellularized harvested dog urethra as an on-lay to replace a 3cm long resected anterior urethral segment in another dog and this was compared in the same study with a control group that had no graft being implanted (Shokeir et al., 2003). The obtained results demonstrated that the regeneration of this urethral defect was possible with and without an acellular matrix providing that the posterior urethral wall was preserved. Motivated by these results, they implanted a tubular graft made of the same matrix to repair a 3cm completely excised urethra in the same animal model and they had 100% failure rate(SHOKEIR et al., 2004). These findings lead them to the conclusion that the presence of a urethral bed was essential for the successful regeneration of a long urethral defect, and therefore long tubular acellular grafts should be avoided. Based on this conclusion it would appear that cell-seeded urethral grafts therefore appeared to be the more clinically relevant grafts to bridge long complete urethral defects.

In 2012, however, two different outcomes had been reported concerning cell-seeded tubular grafts. Shokeir et al reused the same graft as in their previous experiments but this time seeded it with canine smooth muscle and urothelial cells to bridge a 3 cm long urethral defect. Since all 14 dogs in the study subsequently developed urethral strictures, they concluded that the cell-seeded tubular graft was insufficient to replace a 3cm circumferential urethral defect(El-Tabey et al., 2012). In the same year however, Atala et al, successfully regenerated a 6 cm long circumferential urethral defect in dogs using a cell-seeded porcine acellular bladder matrix. In their study, they demonstrated a clear benefit of cell-seeded tubular grafts when compared to acellular tubular grafts as all 6 of the animals that were implanted with the latter graft had developed complications(Orabi,

Aboushwareb, Zhang, Yoo, & Atala, 2013). The only variation between these two studies apart from the biomaterial used to fabricate the graft is that Shokeir et al had utilized stray dogs and Atala et al had used Beagles. It has been postulated that stray dogs have a higher level of immunity thereby potentially mounting a more severe immune rejection towards a foreign material(De Santis et al., 2012).This possibly could be an explanation for the differing results.

As a conclusion, when a graft is utilized as on-lay irrespective if it is acellular, cell-seeded or growth factor loaded, it can regenerate a partial urethral defect in the presence of a healthy urethral bed. Cell based grafts though at times exhibiting contrary results have been shown to reduce side effects when applied on to an engineered graft to repair a partial or complete urethra(Versteegden et al., 2017).

2.5 Regulatory challenges for bioengineered urethral grafts.

In order to achieve clinical translation, a tissue engineered urethral graft has to comply with regulatory requirements. (Figure 2.6)

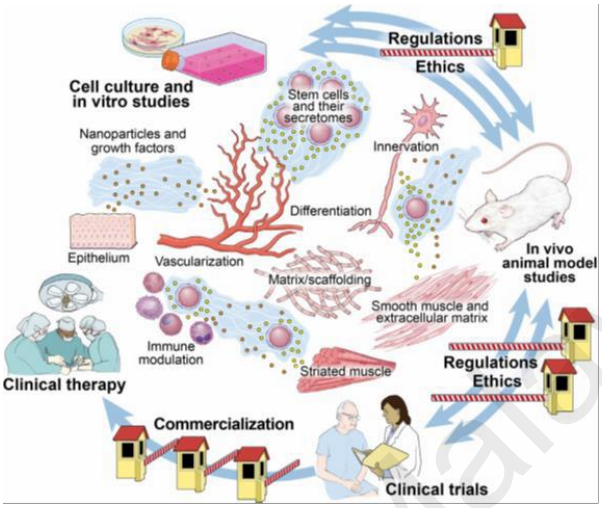

Figure 2.6: Tissue engineering and regenerative medicine: bench to bedside in urology(Karl Dietrich Sievert, 2017)

In Europe, Tissue Engineered Product (TEP), somatic cell therapy-based medicinal products, and gene therapy-based medicinal products are classified under the term Advanced Therapy Medicinal Products (ATMP). ATMP may contain cells or tissues of human or animal origin, or both. It may also contain additional substances, such as cellular products, bio-molecules, and chemical substances. Marketing authorization application for TEPs is processed by the European Medicines Agency. This committee is responsible for assessing the quality, safety, and efficacy of ATMPs and provides the procedure of ATMP classification (European Union law 2007/2009).

In the United States of America, the Food and Drug Authority (FDA) is a science-based regulatory agency in the US Public Health Service. The agency plays a role in product oversight, premarket approval, and post market surveillance and enforcement. Human medical products regulated by the FDA include drugs, tissues, biological products, and medical devices. Due to the complex and integrated nature of the development of tissue engineered products, the US Congress recognized the existence of combination products in its Safe Medical Device Act in 1990. The safe medical device act established that the FDA shall classify a combination product according to its primary mode of action (FDA guidance and regulatory information: Section 503(g) of the FD&C Act [21USC 353(g)). Therefore, a collagen-based tissue engineered urethral replacement graft as envisioned in this thesis with or without cells will come under the jurisdiction of the Center for Biologics Evaluation and Research (CBER). Though there are separate guidelines governed by distinct agencies within the FDA that regulate ''xenotransplantation products'' it should be noted that acellular products of xenogeneic origin do not meet the FDA definition of ''xenotransplantation products'' and are regulated as biological products or medical devices. Therefore, the envisioned graft in this study fabricated from a bovine collagen source is considered as a medical device. In Malaysia, therefore it would need to comply with the guidelines set up by the Medical Device Authority (MDA), an agency under the Ministry of Health if a future clinical trial is envisioned.

2.6 Clinical studies using tissue engineered urethra

In 1999, Atala et al utilized Bladder Acellular Matrix Graft (BAMG) to treat hypospadias. The graft was applied as an on lay while preserving the urethral plate(Atala, Guzman, & Retik, 1999).Out of the 4 patients with previously failed hypospadias repair enrolled in the study, only 1 patient had developed a fistula at the end of the 22-month study. In 2002, Montovanni et al started utilizing porcine small intestine in patients with urethral stricture as a dorsal on lay and subsequently published his long-term outcome in 2011. The study showed a positive outcome in the 40 patients who underwent the procedure (Mantovani et al., 2011; Mantovani, Trinchieri, Castelnuovo, Romanò, & Pisani, 2003). In 2005, Le Roux et al attempted to utilize tubular acellular porcine Small Intestine Submucosa (SIS) to treat urethral strictures endoscopically. The study was stopped after the ninth patient since 8 patients who had been implanted with the graft developed recurrent strictures and only one patient with a 1cm long stricture did not develop any complication (leRoux, 2005). They concluded that long tubular acellular grafts were not able to regenerate strictures longer than 1cm and that in cases with longer defects the graft should be only implanted as an on-lay graft.

In 2012, Palminteri et al published their long-term follow-up on patients implanted with SIS as a ventral on-lay following up on his initial publication from 2007. They had demonstrated good results for strictures shorter than 4cm if SIS was utilized (Palminteri, Berdondini, Colombo, & Austoni, 2007; Palminteri, Berdondini, Fusco, De Nunzio, & Salonia, 2012). This concurred with other studies that noticed that an acellular matrix implanted as an on-lay does not regenerate effectively in strictures that are longer than 4cm(Fiala, Vidlar, Vrtal, Belej, & Student, 2007; Hauser, Bastian, Fechner, & Müller, 2006). El Kassaby et al examined the outcome between buccal mucosa and acellular bladder matrix graft implanted as a ventral on lay and concluded from their clinical trial that acellular matrices should be only used for urethral stricture patients with no previous

intervention and on a healthy urethral bed(El Kassaby, AbouShwareb, & Atala, 2008). Chronic urethral stricture patients who have had multiple surgeries should have a buccal mucosa graft implanted. However the successful utilization of both decellularized human cadaveric urethral grafts and bladder acellular matrix grafts in patients with long complex urethral strictures and with previous multiple urethral procedures by another clinical research team showed that organ specific acellular grafts can be used as an on-lay for these patients(Ribeiro-Filho & Sievert, 2015).

Though showing very promising *in-vivo* data, cell-based tissue engineered urethral grafts only demonstrated a 50-60% success rate in the clinical setting. This was observed when they were utilized for hypospadias repair by Fossum and for urethral stricture patients by Bhargava in 2006 and 2007, respectively(Bhargava, Patterson, Inman, MacNeil, & Chapple, 2008; Fossum, Svensson, Kratz, & Nordenskjöld, 2007). In 2011, Raya-Rivera utilized tubularized polyglycolic acid: poly (lactide-coglycolideacid) scaffolds seeded with smooth muscle and urothelial cells and implanted them in 5 patients with urethral stricture. The length of the tube averaged 6 cm with an internal diameter of 0.2 cm. The six years follow up study showed that no patient had developed any complications(Raya-Rivera et al., 2011b). To date most of these clinical trials have been initiated by academic institution and not conducted by a tissue engineering company.

In 2015, the clinical outcome of a commercial Tissue Engineered Buccal Mucosa (TEBM) product, Mukocell® (Urotiss, Dresden, Germany) engineered from the respective patient buccal mucosa biopsy and implanted in 21 patients with anterior urethral strictures was published. Mukocell® was approved by the European Medicine Agency and is now available as a commercial medical product for urethral stricture indications(Gouya Ram-Liebig et al., 2015).

Nevertheless, there lie some limitations for the widespread utilization of this graft. The patient still needs to have a small sample of their buccal mucosa biopsied and to be sent to the lab for cell multiplication before being seeded on the graft and sent back to the urologist for implantation. The considerable cost involved for patients when utilizing this product when taking into consideration that there is already an available treatment in the form of native oral mucosa is also a point to debate. This has been highlighted recently in an issue of the journal European Urology(Osman & Chapple, 2016). Barbagli mentioned in his recent review the problem with commercial up scaling of the production in a safe and regulated framework for clinical use. Further, he questioned the availability of this technology in a large scale in all parts of the world(Barbagli & Lazzeri, 2015). This tissue engineered product is currently only available in Germany.

Acellular grafts have shown to be able to regenerate efficiently for short urethral defects as an on-lay. The requirement of a healthy urethral bed appears to be an important criterion in these situations. The initial clinical trials with cell-based technology were not so promising, but with the improvement of *ex-vivo* culturing methods over the years, the last clinical trial in 2011 had shown encouraging results. The revolution in the field has begun with this new cell-based tissue engineered product on the market. The widespread utilization of such a method, however, is still uncertain. Progress and innovations in the development and characterization of natural and synthetic biomaterials for the use as urethral grafts have been remarkable (Versteegden et al., 2017). The possible incorporation of bioactive molecules could improve the potential of these grafts for clinical applications. However, a cheap, effective, "off-the-shelf" acellular urethral graft would still have the most widespread utilization in clinical applications. With all this progress, the urologist of the future could potentially benefit by having both acellular matrices with or without bioactive molecules and with personalized medicine have cell-

seeded matrices readily available in his surgical armament, thereby providing patients with the best possible outcome.

CHAPTER 3: THE INVESTIGATION OF A TUBULAR COLLAGEN -BASED GRAFT WHICH CAN BE SUTURED AND USED TO REGENERATE A 2 CM URETHRAL DEFECT WITHOUT THE NEED OF *EX-VIVO* CULTURED CELLS AND GROWTH FACTORS.

3.1 Introduction

The urethra is a tubular structure that evacuates urine from the bladder to the external environment. Both congenital and acquired diseases can affect this organ. 1 in 250 live male births have the risk of being born with an abnormal position of the urethral meatus on the ventral midline; a disease called hypospadias. Trauma, infections, and iatrogenic injuries to the urethra can cause urethral stricture. Both these pathologies can only be treated through surgery. Current therapies require the incorporation of autologous tissue, such as skin or buccal mucosa harvested from other sites in the body. This can results in hair growth, fistula, stricture and fibrotic scar formation. The need for a graft in such surgeries has generated a lot of interest from several research groups. The current consensus is that the incorporation of cells or growth factors into a graft is required to achieve the successful regeneration of a tubular urethral defect. Both these methods have proven to be successful in *in-vivo* research models. However, they have not been translated into clinical practice due to regulatory issues, the complexities involved and high cost required to fabricate such grafts.

Collagen is the most abundant protein in the human extracellular matrix. It has been utilized in numerous medical devices. Collagen alone is not robust enough for clinical use without any modification such as utilizing cross linking or in combination with a mechanically stronger material. These hybrid collagen materials may be surgeon friendly, however they are not ideal for remodeling and degradation in the body; and often results in fibrosis. Therefore, the objective is to utilize untreated collagen as the foundation biomaterial of the graft. Without the addition of other biomaterials, the collagens

architecture is modified to enhance the mechanical properties of the graft. This is to promote cell migration and adherence to the graft that can then be beneficial for urethral regeneration without the need to incorporate cells and/or growth factors. For this reason, we have developed a tubular acellular collagen graft utilizing rat-tail collagen. This tubular collagen graft was implanted in the rabbit animal model, following complete excision of a 2 cm long segment of the native urethra of the rabbit. The animals were evaluated at 1, 3, 6, and 9 months post- surgery using contrast cystography. The urethra was harvested at each time point to be analyzed by histology and immunohistochemistry.

3.2 Literature Review

There are two approaches in tissue engineering; one is to utilize an acellular graft to replace the defect and allow cell infiltration to occur and the other involves the seeding of the graft with the specific cells of the area of interest prior to implantation. Cellular grafts however require longer fabrication period and is generally associated with a biopsy that makes it far less attractive than acellular grafts. The rabbit model is the most common animal model used in the *in-vivo* analysis for urethral regeneration. Acellular grafts have shown good regenerative properties when applied as a patch in this model. However, it seems that if the defect is too long the replaced portion of the urethra becomes atrophic with disordered muscle bundles appearing in the urethral submucosa and ultimately urethral stricture development(Atala, 2004). Dorin et al showed that defects longer than 1 cm in length are critical, as they are too large to allow spontaneous regeneration through cellular ingrowth from the anastomotic edges(Dorin et al., 2008).

Cell seeded grafts for urethral surgery are difficult to fabricate as they require *ex-vivo* cultured cells. The total cost of a cell seeded graft can be up to six times greater than that of cell free matrix making translation of such technology limited(Mangera & Chapple, 2012). In conclusion, a tubular graft to replace segment of the urethra for both hypospadias and urethral stricture surgery that is acellular, cost effective, efficient and "off-the-shelf" graft is far from achievable.

3.3 Materials and Methods

3.3.1 Double layered collagen tube fabrication (dCGT)

Based on a previously described method(Micol et al., 2012a) relating to the preparation of a single- layered rat-tail collagen gel tube (sCGT), a double-layered collagen gel tube (dCGT) was produced under sterile conditions (Fig. 3.1). 6.4 mL of sterile rat-tail type I collagen solution (2.05 mg/ mL in 0.6% acetic-acid, First Link Ltd., West Midlands, UK) was added to 800 µL of 10x MEM, neutralized with 1 M NaOH (Merck, Darmstadt, D), and 800 µL of Alpha MEM was immediately added. This was transferred into a designed steel tubular mold with the following dimensions: 7 cm long and 1.2 cm in outer tube diameter in which a glass mandrel of 3 mm in diameter (Verreries de Carouge, Carouge, CH) was placed in the center to create the lumen of the graft. Gelation was completed by 15 min at room temperature. The sCGT was kept on the glass mandrel. This was followed by rapid removal of excess liquid which was achieved by rolling the tube on a nylon mesh positioned on five layers of double-layer tissue paper (Weita, Arlesheim, CH). To fabricate the dCGT, the sCGT was placed back into the mold and the same procedure was repeated. The dCGT was separated from the glass mandrel and kept in phosphate buffered saline (PBS pH: 7.2) supplemented with 1% Penicillin/Streptomycin (Gibco, Invitrogen, CH) and 2.5 mg/mL Fungizone (Gibco) in a sterile culture tube (VWR International, LLC, Radnor, PA 19087, USA). This tube was placed in a sterile Falcon® tube for transportation and was kept at 4ºC. The final collagen concentration of the dCGT was determined, by calculating from the known volumes and concentration of collagen that was poured into the mold to retrieve the total amount of collagen for each compressed layer (11.2 mg and 9.7 mg, total: 20.9 mg). The total volume of both compressed collagen layers was calculated from measuring with a caliper the average thickness of the double-layered tube and the total length (average volume: 1.22 mL).

To finally obtain the average final collagen concentration of double compressed collagen, tube the total amount of collagen was divided with the volume of double-layered tube (20.9 mg/1.22 mL = 17.1 mg/mL).

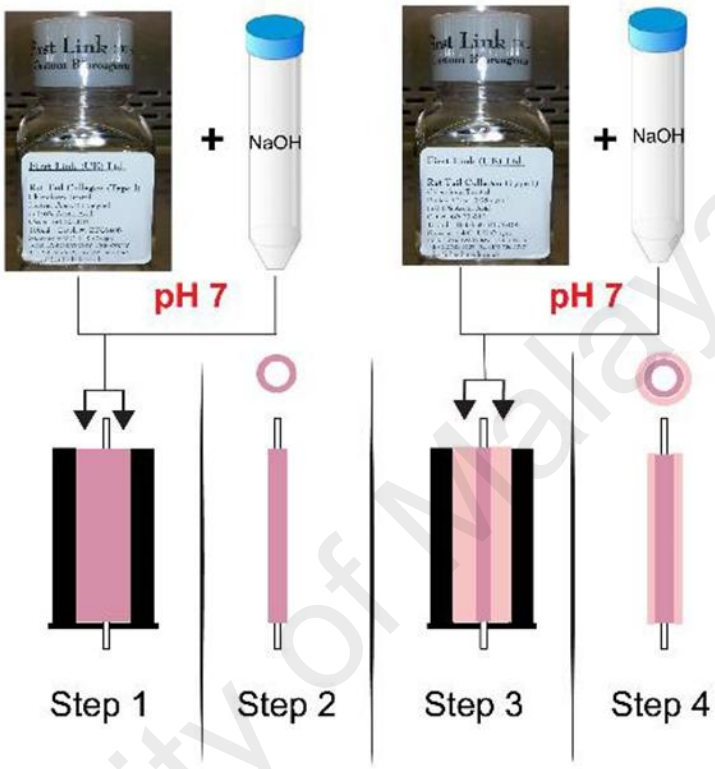

Figure 3.1: Schematic diagram of dCGT tube production. In step 1, liquid rat-tail collagen is neutralized by the addition of NaOH and poured into a mold with a glass rod to shape the molded structure into a hollow tube. The liquid neutralized collagen is allowed to gel at room temperature. In step 2, the gel is removed from the mold and compressed by mechanically rolling the tube on a blotting paper. In step 3, the first compressed layer is placed back in to the same mold as in step 1. Once again, the liquid collagen is neutralized and poured into mold. The second gel is allowed to form into a gel state, before going to step 4, which is once again the mechanical compression resulting in the final double-layered collagen tube.

3.3.2 Scanning electron microscopy of dGCT

To determine the microstructure of the dCGT, scanning electron microscopy (SEM) was performed. 1% tannic acid and 1.25% glutaraldehyde were utilized to fix the samples. This was then washed with 0.1 M cacodylate, and dehydrated in increasing ethanol concentrations prior to critical point drying (CPD). The samples were then coated with gold/palladium and imaged at a voltage of 10 kV using a scanning electron microscope (SEM, XLF30, Philips). 15 random selected pore diameters were measured using Fiji imaging program (ImageJ) in 3 different image locations to determine porosity or the range in pore diameters,

3.3.3 Mechanical properties of sCGT and dGCT

Evaluated tubes had the following dimensions: sCGT had a length of 1 cm, an inner lumen of 3 mm and a wall thickness of 1.3+/-0.2 mm whilst dGCT had a length of 1 cm, an inner lumen of 3 mm and a wall thickness of 1+/-0.1 mm. By utilizing an electronic manometer (Extech instruments HD750) the burst pressure values of the tubes (N=4 in each group) were measured. Pressure was generated in sCGT and dCGT using a syringe pump (flow rate = 360 mL/min) and the pressure changes over time were directly registered in Excel tables with one data point per second. The system was first purged of air bubbles and then filled with a mixture of water and methylene blue (1:1) for better visualization of the leak after bursting. The burst time point was determined by the sudden drop of pressure. A TA.XT plus Texture analyzer (Texture technologies) with a 50 kg load cell and with a sensitivity of 1–3 mN was used to evaluate dCGT' elastic modulus (Young's modulus) and ultimate tensile strength (UTS). A constant strain rate of 1 mm/min was used in all experiments (N = 4). The curves were directly recorded in the program. The Young's modulus (E), which measures the stiffness of the tube, was obtained from the slope of the linear region just after the initial toe region of the stress-strain curve by means of Hook's law (Stress = E _ Strain). UTS was determined from the

maximum tensile stress recorded in the curve. The water loss of the collagen gel after double compression steps was calculated by taking the weight of non-compressed and of compressed gels with a balance (Mettler Toledo) that has a sensitivity of 0.1 mg. The percentage of water loss was calculated as follow: % of water loss = [(weight before compression - weight after compression)/weight before compression]. For measuring the first layers water loss after the second compression step, the second layer was carefully removed and a new recording of the weight of the 1st layer was done.

3.3.4 Surgical testing of dGCT

Surgical testing was done by four different surgeons. Two dCGT grafts were sutured and anastomosed together using Vicryl 5.0 sutures. This was done to test the feasibility of applying suture in an *ex-vivo* condition prior to the animal implantations. After suturing, the tubes were filled with Methylene blue to test if any leakage through the suture was present. This methylene blue leakage test was done without clamping of the distal part of the tube.

3.3.5 *In-vivo* evaluation in a rabbit model of the dGCT

In-vivo experiments were performed in Lausanne and Kuala Lumpur on 20 New Zealand white male rabbits (2.5–3.5 kg; Charles River Laboratories France, and Harlan and Bred, Singapore). The animal experiment was approved by the Animal Ethics Committee of Vaud, Switzerland (Ethical approval number VD2740) and by the Faculty of Medicine of the University of Malaya, Kuala Lumpur (Ethical approval number 2013-09/17/SUR/R/TCR).. Premedication was done utilizing 1 mg/kg Xylasine (Provet Ag CH-3421 Lyssach) and 10 mg/kg Ketamine (Streuli Pharma CH8730 Uznach) which was administered by intramuscular (I.M). A single-dose of prophylactic antibiotics was given Cefazolin 10 mg/kg (Labatec Pharma S.A. Meyrin) by subcutaneous injection (S.C.). General anesthesia was maintained throughout the surgery with 2% Isofluorane. Surgical

disinfection was done with Betadine (Mundipharma). For intra –operative analgesia, Carprofen (Alloga CH-3400 Burgdorf) 4 mg/kg was given by S.C injection after 10 min of surgery and Ketamine was repeated after 45 min. Acellular urethral grafts were implanted using the following surgical method. Prolene-4.0 anchor suture was placed in the glans. A 6F catheter was inserted into the bladder. A 3-cm skin incision was performed just proximal to the glans. Dissection was done until the urethra within the corpus spongiosum was isolated (Fig. 3.2A).

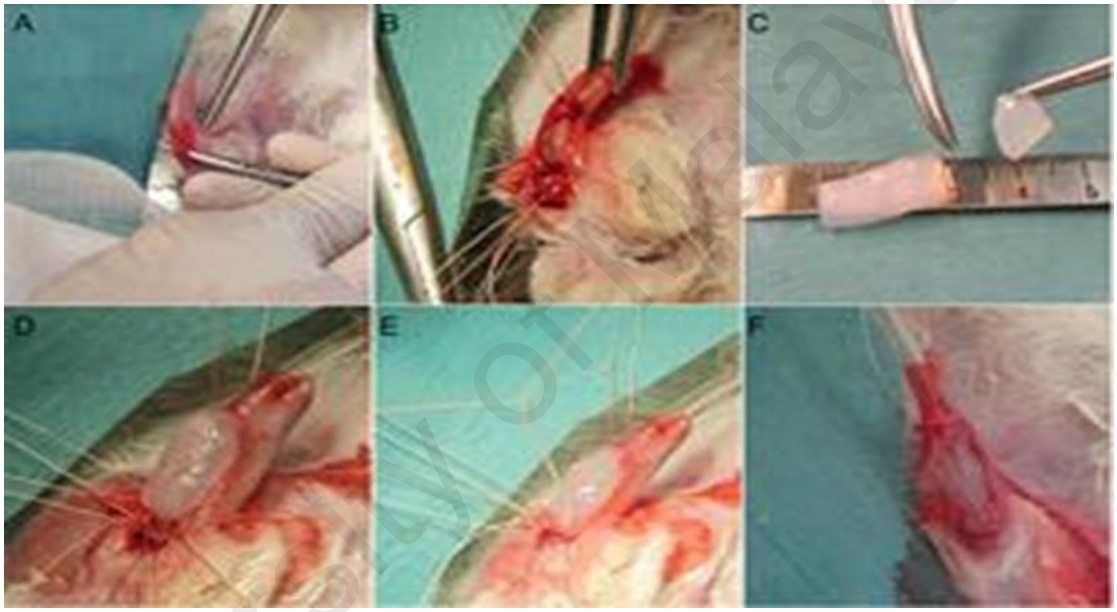

Figure 3.2: Surgical procedure for the implantation of dCGT. (A and B) The urethra was isolated and a 2 cm-long segment was excised creating the artificial urethra defect. (C) A 2 cm-long dCGT graft was prepared for implantation. (D) With the help of a catheter, the tubular graft was positioned in the urethral defect. (E and F) The graft was anastomosed with sutures to the native urethra and the catheter was removed at the end of the procedure.

5.0-Vicryl stay sutures were placed as stay sutures in the proximal and distal urethra. The middle part of the urethra along with the corpus spongiosum was excised to create a 2 cm long defect (Fig. 3.2B), at 0.5 cm proximally from the base of the glans. A 2 cm-long dCGT graft was then loaded on the catheter (Fig. 3.2 C and D) Anastomoses was performed to the native urethra with interrupted sutures (Vicryl-6.0) (Fig. 3.2E). The anastomosis was further reinforced with the application of 0.1 mL of fibrin glue (Tisseel,

Baxter, Volketswil, CH) (Fig. 3.2F). Finally, the skin was sutured with Vicryl-5.0 interrupted sutures. At the end of the surgery the catheter was removed and a leak test was performed. Post –operative analgesia with Carprofen 4 mg/kg/day was continued for 5 days.

3.3.6 Follow-up at 1, 3, 6 and 9 months post-surgery

With the animals under general anesthesia a macroscopic evaluation and 2 voiding cysto-urethrographies (Visipaque 270 mg/mL) were performed at the time of euthanasia for all the animals in the 1, 3, 6 and 9 months group. All images were collected using a Philips BV Pulsera. The diameter of the urethra was measured utilizing a scale. Knowing that the graft was sutured at 0.5 cm from the base of the glans and it measured 2 cm in length, the graft's position could be determined on the radioscopic image. It was then possible to estimate the presence of a stricture and their location. As it is a dynamic examination, a stricture was defined as a 50% reduction of the diameter of the urethra at the same location during two repeated examinations. Euthanasia was performed using a lethal intra-venous pentobarbital (Esconarkon ad.us VET Streuli) injection at 1, 3, 6, and 9 months post-surgery respectively. The entire penis was harvested and fixed in 4% Formalin (PFA), embedded into paraffin, and 8µm sections were prepared for histology and immunohistochemistry. Antibodies used for immunohistochemistry are summarized below:

Table 3.1: List of antibodies used for immunohistochemistry dCGTs

Primary Antibodies	**Provider**	**Dilution**
Mouse anti-alpha smooth muscle actin	Abcam, CH	1:150
Mouse anti-smooth muscle myosin heavy chain 11	Abcam, CH	1:150
Mouse anti-	Abcam, CH	1:500
Goat anti-uroplakin2	Labforce, CH	1:150
Secondary Antibodies	**Provider**	**Dilution**
Donkey anti mouse-Alexa647	Abcam, CH	1:500
Donkey anti mouse-Alexa647	Abcam, CH	1:500

Lumen shape, urothelial, smooth muscle and connective tissue regeneration, as well as possible inflammatory responses and collagen degradation were evaluated on Hematoxylin & Eosin (H&E) and Masson's Trichrome stained slides. Images were taken using a Leica DM5500 microscope (Leica, D) and a LSM 700 confocal laser-scanning microscope (Zeiss, D). Obtained images from immunohistochemistry were processed using the Fiji imaging program (ImageJ) for quantification of muscle specific proteins. Smooth Muscle Actin (SMA) and Myosin Heavy Chain (MyoHC) positive areas were calculated as a percentage from four different selected regions within the grafted tissue using Fiji software.

3.3.7 Statistical analysis

A two-tailed unpaired Student's t-test was used to analyze if a significant difference between the sCGT and the dCGT was present for burst pressure, ultimate tensile strength and Young's modulus. Also, a two-tailed unpaired Student's t-test was used to analyze if a significant difference in the protein expression at different time points was present in immunohistochemistry. A p-value of less than 0.05 was considered significant. Error bars represent the standard deviation (SD) of 4 independent samples (n = 4).

3.4 Results

3.4.1 Structure and mechanical properties of the sCGT and dCGT

The microstructure and porosity of dCGTs (collagen concentration 17.1 ± 4.9 mg/mL) were examined using SEM. The uneven manual compression created varying wall thickness, which is the reason for the high standard deviation of the collagen concentration seen above. Differences in wall thickness were observed at different positions of the graft (Fig. 3.3A). Furthermore, two distinct layers were clearly seen in the dCGT due to the double-layered molding technique. The porosity difference between the inner and outer layer was not significant with a range of pores measuring from 0.3 µm to 3 µm (Fig. 3.3B and C). Both sCGT and dCGT scaffolds were compared in terms of burst pressure values, ultimate tensile strength (UTS) and Young's modulus. dCGT showed a significantly higher burst pressure value (77.4 ± 2.4 cm H2O) compared to sCGT scaffolds (42.4 ± 10.2 cm H2O) (Fig. 3D). The UTS of sCGT was 3.4 ±0.8kPa with an average load measurement of 0.06 N and the Young's modulus was 7.7 ±3.0 kPa (Fig. 3E, and F). The UTS of dCGT was 5.9 ±1.5 kPa with an average load measurement of 0.14 N and the Young's modulus was 28.4 ±5.3 kPa. There was a significant difference in UTS and Young's Modulus, between the double and single layered tubes (N= 4). The average water loss due to compression of the sCGT was approximately 73% (w/w) while it was approximately 67% (w/w) for the dCGT. However, the inner layer of the dCGT had lost 80% (w/w) of water after the second compression step.

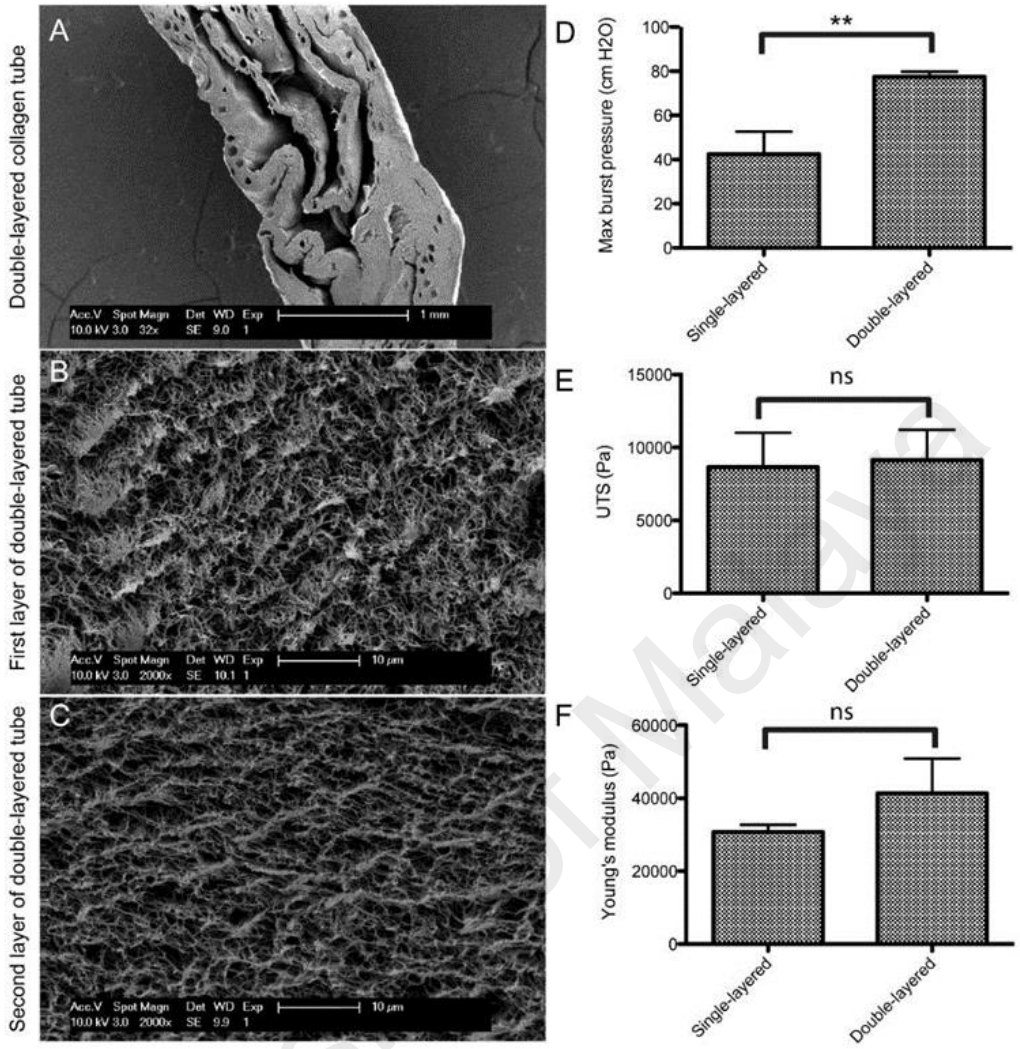

Figure 3.3: Surface structure and mechanical properties of dCGT (A) SEM image of a double-layered collagen tube. (B and C) SEM images of the cross-section of the first layer and the second layer of a double-layered collagen tube. (D) Burst pressure of single- and double-layered collagen tubes. (E) Ultimate tensile strengths calculated from the maximum stress in the stress-strain curves of pulled single and double-layered collagen tubes. (F) Young's Modulus calculated from the slopes of initial linear region of the stress-strain curves of pulled single and double- layered collagen tubes. Error bars represent the standard deviation of four independent samples.

3.4.2 dCGT tube evaluation by surgeons

Three other surgeons Prof Peter Frey, Prof C. R. Thambidorai, Dr.Kalitha Pinnagoda and myself could suture and anastomose two dCGT together. No visual leakage of methylene blue was seen through the sutures when a leakage test of the anastomosed tubes with open distal ends was performed.

3.4.3 *In-vivo* implantation outcome of dCGT

20 rabbits survived the surgical implantation and could void within 48 h after surgery. Voiding cysto-urethrography done at the time of euthanasia demonstrated no complications in 60% of the rabbits (Fig.3.4 A, B, and E), distal fistulae in 20% of the rabbits (Fig. 3.4 A, C, and F), and distal stricture associated with secondary fistula in 20% of the rabbits (Fig. 3.4 A, D and G). No proximal stricture, potentially lethal in the rabbit model, was observed in the study.

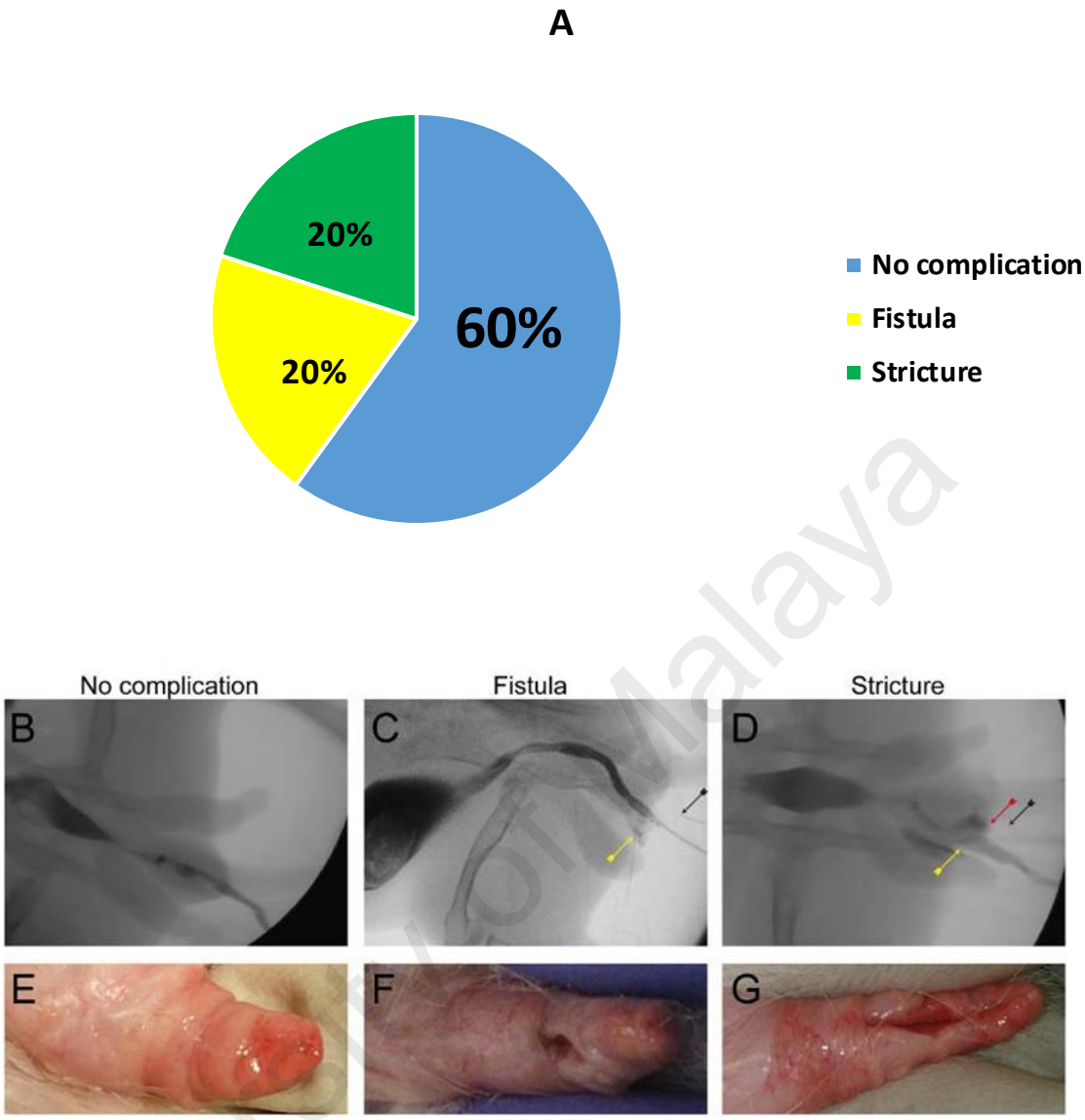

Figure 3.4: Surgical outcome of dCGT implanted in 20 male rabbits. (A) Histogram of the frequency of observed complications. Voiding cysto-urethrographies (B, C, D) and macroscopic images (E, F, G) showing (B and E) a rabbit with no complications, (C and F) a rabbit with a fistula, and (D and G) a rabbit with a clear fistula after stricture. Note: Black arrows indicate tip of penis, yellow arrows indicate fistula location, and red arrows indicate stricture point.

3.4.4 Histology

At 1, 3, 6, and 9 months post-surgery, longitudinal HE-stained sections of the grafts showed gradual cell infiltration over time (Fig. 3.5). At 1 month, spots with single or multi-layered urothelium were observed in the grafted area and vascular structures were already present at 1 month (Fig. 3.5A–D). A mild inflammatory response was only present at the first month. At 3, 6, and 9 months, the urothelium showed stratification comparable to the native urethra (Fig. 3.5B–D). At 1 month no smooth muscle were seen (Fig. 3.5A) and at 3 months they were sparsely present (Fig. 3.5B). At 6 months muscle bundle formation was observed for the first time (Fig. 3.5C), which was even more extensively developed after 9 months (Fig. 3.5D). Transverse-tissue sections were analyzed at the same time points and confirmed the findings seen on longitudinal tissue-sections. (Fig.3.6).

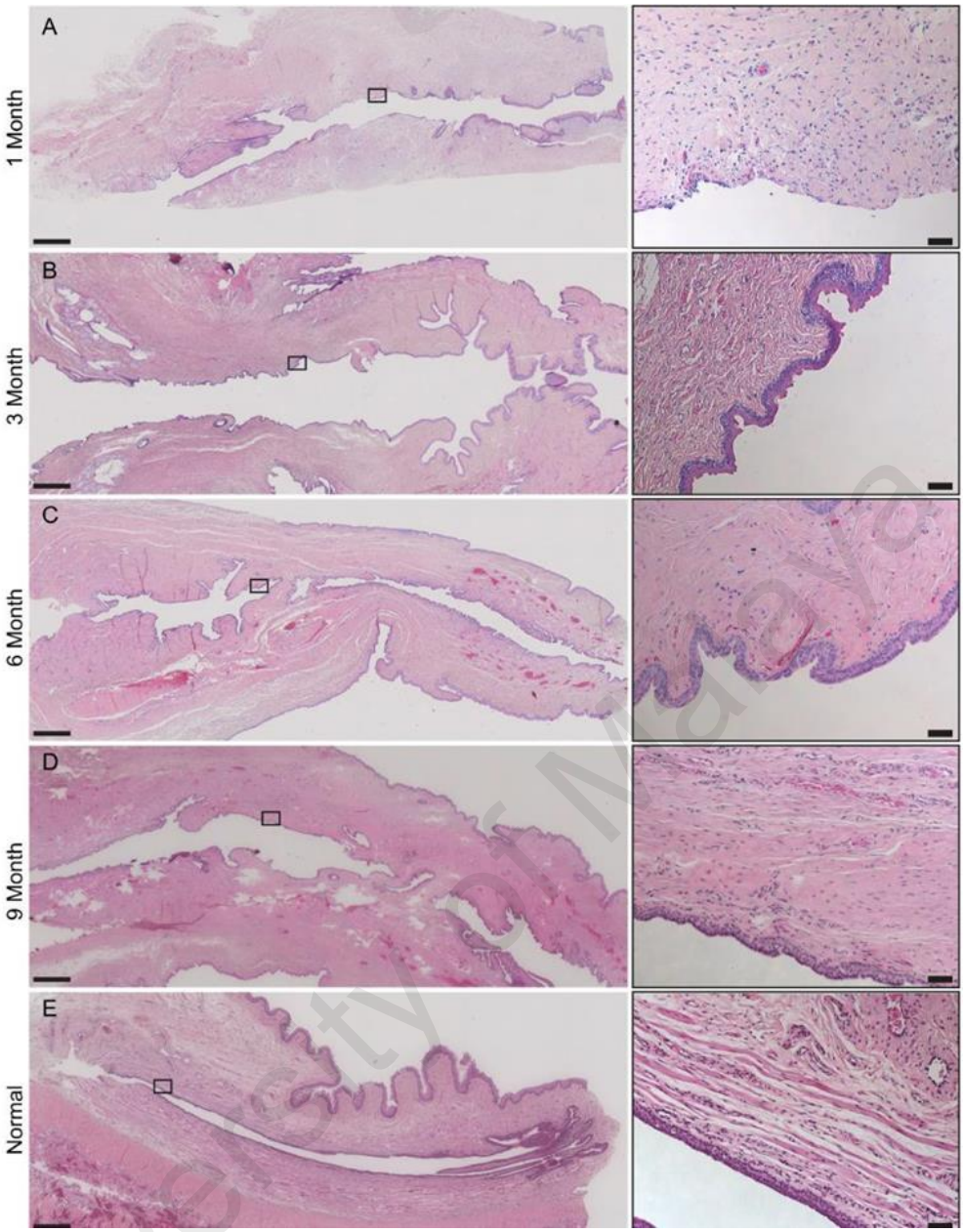

Fig 3.5: Longitudinal H&E sections of dCGT implanted in rabbits. dCGT were implanted into a critical size urethra defect in a rabbit model. Animals were sacrificed 1, 3, 6, and 9 months post-surgery. (A) 1 month, (B) 3 months, (C) 6 months, and (D) 9 months after surgery. (E) A native/normal rabbit urethra. Note: Scale bars represent 1mm (left images) and 50 µm (right images)

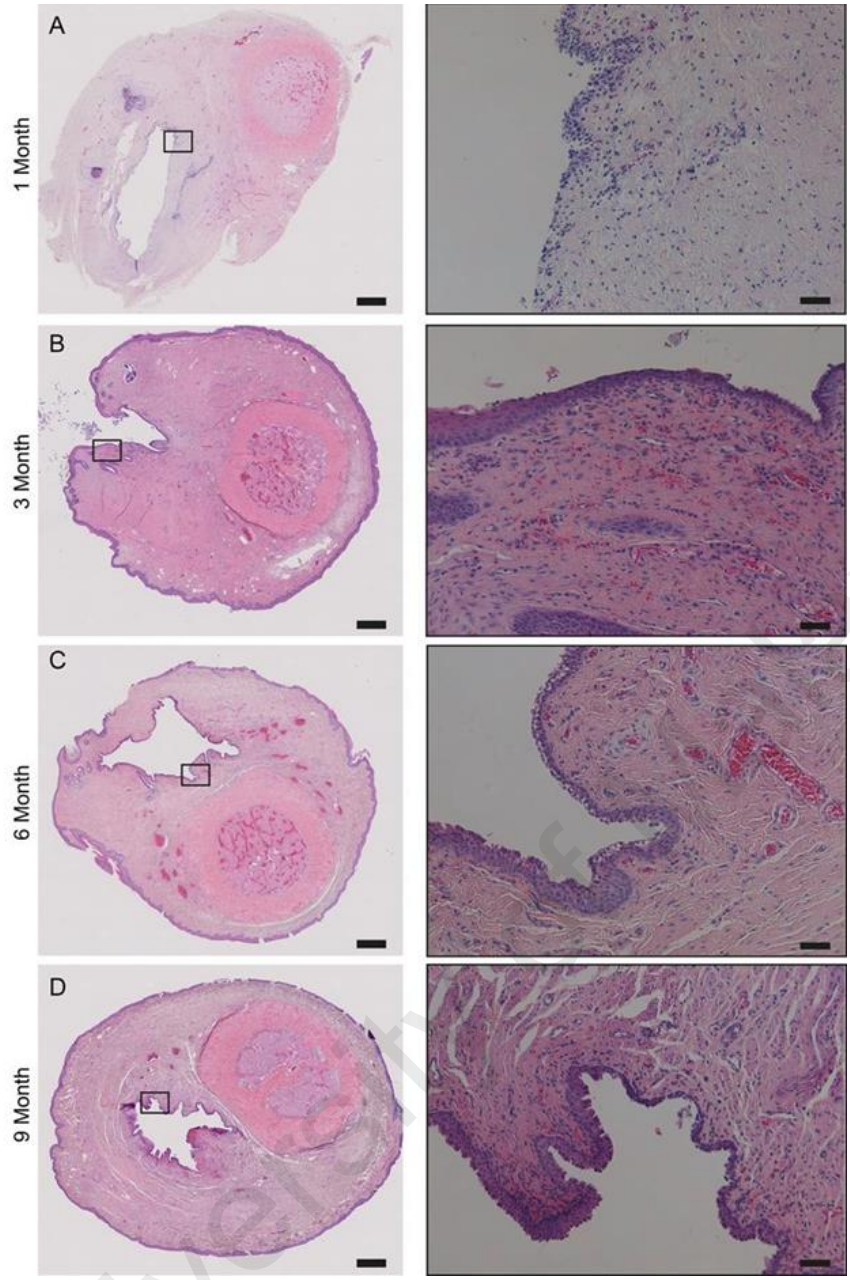

Fig 3.6: H&E-stained cross-sections of the graft site. dCGT were implanted into critical size urethra defects in rabbits for (A) 1 month, (B) 3 months, (C) 6 months, and (D) 9 months. Note: Scale bars represent 0.75mm (left images) and 50 μm (right images).

A time dependent progressive degradation and remodeling of the collagen scaffold could be observed in the Masson's Trichrome stained sections (Fig. 3.7). At one month, collagen was still seen in the grafted area and a high number of native cells were already present. However, they were not organized at that point and a mild inflammation was observed with the increased in ingrowth of epithelial cell types. From 6 to 9 months, the cells were progressively more organized and the tissue structure was similar to a native rabbit urethra. In Masson's Trichrome sections, a time-dependent gradual increase of muscle fibers was seen increasing in red from 1 to 9 months.

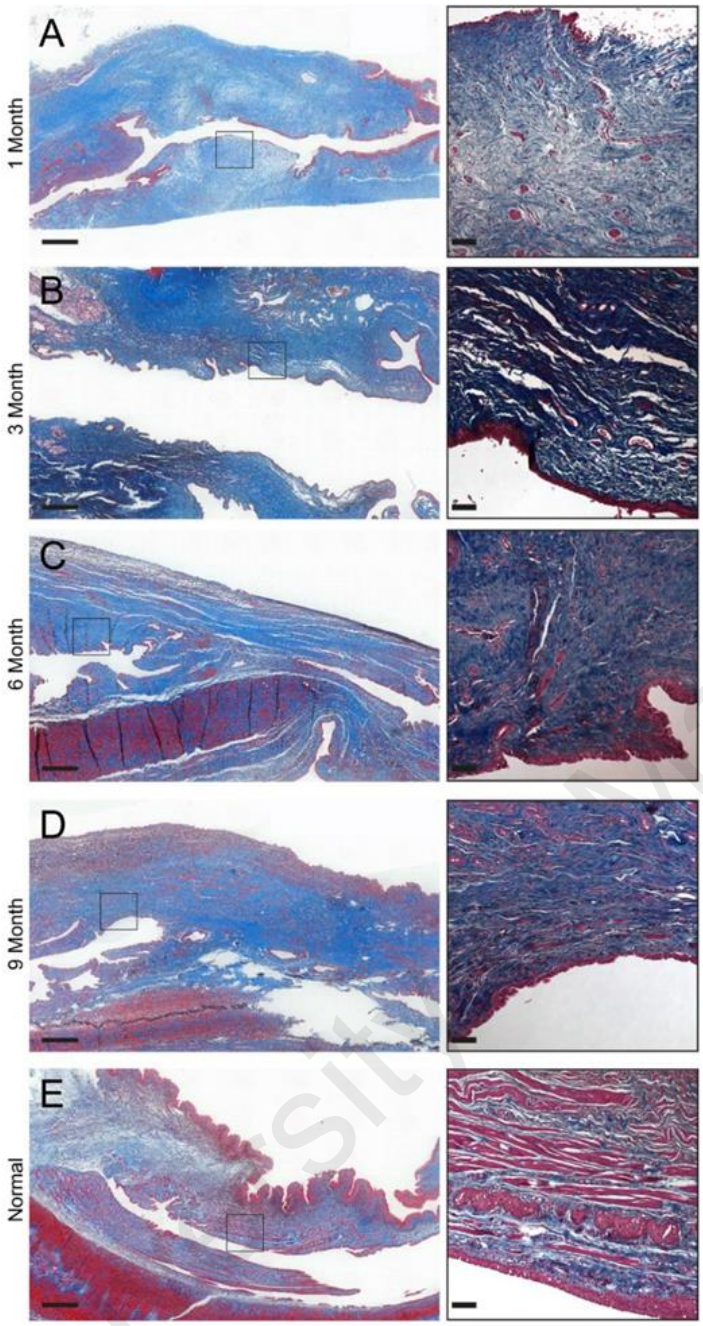

Figure 3.7: Longitudinal Masson's Trichrome sections of dCGT implanted in rabbits. Blue staining represents collagen and red staining muscle fibers and keratin. (A) 1 month, (B) 3 months, (C) 6 months, and (D) 9 months after surgery. (E) Normal/Native rabbit urethra. Note: Scale bars represent 1mm (left images) and 50 µm (right images).

3.4.5 Immunohistochemistry

The presence of smooth muscle cells (SMC) was confirmed by immunohistochemistry showing smooth muscle alpha actin (SMA) expressing cells in the grafted area as early as the first month and progressively increasing over the observation period (Fig. 3.8A–E). To demonstrate the progressive muscle bundle formation, a more specific smooth muscle cell bundle protein marker, myosin heavy chain (MyoHC), was utilized. As seen in Fig. 3.8F–J, smooth muscle cell bundles were not present in the grafted area at 1 month, but started appearing at 3 months, were fully formed at 6 months and well organized at 9 months. The native urethra had a higher SMC density when compared with the 9 months group. This confirms the results obtained from the Masson's Trichrome staining. Furthermore, quantification of SMA and MyoHC showed that after 9 months the smooth muscle cell expression was not as dense as seen in the native rabbit urethra (Fig. 3.8P and Q). However, there was a significant difference in SMC expression between the 1 and 9 months groups; thus validating a time-dependent ongoing regeneration process. At 3 months, a stratified urothelium in the grafted area was demonstrated by Cytokeratin 5/8 staining (Fig. 3.8K–O), a general urothelial cell protein marker. Urothelial cell differentiation was also demonstrated by the expression of the urine barrier protein, Uroplakin-2 (Fig. 3.8K–O).

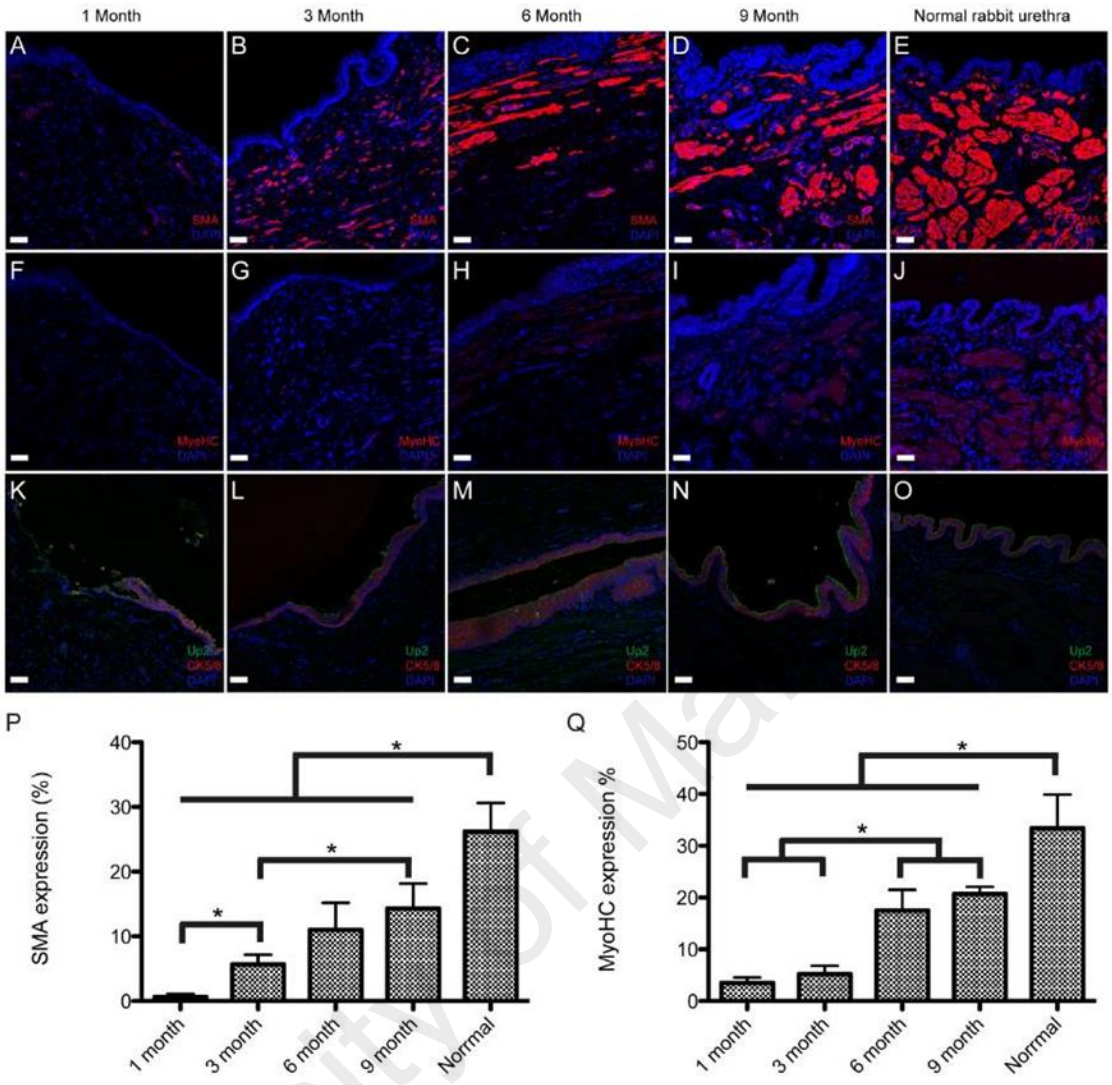

Fig 3.8: Immunohistochemistry of the graft site. dCGT were implanted into a critical size urethra defect in a rabbit model. Animals were sacrificed at 1, 3, 6, and 9 months post-surgery. Functional tissue regeneration was determined by immunohistochemistry using anti-smooth muscle alpha actin (SMA) (A-E), anti-myosin heavy chain (MyoHC) antibodies (F-J), and combined uroplakin-2 with Cytokeratin-5/8 (Up2, CK5/8) antibodies (K-O). As a control, a normal/native rabbit urethra is shown (E, J and O). (P and Q) Quantification of SMA and MyoHC expression in the graft area based on immune-stained sections images. Four different areas within the grafted area were analyzed. The quantifications were compared to non-operated/ native rabbit urethras as well as the different sacrifice time points. Note: Stars (*) indicate at least a $p < 0$ for n=4 areas. Scale bars indicate 50 µm.

3.5 Discussion

The objective of this study was to investigate if a tubular acellular collagen based graft could be sutured and used to regenerate a 2cm urethral defect without the need of *ex-vivo* cultured cells and growth factors. An existing platform of collagen fabrication was previously described by the group of Prof Peter Frey where a single layered collagen tube was developed and implanted into a similar animal model (Micol et al., 2012). The current study improved on the previous developed tubular graft by creating a double-layered collagen tube, which had better mechanical properties in comparison to its predecessor. These double-layered collagen tubes could be sutured to the native rabbit urethra, something that was not possible with the single layered collagen tubes.

The study, which spanned a total duration of 9 months, showed a progressive, time dependent regeneration of the implanted acellular collagen graft. At 9 months, histology and immunohistochemistry showed a regenerated urethra that was almost similar compared to the extracellular matrix and cell architecture of a native rabbit urethra. Even so, the regeneration was not complete after nine months, due to the progressive regeneration taking place over time. One could argue that if the study group was kept for longer periods potentially, the remodeling would be completed. This study proves that an acellular tubular graft can regenerate a tubular urethral defect of 2 cm without the requirements of *ex-vivo* cultured cells contrary to what Dorin et al concluded from their study(Dorin et al., 2008). Other research groups have also demonstrated that the limits of acellular tubular graft regeneration can go beyond the aforementioned 0.5cm,(Ribeiro-Filho & Sievert, 2015).

The histological data shows a progressive remodeling of the collagen graft. The graft was present in the first month, but completely reabsorbed by the native tissue after three months as was seen in the Masson Trichrome sections. The collagen remodeling and the

presence of a more organized urothelial layer at 3 months probably favored the well-organized ingrowth of smooth muscle cells. This is demonstrated by the increasing density of the smooth muscle cell specific markers from the 3rd month and onwards. This ingrowth of smooth muscle cells at 3 months in coordination with the development of a complete urothelial layer could be due to the fact that the urothelium, a multi-layered tissue that functions primarily as a first line barrier against pathological bacteria and urine, exhibits important signaling properties that potentially attract the ingrowth of smooth muscle cells(Birder & de Groat, 2007; Khandelwal, Abraham, & Apodaca, 2009). The ingrowth of urothelial cells either from the edges of the native urethra or from progenitor cells in the urine showed that the need to pre-seed *ex-vivo* cultured urothelial cells is not a necessity for 2 cm long urethral defects. Parnigotto et al seeded their scaffolds with urothelial cells and implanted them into the rabbit to replace a 1 cm tubular defect. Nevertheless, they concluded a similar observation as us and stated in their paper that the coverage of the matrix with urothelial cells did not seem to be mandatory prior to implantation. 10 days after the surgery in their study, the implanted area had already appeared completely covered by urothelium formed by epithelial cell migration from the edges of the graft(Parnigotto, Conconi, Gamba, & Midrio, 2000).

Our current results show a 40% rate of complications, higher in contrast to other groups who have utilized a cellular approach(Fu & Cao, 2012). The 40% complication rate seen in this study could have been avoided if a catheter has been placed post-operatively as it has been done in the clinical scenario. Such an undertaking was not done in this study taking into consideration the requirements of the animal ethical committee and the welfare of the animals. Our complications might have been caused by the composition of the rabbit's urine. The rabbit often produces milky or cloudy urine due to high levels of calcium present in many commercial feeding pellets(Loo & Diamond, 1985). The acellular collagen graft has a strong adsorption capacity. These salts could

easily be impregnated into the collagen network causing a distal urinary obstruction and the subsequent development of stricture or fistula as seen in the study. Similar complications have also been reported in clinical trials using acellular matrices for urethral reconstruction in patients with hypercalciuria and hyperuricosuria (Ribeiro-Filho & Sievert, 2015).

It should be cautioned that the pursue of improving the mechanical properties of a collagen scaffold either by adding synthetic materials or performing cross-linking to facilitate its handling should not be done at the cost of compromising its regenerative potential. The major advantage of using natural proteins without modifications is that they cause less inflammation and therefore are more favorable in terms of regeneration(Yang, Ritchie, & Everitt, 2017). When collagen is used without cross-linkers or synthetic polymer addition, a very mild inflammatory reaction is seen in the rabbits as demonstrated in this study. Even at one month, it was observed that the implanted collagen was already remodeled by the invading host cells as shown in the H&E and Masson Trichrome sections (Figure 3.5-3.7).

Porcine-based decellularized Small Intestine Submucosa (SIS) has been used as a biomaterial to develop grafts for urethral regeneration studies(Kropp et al., 1998). It is believed that these decellularized matrices have far better regenerative potential than pure collagen based matrices such as the dCGT fabricated in this study. This is due to the fact that they consist of structural and functional molecules secreted by the resident cells of the respective tissue and organ from which they are derived. However the clinical grade version of this biomaterial produced by industry has shown to have high amounts of porcine DNA residues(Zheng et al., 2005), which could be responsible for some of the cytotoxic effects observed on urothelial cells influencing their final regenerative outcome. Also these decellularized matrices vary in the extracellular matrix constituents and

composition from batch to batch depending on the tissue source(Badylak, Freytes, & Gilbert, 2015). Certain research groups have proposed a better outcome if one utilizes an organ–specific allograft(K D Sievert & Tanagho, 2000). Though this approach has been translated into clinical practice in certain centers in the world, one must be aware of the legal and ethical requirements of human organ donation, which might be a drawback for widespread utilization of such techniques globally(Lim et al., 2013).

A double layer molding technique was used for the manufacturing of the dCGT graft, this is compatible to the production of different sized tubes. This can be done without the addition of any synthetic mesh or sutures. However, the manual compression technique used here has its limitations since the uniformity of the compression cannot be controlled. The development of an automation procedure could easily address these issues in the future if mass production is required. On the mechanical property of the engineered graft there was a significant difference between the dCGT and the sCGT in terms of burst pressures, UTS and Young's modulus. This could be explained by the fact that the internal layer of the dCGT had more water removed than the single layer of the sCGT since the former undergoes two compression steps. It is known that the mechanical property of collagen are linked to the water content within the compressed collagen gels(Abou Neel, Cheema, Knowles, Brown, & Nazhat, 2006; R. A. Brown, Wiseman, Chuo, Cheema, & Nazhat, 2005). The UTS and Young's modulus values are there for proportional to the amount of water removed from the collagen gels, since the collagen fiber density increases with the removal of water. The collagen fiber density of the dCGT was calculated to be 3.6% (w/w) using a described formula(Ghezzi, Marelli, Muja, & Nazhat, 2012). In the same publication, a linear trend between collagen fiber density and UTS was described. By extrapolating a linear line in their graph, a 3.6% (w/w) collagen fiber density would measure a UTS below 10 kPa. This validates the result obtained for the mechanical measurement of a UTS of around 5.9 kPa for the dCGT (Figure 3.3 E).

A graft that is utilized for clinical application needs to be robust enough to be easily handled by the surgeon and to be sutured securely at the intended site. In urethral surgeries, the applications of sutures for securing a watertight anastomosis is of paramount concern for the surgeons. Suture retention test was attempted for the dCGT tube utilizing the A TA.XT plus Texture analyzer (Texture technologies) with a 50 kg load cell and with a sensitivity of 1–3 mN but the value was too low to be recorded. However, the graft could still be sutured to the native urethral tissue in rabbits. Urethral grafts unlike vascular grafts also do not have standards or provisions as predetermined by agencies such as the American National Standards Institute / Association for the Advancement of Medical Instrumentation (ANSI/AAMI) as guidelines to be followed for such biomechanical evaluations (Cardiovascular implants-vascular prostheses. Association for the Advancement of Medical Instrumentation, ANSI/AAMI VP20-1994(Revision of ANSI/AAMI VP 20- 1986), Association for the Advancement of Medical Instrumentation, Arlington , VA,1994) For vascular applications, for example there is a consensus that a material needs to resist to approximately 1.85 N in a suture retention test to fit surgical requirements(Huynh et al., 1999). Clearly, the current scaffold could not be used for vascular surgeries but as demonstrated in the rabbit model it fits very well for urethral surgeries. The burst pressure testing of the tubes revealed values well above the maximal pressure present within the native human urethra(Müller, Ratia Garcia, Marti, & Leippold, 2008).

The strength of this study lies not only in the fact that the graft could regenerate a tubular urethral defect of 2 cm length without the incorporation of *ex-vivo* cultured cells but that this was achieved by four different clinicians and in two different centers across the globe. The future direction of the study will be in improving the regenerative properties of the scaffold with regards to urothelial cell and smooth muscle cell in growth to ensure a more consistent positive surgical outcome with fewer complications. The other

challenges to be considered is also to induce regeneration in even longer segments that are of clinical relevance and addressing the issue of surgical performance versus regenerative potential which will be further investigated in subsequent chapters.

3.6 Conclusion

This study demonstrated that a tubular acellular collagen based graft could be sutured and used to regenerate a 2cm urethral defect without the need of *ex-vivo* cultured cells and growth factors. The urothelial layer was the first cell layer to completely regenerate on the inner lumen of the graft by 3 months. Though the ingrowth of smooth muscle cells within the graft was seen as early as 3 months, it had not completed its regeneration as per native urethral tissue even by 9 months. The regeneration for the acellular tubular graft can be concluded to be time dependent. Though a 40% surgical complication was seen. The insertion of a postoperative catheter could have further reduced this rate. Without the requirement of prior biopsy, *ex-vivo* culturing of cells, and expensive growth factor delivery technology, an acellular graft as described in this study is therefore cost effective and practical for clinical translation.

CHAPTER 4: CELLULAR ENGINEERING OF A COLLAGEN GRAFT WITH INCREASED DENSITY FOR BETTER UROTHELIAL AND SMOOTH MUSCLE REGENERATION

4.1 Introduction

The urological system is made up of the urethra, bladder, ureter and kidney. Both congenital and acquired diseases affect these organs. Most often these diseases have to be treated by surgical intervention. In the kidney, the current gold standard for treatment of kidney failure is kidney transplantation which is associated with limited donor availability and long- term immunosuppression therapy(Sandovici, Deelman, Benigni, & Henning, 2010). However, for an organ such as the urethra, transplantation is not required and the current benchmark therapy utilizes autologous tissue harvested from the buccal mucosa of the patient. This is however associated with complications such as numbness or paresthesia at the oral cavity. Furthermore, harvesting of buccal mucosa is associated with prolong surgery requiring longer anesthesia and therefor higher operative cost. This need for a replacement tissue has driven the field of tissue engineering to develop innovative biomaterials as an alternative. The current available biomaterials have shown to be only effective if utilized along with *ex-vivo* cultured cells(Christopher Chapple, Osman, & MacNeil, 2013). This is associated with higher cost and has thus limited the wide spread utilization of such a platform. If the biomaterials' innate property can be modified to increase the ingrowth of host cells than the incorporation of *ex-vivo* cultured cells is not mandatory. One method attempted and is currently utilized in regenerative medicine is by utilizing naturally occurring biomaterials composed of extracellular matrix (ECM) that is the secreted byproduct of resident cells of each native tissue. This biomaterial undergoes a process called decellularization to remove its cellular components while still preserving its native ECM architecture. These biomaterials has been shown to have biological cues that are favorable for cell proliferation (Kuraitis, Giordano, Ruel, Musarò, & Suuronen, 2012).

Cell behavior is also known to be influenced by the microenvironment of the matrix. Mechanical properties such as stiffness therefor can influence cell differentiation (Engler, Sen, Sweeney, & Discher, 2006). The aim of this project part was to engineer a tubular collagen graft by changing its stiffness and allowing human smooth muscle cells to modify the ECM composition of the graft to enhance the tissue regeneration capacity *in-vivo*. Initially by using Collagen-Fibrin-Collagen sheets that had already been developed in the group for bladder tissue engineering applications a proof-of technology experiment was undertaken. These 3D sheets fabricated from rat-tail collagen were cultured with human smooth muscle cells eventually engineering a final more-dense, stiffer and a human collagen type I containing matrix. As an off-the shelf graft is easier to translate to the clinical setting, these "humanized" cellular sheet were then decellularized. Following the proof of concept, this fabrication and decellularization protocol was then implemented to engineer a denser and "humanized" tubular collagen grafts aimed for urethral replacement surgery. The decellularized tubular grafts had a final composition made up of human ECM deposited by human urinary tract smooth muscle cells. This new biomaterial was evaluated *in-vivo* in the rabbit urethral model for its efficacy to induce urethral regeneration.

4.2 Literature Review

The types of available biomaterials to be utilized to fabricate grafts can be broadly classified into naturally derived, cell-free tissue and synthetic polymer. Collagen is the most common naturally derived biomaterial. Collagen makes up 25% of the dry weight in mammals. It is made up of three α chains that are assembled together. Every α-chain is composed of more than a thousand amino acids based on the sequence -Gly-X-Y-. The presence of glycine is essential at every third amino acid position in order to allow for a tight packaging of the three α-chains in the tropocollagen molecule and the X and Y positions are mostly filled by proline and 4-hydroxyproline (Prockop & Kivirikko, 1995; van der Rest & Garrone, 1991). There are many types of collagen that have been identified. The most common collagen type utilized in tissue engineering applications is type 1(Charriere, Bejot, Schnitzler, Ville, & Hartmann, 1989). However, collagen is noted to have inherently weak mechanical properties. In the previous version of our tubular collagen grafts utilized for urethral regeneration in the rabbit model within the Frey group, the fabricated graft could not even be sutured (Micol et al., 2012b).

It has however been demonstrated that by increasing the density of a collagen scaffold we can increase its mechanical properties. At the same time, this denser collagen scaffolds have also shown good cell proliferation when seeded with fibroblast(Ghezzi et al., 2012).A biomaterials mechanical property and its effect on cell fate choice has been clearly demonstrated. Cells are not only responsive to the dynamic mechanical loading in the biomaterial but also sensitive to the stiffness of the microenvironment within. It has been demonstrated that the differentiation of mesenchymal stem cells to specific cell types can be greatly influenced by microenvironment stiffness(Engler et al., 2006).

In this study therefore in order to modify the density of the collagen biomaterial a method will be applied that has been described in the fabrication of vascular tissue engineered grafts. The method described the culturing of smooth muscle cells (SMCs) from cadaveric donor on to prefabricated rapidly degradable polyglycolic acid (PGA) tubular scaffolds(Dahl et al., 2011).

During the culture period, they noted that the SMCs secreted extracellular matrix proteins, predominantly collagen that modified the PGA tubular scaffolds(Niklason, 1999). The cell-modified graft underwent decellularization, leaving only the extracellular matrix, which had a similar dsDNA amounts as demonstrated by clinically acceptable decellularized scaffolds on the market(Derwin, Baker, Spragg, Leigh, & Iannotti, 2006). This cell-modified graft had demonstrated good integration at the anastomotic site along with infiltration of vascular smooth muscle cells when implanted in a large animal model. The benefit of this method compared to cell based therapy is that one biopsy can be used to fabricate multiple grafts and that biopsy does not have to be autologous. The waiting time for patients is reduced and the engineered graft is cheaper and can be stored for longer periods of time than cell-seeded grafts (Pascual et al., 2001). This vascular graft is currently undergoing a Phase 2 clinical trial in the United States.

The use of biomaterials derived from decellularized tissue is increasingly frequent in the field of regenerative medicine. There are already clinical products available in the market that is derived from a variety of allogenic and xenogenic sources. These biomaterials are said to possess properties that can influence cell mitogenesis and chemotaxis(Barkan, Green, & Chambers, 2010; Bornstein & Sage, 2002; Nagase, Visse, & Murphy, 2006; Nelson & Bissell, 2006; Taylor, 2006; Vorotnikova et al., 2010; Werner & Grose, 2003). Biological cues left behind by the cells help to direct cell differentiation(Allen et al., 2010; Cheng, Estes, Awad, & Guilak, 2009; Cortiella et al., 2010; Ross et al., 2009; Sellaro et al., 2010), and induce constructive host tissue remodeling responses(Parekh et al., 2009; Valentin, Turner, Gilbert, & Badylak, 2010). This is due to the microenvironment, three- dimensional ultrastructure and the composition inherent in the native tissue that has undergone decellularization. Therefore, the preparation of the tissue and the decellularization protocol employed is important to ensure that these properties are not loss. Aggressive removal of all cellular components is not ideal as residual cellular material left behind is said to further promote and signal tissue remodeling. It has been recommended that the final decellularized matrix fulfill the following criteria :(Nagata, Hanayama, & Kawane, 2010; Zheng et al., 2005)

1) <50 ng dsDNA per mg ECM dry weight

2) <200 bp DNA fragment length

3) Lack of visible nuclear material in tissue sections stained with 4',6-diamidino-2-phenylindole (DAPI) or H&E

This is to ensure that the unwanted cytocompatibility problems *in-vitro* and adverse host responses *in-vivo* are avoided.

In this chapter, collagen is utilized in its native form and its fiber property is to be modified by the implantation of smooth muscle cells followed by decellularization. The objective is to fabricate a "humanized "ECM graft which can improve the ingrowth of urothelial and smooth muscle cells for urethral tissue engineering applications.

4.3 Materials and Methods

4.3.1 Ethical human and animal research approvals

Ethical approval for working with human biopsies was given by the ethical board of the "Centre Hospitalier Universitaire Vaudois" (CHUV, Lausanne, CH). Furthermore, urinary tract biopsies were harvested in children following signed consent by the patients or their guardians. All animal procedures were approved by the "Office Vétérinaire Cantonal" (Vaud, CH) (Ethical approval number VD2740) and the Animal Ethics Committees Faculty of Medicine of the University of Malaya, Kuala Lumpur (Ethical approval number 2013-09/17/SUR/R/TCR).

4.3.2 Cell culture of human smooth muscle and urothelial cells

Excisional samples were harvested at open ureter or bladder surgery for correction of congenital malformations in children, performed by Prof Peter Frey. Tissue specimens were cut into small pieces and digested with Liberase Blendzymes I (Roche, Basel, Switzerland) at 37 ◦C for 1.5–2 h. The cell suspension was passed through a 70 µm cell strainer (BD Biosciences, Allschwil, Switzerland) prior to centrifugation (800 rpm, 4 ◦C, 5 min). The cell pellet was resuspended in α-MEM medium (Cambrex Bio Sciences, Verviers, Belgium) supplemented with 10% fetal bovine serum (FBS; Gibco, Invitrogen, Lucerne, Switzerland), 2 mM L-glutamine (Invitrogen) and 1% penicillin–streptomycin (Invitrogen). Urothelial cells (UCs) were isolated by positive selection with antibody-conjugated magnetic beads (Dynabeads, Invitrogen/ Dynal Biotech, Basel, Switzerland). Beads conjugated with anti-human epithelial antigen (clone Ber-EP4; Dakocytomation M0804, Baar, Switzerland) were mixed in the cell suspension at 4 ◦C for 15min to isolate UCs. Collected beads were resuspended in keratinocyte serum-free medium (KSFM; Invitrogen) supplemented with bovine pituitary extract (BPE), epidermal growth factor and 30 ng/ml cholera toxin, as previously described (Southgate et al., 1994). Beads were plated in a 25 cm2 Primaria T-Flask (BD Biosciences) containing 10 ml supplemented KSFM. Contaminating fibroblasts were removed using beads coated with fibroblast-specific antibodies (ASO2, mouse IgG1, CD90, Thy-1; Dianova, Hamburg, Germany). Negative isolation of smooth muscle cells (SMCs) was performed on the remaining supernatant after the positive selection of

UCs and fibroblasts. The supernatant was centrifuged (800 rpm, 4 ◦C, 5 min) and the cell pellet was resuspended in supplemented α-MEM medium and plated in a 25 cm2 T-Flask. The cells were grown until confluent and a cell bank was generated. SMCs and UCs were cultivated in supplemented α-MEM and KSFM medium, respectively, in a humidified atmosphere at 37 ◦C and 5%CO2. The cells were passaged every 3–4 days(Engelhardt et al., 2011). Experiments were performed with SMCs and urothelial cells between passages 6 and 8. GFP lenti- virus transduced human urothelial cells were seeded on substrates in a droplet of fibrin gel.

4.3.3 Preparation of compressed Collagen-Fibrin-Collagen sheets with and without cells for proof of concept for cellular engineering of collagen grafts with increased density.

Collagen-fibrin-Collagen (CfC) sheets were prepared by using square-shaped molds (2.5 x 3 x 2.5 cm) similar to a method described by Vardar et al(Vardar et al., 2016). Briefly, 3 mL of neutralized collagen solution (80% of Rat tail collagen (2.05mg/mL, First-link, UK), 10% of 10X MEM, 10% of alpha-MEM and 1M NaOH) were casted into the molds and incubated in a 5% CO2 incubator at 37°C for 20 minutes. After collagen polymerization, 300 µL of fibrin solution was casted onto the first layer of collagen gel followed by the addition of a second volume of neutralized collagen solution on top of the fibrin layer. The fibrin solution contained 4 mg/mL of human fibrinogen (plasminogen, fibronectin- depleted; Enzyme Research Laboratories, South Bend, IN, USA), 2 U/mL factor XIIIa (Fibrogammin, CSL Behring, UK), 2 U/mL human thrombin (Sigma Aldrich, Switzerland), and 5 mM Ca2+ in tris-buffered saline (TBS). Scaffolds were placed inside an incubator at 37°C for 45 min to ensure full fibrin polymerization and polymerization of the second collagen layer. Multilayered gels were then subjected to plastic compression for 3 minutes using a method previously described(R. A. Brown et al., 2005). For preparation of cellular collagen sheets, 1*106 hSMC in cell culture media were added into each collagen solution instead of alpha-MEM prior to casting. Areas of cultured cellular sheets were measured using a regular ruler. Metabolic activity was measured each week using an Alamar blue assay (AbD Serotec, UK).

4.3.4 Preparation of tubular collagen grafts seeded with smooth muscle cells for cellular engineering of tubular grafts with increased density.

Tubular collagen grafts were fabricated utilizing liquid type 1 bovine collagen (5mg/ml) provided by Symatese (France). Sterile collagen solution was added to 10x MEM and neutralized with 1M NaOH. This solution was then poured into a 7 cm long tubular steel mold having an outer tube diameter of 1.2 cm. To create the final tubular lumen, a glass mandrel (Verreries de Carouge, CH) was placed inside the tubular mold. The diameter of the glass mandrel was 3 mm. Full collagen gelation was achieved in 15 minutes at RT. For the preparation of cellular tubes, 4 million hSMC were added to the 5mg/ml of neutralized bovine collagen before casting it into the mold for polymerization. Cell-seeded tubes were kept in culture of alpha-minimum essential medium (Gibco) supplemented with 2mM L-glutamine, 10% fetal bovine serum, and 1% penicillin/streptomycin (100 units/mL) for a period of 4 weeks before decellularization.

4.3.5 Decellularization of cell-seeded tubular collagen grafts and validation of the treatment

Decellularized cellular grafts were prepared using a previous established protocol with minor modifications to ensure a low dsDNA content(Kim et al., 2012). Briefly, cellular grafts was placed in detergent bath for 72 hours (Triton-X and ammonium hydroxide), followed by numerous washing steps in PBS and distilled water. The decellularized grafts were stored in PBS supplemented with 1% Penicillin/Streptomycin and Fungizone at 4 °C until used. DNA from decellularized grafts were isolated by following a previously published protocol (Bullers, Baker, Ingham, & Southgate, 2014). Briefly, decellularized grafts were broken down using papain and the DNA content was measured using Picogreen (Life technologies, CH) following the provider's instructions. Endotoxin levels of decellularized matrices were quantified using the HEK-Blue hTLR4 cell assay from InvivoGen (San Diego, CA, USA).

4.3.6 Scanning electron microscopy (SEM)

1% tannic acid and 1.25% glutaraldehyde were utilized to fix the samples. This was then washed with 0.1 M cacodylate, and dehydrated in increasing ethanol concentrations prior to critical point drying (CPD). The samples were then coated with gold/palladium and imaged at a voltage of 10 kV using a scanning electron microscope (XLF30, Philips).

4.3.7 Mechanical stress-strain test

Linear modulus (E) values of matrices were determined using a tensile machine (Instron Norwood, MA, USA) following the same technique as Vardar (Vardar et al., 2016). Briefly, samples were fixed within the machine and then pulled with a 250 N load cell at a strain rate of 1 mm/min until break. E values represent the slope of the initial linear region of the stress/displacement curves of the samples.

4.3.8 Urethral replacement surgery in rabbits using decellularized tubular collagen grafts

In-vivo experiments were performed in Lausanne, Switzerland and Kuala Lumpur, Malaysia on twelve New Zealand white male rabbits (N=12; 2.5–3.5 kg; Charles River Laboratories France, and Harlan and Bred, Singapore). Premedication was done utilizing 1 mg/kg Xylasine (Provet Ag CH-3421 Lyssach) and 10 mg/kg Ketamine (Streuli Pharma CH8730 Uznach) which was administered by intramuscular (I.M). A single-dose of prophylactic antibiotics was given Cefazolin 10 mg/kg (Labatec Pharma S.A. Meyrin) by subcutaneous injection (S.C.). General anesthesia was maintained throughout the surgery with 2% Isofluorane. Surgical disinfection was done with Betadine (Mundipharma). For intra –operative analgesia, Carprofen (Alloga CH-3400 Burgdorf) 4 mg/kg was given by S.C injection after 10 min of surgery and Ketamine was repeated after 45 min. Acellular urethral grafts were implanted using the following surgical method. Prolene-4.0 anchor suture was placed in the glans. A 6F catheter was inserted into the bladder. A 3-cm skin incision was performed just proximal to the glans. Dissection was done until the urethra within the corpus spongiosum was isolated.

5.0-Vicryl stay sutures were placed as stay sutures in the proximal and distal urethra. The middle part of the urethra along with the corpus spongiosum was excised to create a 2 cm long defect, at 0.5 cm proximally from the base of the glans. A 2 cm-long decellularized graft was then loaded on the catheter. Anastomoses was performed to the native urethra with interrupted sutures (Vicryl-6.0). The anastomoses were further reinforced with the application of 0.1 mL of fibrin glue (Tisseel, Baxter, Volketswil, CH). Finally, the skin was sutured with Vicryl-5.0 interrupted sutures. At the end of the surgery the catheter was removed and a leak test was performed. Post –operative analgesia with Carprofen 4 mg/kg/day was continued for 5 days.

The animals were followed up for a period of 1, 3, and 6 months with N=4 in each group. With the animals under general anesthesia a macroscopic evaluation and 2 voiding cysto-urethrographies (Visipaque 270 mg/mL) were performed. All images were collected using a Philips BV Pulsera. The diameter of the urethra was measured utilizing a scale. Knowing that the graft was sutured at 0.5 cm from the base of the glans and it measured 2 cm in length, the graft's position could be determined on the radioscopic image. It was then possible to estimate the presence of a stricture and their location. As it is a dynamic examination, a stricture was defined as a 50% reduction of the diameter of the urethra at the same location during two repeated examinations. Euthanasia was performed using a lethal intra-venous pentobarbital (Esconarkon ad.us VET Streuli) injection at 1, 3, and 6 months post-surgery respectively. The entire penis was harvested and fixed in 4% Formalin (PFA), embedded into paraffin, and 8µm sections were prepared for histology and immunohistochemistry.

4.3.9 Immunohistochemistry

Harvested tissue samples were fixed in 4% PFA and embedded in paraffin. Sections were prepared at a thickness of 8 µm. Primary and secondary antibodies used for immunohistochemistry are summarized in Table 4.1. Images were taken with a Leica DM5500 microscope (Leica, D) and with a LSM 700 confocal laser-scanning microscope (Zeiss, D). Alpha smooth muscle actin (SMA) expression was quantified in the grafted area with Fiji imaging program (ImageJ). Fluorescent images of only the SMA fluorescent channel were separated from the other used fluorescent channels and were made binary. The SMA positive areas were calculated as percentage of black and white signal. From n=4 different selected areas for the different time points, a mean and standard deviation was calculated. Antibodies used are summarized below:

Table 4.1: List of antibodies used for immunohistochemistry decellularized grafts

Primary Antibodies	**Provider**	**Dilution**
Mouse anti-alpha smooth muscle actin	Abcam, CH	1:150
Rabbit anti-Collagen type	Abcam, CH	1:250
Goat anti-uroplakin2	Labforce, CH	1:150
Secondary Antibodies	**Provider**	**Dilution**
Donkey anti mouse-Alexa647	Abcam, CH	1:500
Donkey anti rabbit-Alexa546	Abcam, CH	1:500

4.3.10 Statistical Analysis

A two-tailed unpaired Student's t-test was used to analyze if a difference in two data sets was statistically significant. A p-value of less than 0.05 was considered significant. Error bars represent the standard deviation (SD) of n=4 independent samples.

4.4 Results

4.4.1 Fabrication of a dense, acellular "humanized "collagen sheet by culturing human smooth muscle cells on a 3D rat collagen gel followed by decellularization.

Human smooth muscle cells were cultured within our surgically compatible collagen–fibrin-collagen hybrid graft (hereafter referred to as acellular sheet graft) that was previously developed by the group (Vardar et al., 2016). Utilizing a human specific collagen type I antibody, it was possible to monitor the human collagen type 1 deposition over time in the rat collagen matrix. A gradual increase of human collagen type I could be seen over the culture time (Figure 4.1A-D). At 4 weeks, a strong and dense expression of human collagen type I protein in the previous rat collagen based scaffold was seen (Figure 4.1D). Decellularization of grafts 4 weeks after cell seeding was achieved by utilizing an established decellularization protocol. DAPI staining confirmed the absence of cell nuclei within the decellularized grafts. The decellularized acellular collagen sheet demonstrated a dense and intact human collagen extracellular matrix. This could be validated by staining for human collagen type I (Figure 4.1F). Furthermore, the dsDNA level present within the decellularized matrices was below the set standard of 50ng dsDNA/mg of ECM (Figure 4.1E).

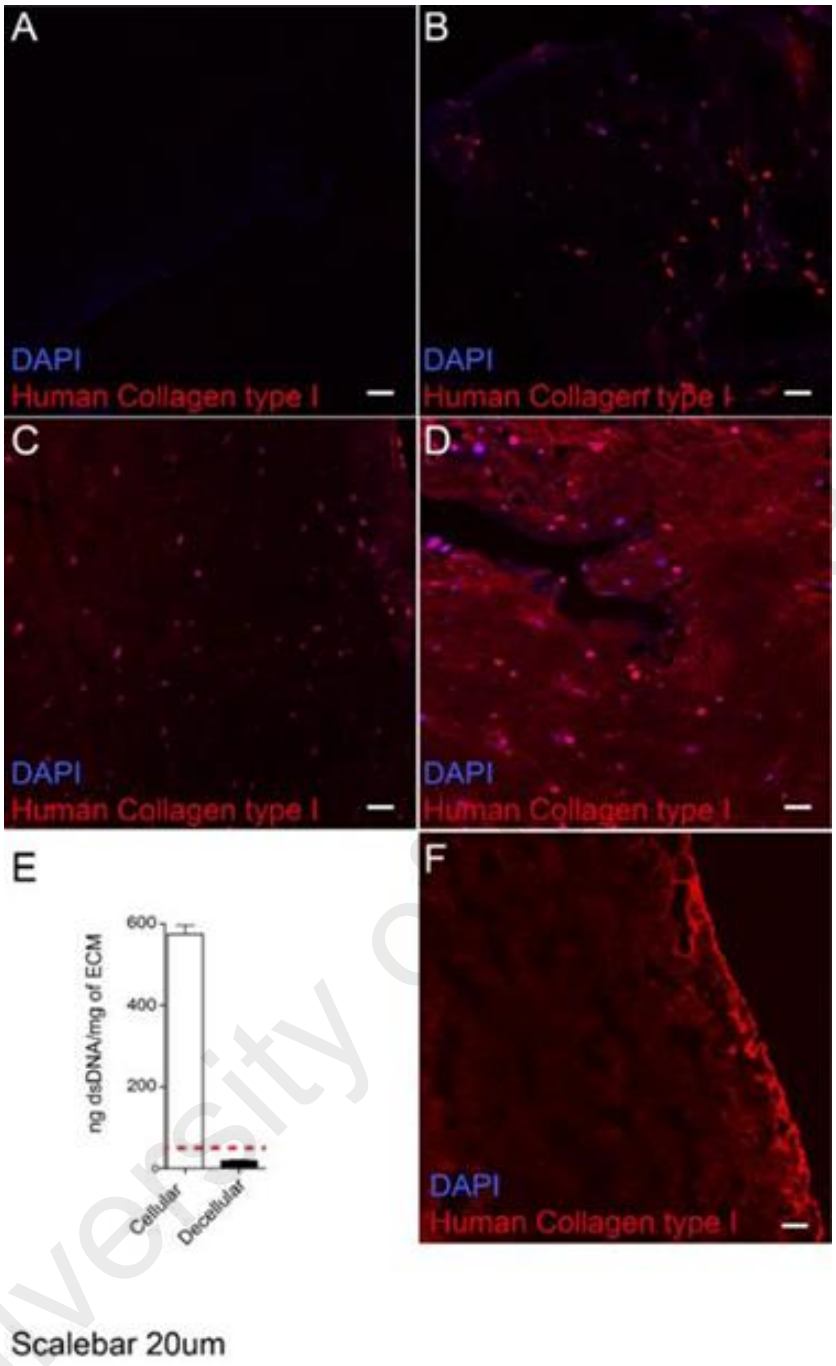

Figure 4.1: Production of decellularized human type 1 collagen sheets. 4 million SMCs were seeded within collagen-fibrin-collagen gels. The gradual turnover of rat to human type 1 collagen in the graft was visualized by immunohistochemistry using anti- human collagen type 1 specific antibodies (red). DAPI staining visualizes cell nuclei (blue). (A) Stained sections of acellular matrices showing an acellular rat collagen gel before cell seeding as control (B-D) Representative stained sections of cell-seeded gels 7, 14, and 28 days after cell seeding. (E)The level of ds DNA on decellularized matrices was determined by picogreen staining. As comparison, the dsDNA level of a cell-seeded matrix prior to decellularization is shown. Red lines mark the set standard for dsDNA content of decellularized matrices. (F) Decellularized collagen matrix where the cells had been removed after 28 days of cell seeding showing absence of DAPI. Scale bars represent 20 um.

4.4.2 Characterization of decellularized and acellular collagen –fibrin-collagen sheets.

It was observed that the decellularized collagen collagen–fibrin-collagen sheets had a much denser collagen distribution as compared to the acellular sheets as observed from the Sirius red stained sheets under bright field and polarized light (Figure 4.2A and 4.2B). Observations under the scanning electron microscope confirmed the difference in the collagen fiber density between the two sheets. The stiffer decellularized sheets showed a denser structural collagen fiber arrangement compared to the acellular sheets (Figure 4.2C and 4.2D). To prove that the denser decellularized sheets had a higher stiffness than the less dense acellular sheets, a stress-strain measurement of the sheets was done. Decellularized sheets recorded a Young's Modulus of 0.195 MPa in comparison to 0.065MPa for acellular sheets. These measurements proved that the decellularized sheets were stiffer. Proliferation, migration, and cell morphology of human urothelial, GFP-positive cells seeded on acellular and decellularized sheets were analyzed on day 1, 3, and 7. It was observed that a pro-migratory urothelial phenotype with a zero-proliferative index was exhibited from the GFP-positive cells seeded onto acellular sheets over time (Figure 4.2E). Urothelial cells had a more rounded cellular phenotype, similar to a senescent urothelial cell phenotype when growing on acellular sheets. On the contrary, cells seeded onto decellularized sheets, exhibited a low migratory urothelial phenotype and a more colony forming urothelial phenotype (Figure 4.2F). The urothelial cells were also nicely spread when growing on top of decellularized sheets. Though the proliferative index that was exhibited was low, decellularized sheets still had a significantly higher proliferative index than the acellular sheets (Figure 4.2G).

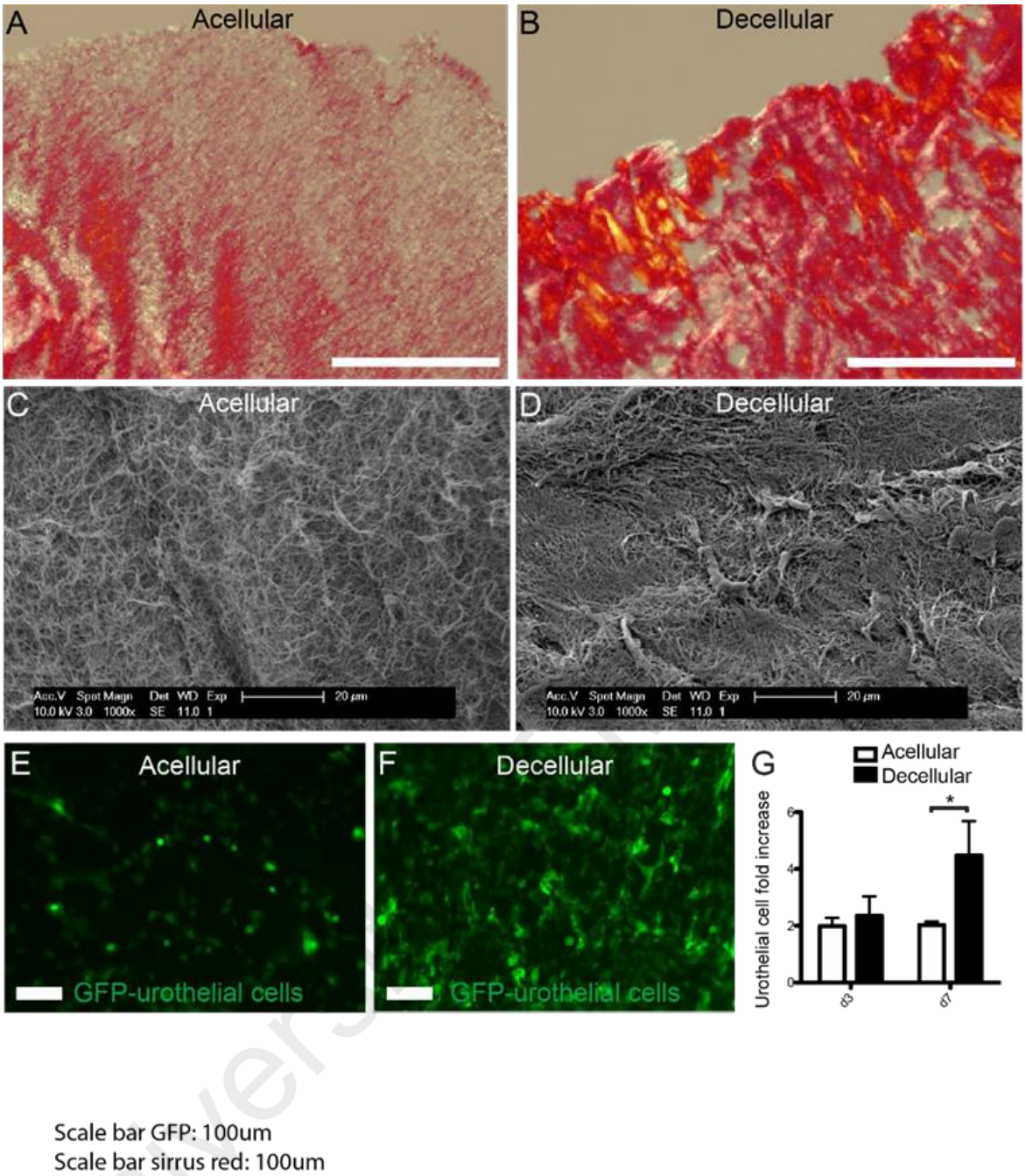

Scale bar GFP: 100um
Scale bar sirrus red: 100um

Figure 4.2: Comparison of decellularized and acellular collagen sheets. (A) Sirius red stained paraffin sections of an acellular and (B) a decellularized graft visualizes the collagen structure. (C) Scanning electron microscope images show the surface structure of an acellular and a (D) decellularized graft (E-F) Images taken under a fluorescent microscope show GFP-expressing human urothelial cells on the surface of an acellular and a decellularized matrix 7 days after seeding. (G) Cells were counted on images taken under the fluorescent microscope and the cell number was normalized to the amount of cells that was initially seeded. The cell fold increase on acellular and decellularized matrices 3 and 7 days after cell seeding is shown. Error bars represent the standard deviation of 4 independent samples. Scale bars represent 100 um.

4.4.3 Characterization of decellularized tubular urethral grafts

The collagen structure of the decellularized tubular urethral grafts were analyzed using Sirius Red staining before cell- seeding (acellular matrix), 4 weeks after the culture of human smooth muscle cells, and after the decellularization process (Figure 4.3). An increase in collagen deposition was observed during the 4 weeks of cell culture (Figure 4.3A and 4.3B). The decellularization process appears to have not modified the collagen architecture of the graft when compared to the cell-seeded graft at 4 weeks (Figure 4.3B and Figure 4.3C).

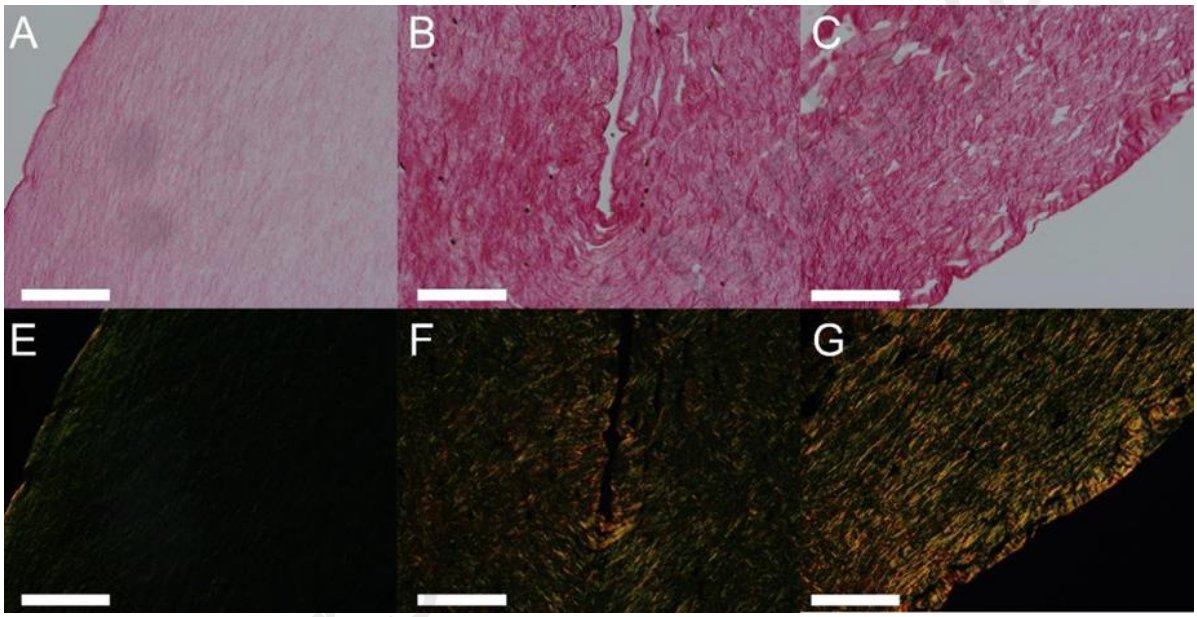

Figure 4.3: Characterization of a decellularized tubular urethral collagen graft. Human smooth muscle cells were cultured within the scaffold for 4 weeks prior to decellularization. Acellular scaffolds (A, E), cell-seeded scaffolds after 4 weeks of culture (B, F), and decellularized scaffolds (C, G) were fixed and embedded into paraffin. The collagenous structure of the scaffold was visualized by Sirius red staining. Images were taken by bright field microscopy (A-C) and under polarized light (E-G). Scale bars represent 100 um.

4.4.4 Surgical outcome of implanted tubular urethral grafts in a rabbit model

All the rabbits (N=12) survived the surgical implantation and could void within 48 h. No complications were observed macroscopically and on voiding cysto-urethrography in 75% of the rabbits (Fig.4.4A and 4.4B). 25% of the rabbits presented a non-lethal distal fistula in this study.

4.4.5 Histology and immunochemistry of decellularized tubular graft implantation study

One of the absorbable sutures utilized to anastomose the graft in place could be clearly seen on H&E and Masson's Trichrome (MT) stained sections 1-month post-surgery (Figure 4.4C and Figure 4.4F). Both H&E and MT staining showed an early onset of urothelial repopulation of the grafted area even at 1 month. By 3 months, the urothelial cell layer appeared to show a stratification similar to the one of a native urethra (Figure 4.4D and Figure 4.4G). At 1 month, no muscle fibers were seen (Figure 4.4F). By 3 months and by 6 months muscle bundle formation was demonstrated (Figure 4.4G and Figure 4.4H). This was clearly shown by the MT stained sections, with a time- dependent gradual increase of muscle fibers shown by the increase in red from 1 to 6 months. Urothelial cell differentiation in the grafted area was shown by the expression of the urine barrier protein, Uroplakin-2. At 1 month, no Uroplakin-2 expression could be detected by immunohistochemistry, but a multilayered urothelial architecture was shown by DAPI staining (Figure 4.5A) this multilayered urothelial architecture became more organized by 3 months. Uroplakin-2 eventually completely covered the urothelial layer at 3 and 6 months post-surgery (Figure 4.5B and 4.5C) similar to the native rabbit urethra (Figure 4.5D). Smooth muscle cells appeared to invade the grafted area from the wound edges at around 3 months as seen by the expression of smooth muscle actin in red (Figure 4.5F). A significant increase in the regeneration of the smooth muscle cells was seen from 3 to 6 months in the grafted area (Figure 4.5G). There was no significant difference in the ingrowth of smooth muscle cells between the 6-month group and the native rabbit urethra (Figure 4.5I).

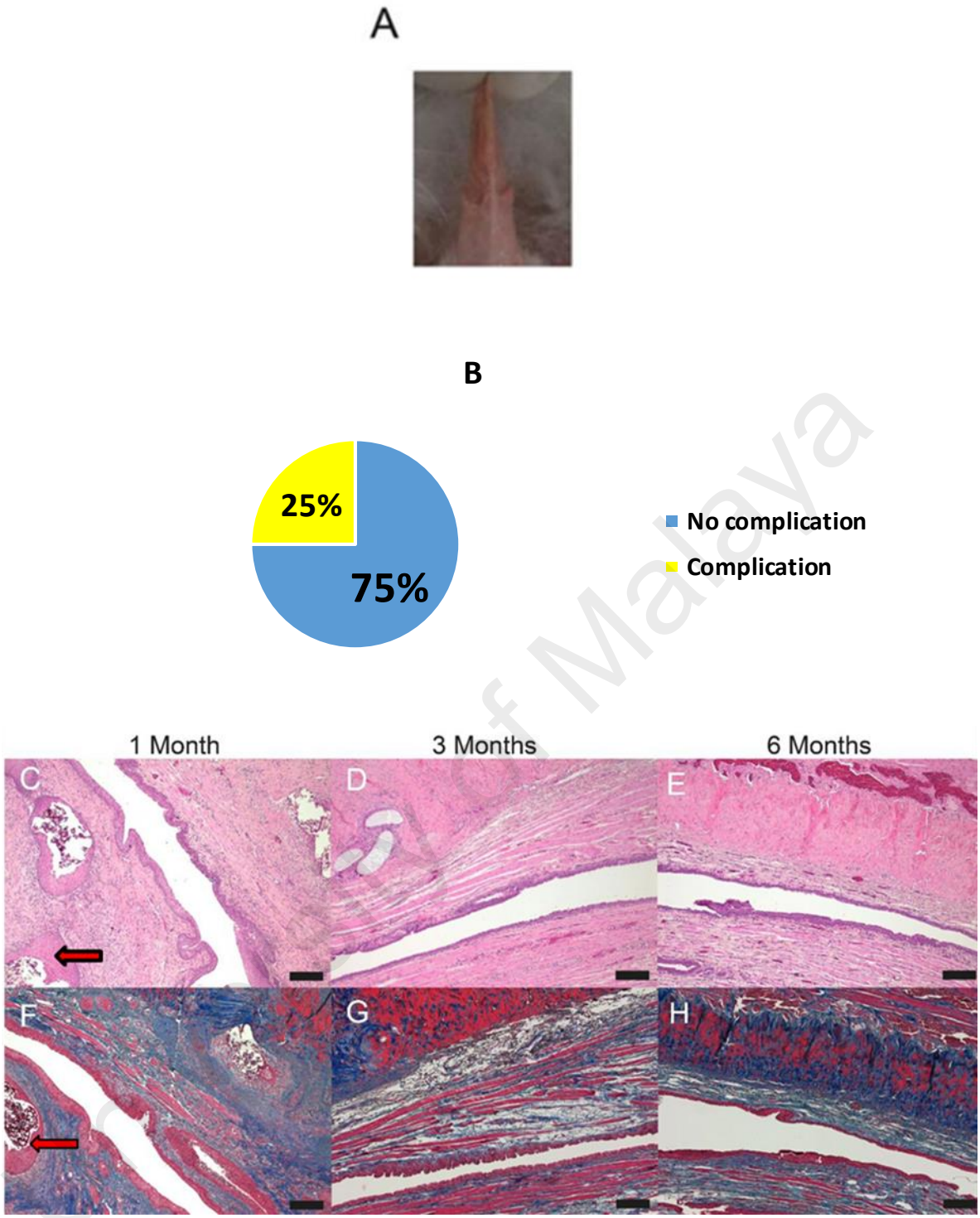

Figure 4.4: Surgical outcome and histology of *in-vivo* implantation of decellularized urethral graft. Decellularized tubular grafts were implanted in an artificially created urethral defect of 2cm in the rabbit model. Animals were sacrificed at 1, 3 and 6 months post-surgery (N=12). A) Macroscopic image of normal rabbit penis post-surgery showing no complications(B) Histogram of the frequency of the observed complications based on macroscopic examination and micturating cystourethrography (C-E) H&E stained paraffin sections show the tissue morphology (C) 1month, (D) 3 months, and (E) 6 months post-surgery. (F-H) MT stained paraffin sections visualize the grafted area (F) 1month, (G) 3 months, and (H) 6 months after implantation. Collagenous structures are stained in red. Arrow in red shows sutures used for anastomosis of graft. Scale bars represent 100um.

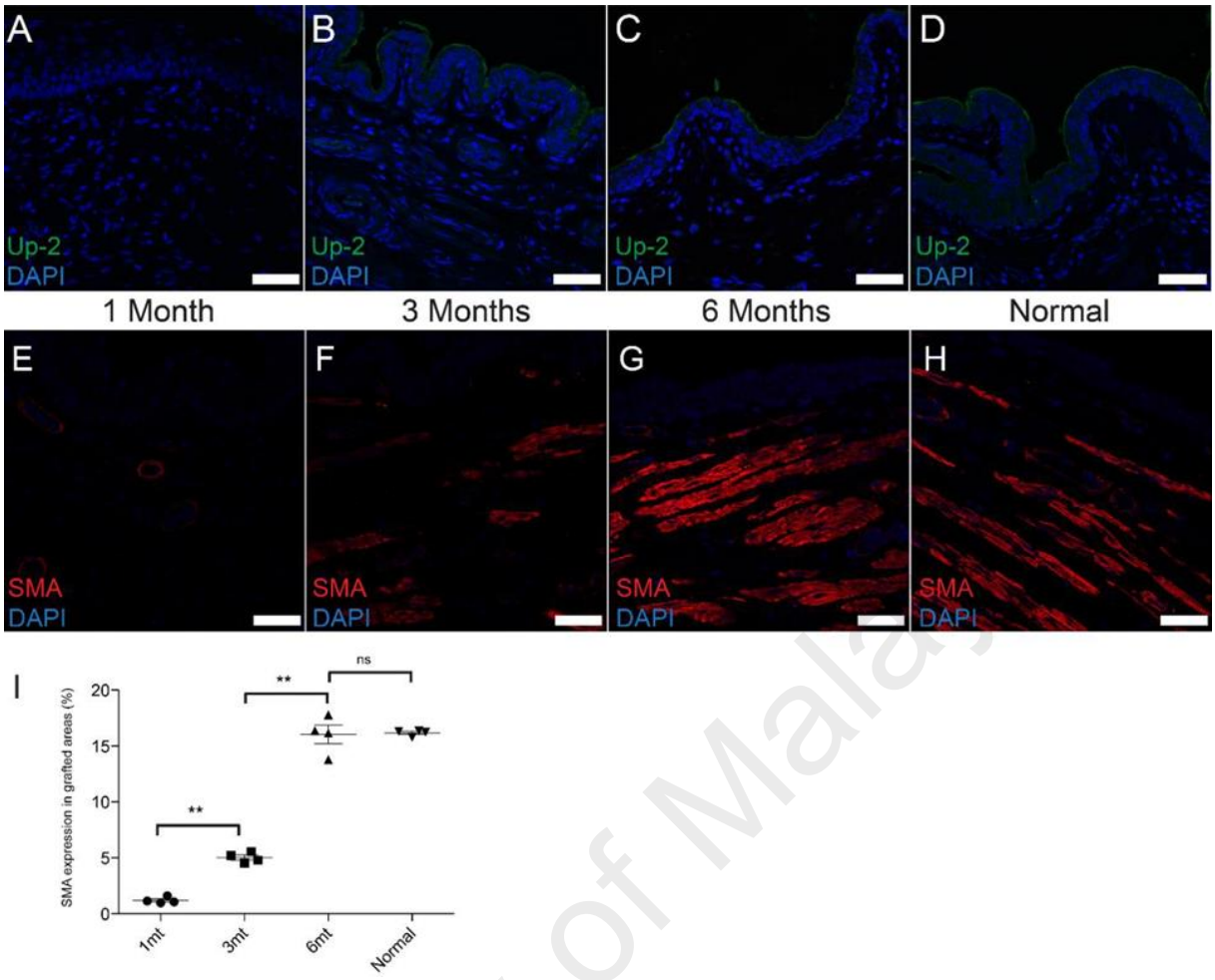

Figure 4.5: Immunohistochemistry images of the decellularized tubular grafted site. Decellularized tubular urethral collagen grafts (2cm in length) were implanted into a critical size urethra defect in a rabbit model. Animals were sacrificed 1, 3, and 6 months post-surgery. Functional tissue regeneration was determined by immunohistochemistry using either anti-uroplakin-2 antibodies (Up2) (A-C), or anti-smooth muscle alpha actin (SMA) antibodies (E-G). As a control, a native/normal rabbit urethra is shown (D and H). (I)The smooth muscle alpha actin expression was quantified on images taken of anti-SMA stained sections. Four different areas were analyzed within each stained section using the FIJI- software. SMA expression was compared at different sacrifice time points and to the expression within a non-operated (native) rabbit urethra. Note: Stars (**) indicate $p < 0.01$ for n=4 different and independent areas. Scale bars indicate 50 µm.

4.5 Discussion

The aim of this study was to fabricate a graft that could accelerate the regeneration of functional urothelial and smooth muscle tissue from the host tissue upon implantation for urethral tissue engineering application. The hypothesis was that by modifying the density of the collagen matrix we could enhance its tissue regeneration capacity. However the challenge was the choice of method that was to be employed to obtain this objective. Collagen as a biomaterial has inherent weak mechanical properties that makes it difficult for its use for surgical applications. Even within the experience of my research group, the first graft we had implanted for urethral regeneration in the rabbit model in 2012 had to be glued to the native urethra as it could not be sutured. As described by Gheezi et al there exists a linear relationship between collagen fiber density and ultimate tensile strength. Therefore, by increasing the density of the collagen matrix, the aim was to improve the mechanical property of the graft. As previously described, the utilization of cross-linking methods and/or the addition of polymers to collagen matrices have been utilized to improve its mechanical property, but these modifications have been shown to be associated with increased inflammatory reactions from the host tissue and could impede the regeneration potential of the graft. In this study, smooth muscle cells were seeded followed by a decellularization step to modify the architecture of the collagen graft. Such a method has been described for the fabrication of tissue engineered vascular endothelial grafts by Shannon et al (Dahl et al., 2011) which has been modified and applied here for urological tissue engineering applications. The graft engineered by this platform would also have biological cues and structural alterations by the cells making it an attractive matrix for cellular ingrowth when implanted. Utilizing the described technique, a modification was done to the initial collagen matrix by seeding the collagen matrix with human smooth muscle cells followed by decellularization. Both the decellularized collagen-fibrin-collagen sheets that were attempted initially and the final tubular urethral grafts had demonstrated a denser collagen architecture when analyzed on Sirius Red- stained sections than their predecessor acellular grafts. SEM images also showed a more tightly arranged collagen fiber orientation within the decellularized grafts compared to the

acellular grafts. This increase in fiber density also correlated with a statistically significant difference in the Young's Modulus of the decellularized sheets in comparison to the mechanical property of the acellular sheets. Both the variation in the imaged architecture and the mechanical property exhibited by the decellularized scaffolds confirmed that the initial matrix was remodeled into a new matrix by the seeded smooth muscle cells. This decellularized collagen matrix showed a specific staining for human collagen type 1 where the stained area increased with longer cell culture times. This "humanization" of the collagen matrix explains the architectural difference of the decellularized matrix when compared to the initial matrix prior to cell-seeding. A well described decellularization protocol was utilized to minimize the risk of immunoreaction from the host tissue to the implanted decellularized matrix. The decellularized grafts fabricated here fulfilled established safety criteria used by clinical grade decellularized biomaterials available in the market, by demonstrating a low level of dsDNA (of less than 50ng dsDNA/mg of ECM) and DAPI staining confirming the absence of cell nuclei.

The decellularized tubular grafts were then implanted in the rabbit urethral model to examine the urethral regeneration potential of this denser "humanized" matrix. A 2 cm long tubular graft was used to close a circumferential, artificially created urethral defect. The graft was anastomosed to the native ends of the rabbit urethra. A far better functional outcome was demonstrated in comparison with the previous described dCGT graft from chapter 3. The functional outcome was improved with 75% of the rabbits showing no complication rates in comparison to 60% seen in the previous study. This study showed once more of the translatability of the technology as it was again conducted in 2 different parts of the world and by 4 different surgeons. The decellularized implanted tubular urethral graft showed an early ingrowth of urothelial cells at 1 month and was completely remodeled by urothelial cells at 3 months post implantation.Uroplakin-2 expression which is a marker for terminally differentiated urothelial cell was shown to completely cover the urothelial layer as early as 3 months post-surgery thus demonstrating that a successful urothelial cell differentiation had taken place. This finding and the appearance of smooth muscle bundles at 6 months post-surgery showed that the new

decellularized grafts had an improved regeneration potential than that of the previous dCGT grafts. This method of modifying the collagen matrix into a denser and humanized collagen matrix is more time consuming than the previously described fabrication method. However it is still far more translatable for clinical application than grafts with *ex-vivo* cultured autologous cells. This denser and "humanized" graft remains an "off-the-shelf" product ready to be shipped across the world as demonstrated in this multicenter study. The utilization of a standard decellularization protocol ensures that the matrix can be implanted into anyone without the risk of a major histocompatibility rejection due to the cell removal procedure(Charriere et al., 1989). The improved ingrowth of smooth muscle cells in coordination with the early development of a complete urothelial layer could be due to the fact that the urothelium, which functions primarily as a first line barrier against pathological bacteria and urine, might exhibit important signaling properties that potentially favor the ingrowth of smooth muscle cells(Birder & de Groat, 2007; Khandelwal et al., 2009; Wu, Kong, Pellicer, Kreibich, & Sun, 2009). The subsequent challenge would be to see similar results in a large animal model and to explore the potential of modifying the collagen matrix with other methods to obtain improved regeneration. This would ideally be done without the incorporation of cells and a decellularization step to ensure a simple and cost-effective fabrication method that would guarantee a better possibility for future clinical translation of the final developed urethral graft.

4.6 Conclusion

This study demonstrated that an animal collagen matrix could be transformed into a denser collagen matrix with increased human collagen type 1 using cellular engineering techniques. This is achieved by culturing human smooth muscle cells followed by decellularization. The decellularized tubular urethral grafts performed better with a 75% no complication rate and faster regeneration than the previously implanted dCGT graft. The development of a differentiated urothelial layer within three months and an increasing smooth muscle bundle formation over time showed the excellent regeneration capacity of this graft for urinary tract tissue engineering applications.

CHAPTER 5: SPATIALLY CONTROLLED ENGINEERED ACELLULAR COLLAGEN GRAFT WITH DENSITY GRADIENT PERFORM BETTER FOR URETHRAL RECONSTRUCTIVE SURGERY WITH IMPROVED UROTHELIAL CELLS AND SMC INGROWTH.

5.1 Introduction

Growing number of urethral diseases are seen in developing and underdeveloped regions of the world where the number of operative theatres and children access for basic surgical care are still very limited(Bickler & Rode, 2002; Chirdan, Ameh, Abantanga, Sidler, & Elhalaby, 2010). Though many surgical techniques and grafts have been described, the outcome is far from perfect with complication rates of up to 21% fistula rates being reported along with other complications such as recurrent stricture, meatal stenosis, diverticulum, dehiscence and recurrent penile curvature. Both acellular, cellular and growth factor incorporation into existing biomaterials to fabricate urethral grafts have been attempted. Acellular grafts have only been managed to be utilized in short urethral defects as an on–lay graft. The need for having a healthy base on one side of the urethra to place the graft has limited their wide spread clinical utilization. In 2015 the clinical outcome of a commercial cell seeded Tissue Engineered Buccal Mucosa (TEBM) product, implanted in 21 patients with anterior urethral strictures was published. Prior buccal biopsy from the patient, *ex-vivo* culturing in a GLP facility and cell seeding is required when utilizing this product. This can lead to a delay in the time of biopsy to surgery. The final grafts success is dependent on the quality of the cells cultured and seeded, of which can be variable.

The multiple procedures required prior to implantation in the patient will definitely be added to and increase the final cost of production. It is unlikely therefore that this approach will become standard clinical practice or will be useful for patients with limited financial resources. Therefore, the focus should be on developing an off the shelf acellular tubular urethral graft that is cost effective and easy to be used in any hospital in the world. The dCGT graft engineered in Chapter 3 showed the potential to regenerate a 2cm artificially created urethral defect using an acellular graft. By modification in the architecture and the extracellular matrix protein composition of the

collagen graft, a better regeneration outcome was achieved with the subsequent decellularized 'humanized'' graft in Chapter 4. In this chapter however a simple fabrication method without the utilization of cells was explored. Inspiration on urethral graft design was obtained by analyzing the architecture of the extracellular matrix of the native rabbit urethra. Urothelial and smooth muscle cell behavior on different collagen density was also examined to optimize the collagen graft fabrication. Utilizing this knowledge and by varying the amount of fluid extracted from the collagen matrix, 2 different tubular bio-engineered grafts with different density were fabricated. The evaluation of the function of the two versions of the graft was done in the similar rabbit model to regenerate a 2 cm artificially created urethral defect. Sterilization was then done later on the better performing graft of the two as per standard regulatory requirements for medical device for future clinical translation. The sterilized graft was also implanted in the similar animal model to look for the effects on graft behavior post sterilization.

5.2 Literature review

Using tissue engineering platforms to regenerate an organ like the urethra has advantages. The urethral wound bed is very well vascularized. Hence failure of acellular tissue-engineered grafts due to delayed vascularization as seen in other indications may not occur in the urethra (Bhargava et al., 2008). Therefore, this vascular rich environment could be the perfect organ for a successful regeneration utilizing an acellular graft. Currently however oral mucosa still represents the most popular substitute material for urethral reconstruction. From 1966 to 2006, 1,267 studies were reported in literature on the use of oral mucosa in urethral reconstructive surgery. In these reports, 724 urethroplasties (53.5%) were performed for urethral strictures, while 629 (46.5%) were performed for hypospadias/ epispadias repair. Out of these surgeries only 66.5% of buccal mucosal graft implantation in urethral stricture reconstruction were successful and 76.4% uptake of the graft was seen when utilized for children undergoing hypospadias/epispadias repair(Markiewicz, Margarone, Barbagli, & Scannapieco, 2007).

Autologous buccal mucosa also cannot be utilized for all patients undergoing urethral reconstruction. Certain patients may have some normal oral conditions that may necessitate delaying oral mucosa harvest until site conditions improves and others pathologic oral conditions which are strict contraindications for oral mucosa harvesting (Markiewicz et al., 2007).In 2010, Barbagli et al. reported on a group of 350 patients with oral mucosa harvested from the cheek. They recommended that patients having an ongoing infectious disease of the mouth (Candida, varicella virus, herpes virus) are advised to have their urethral reconstruction utilizing genital or extra genital skin because these pathologic oral conditions are contraindications for oral mucosa harvesting(Barbagli et al., 2010). The Finnish Family Human Papilloma Virus (HPV) Study published by Kero and colleagues reported a high prevalence of male oral HPV, ranging from 15% to 31%. The most frequent genotype was HPV-16. They concluded that the oral mucosa is an important reservoir for the virus(Kero, Rautava, Syrjänen, Grenman, & Syrjänen, 2012). Though the literature does not provide any information about the incidence of HPV related disease in patients who undergo transplantation of oral mucosa into the urethra. However, this

increasing trend would definitely change the practice of urologist. Clinicians would have to possibly schedule all patients intended for oral mucosa harvesting to have a preoperative oral scrapping to screen for HPV. Ultimately, using a tissue-engineered material for urethroplasty might solve these issues.

Tissue-engineered oral or urethral mucosa is now available in some countries, and these technologies are ready to be used worldwide but at a cost. Certain centers in Europe are now starting to use this technique as standard procedure for their anterior urethroplasty, thus avoiding problems related to harvesting oral mucosa from the patient, including the risk of infection (G. Ram-Liebig et al., 2012; Gouya Ram-Liebig et al., 2017). Indeed, this novel technology has revolutionized the field of urethral tissue engineering. However it is still not a cost-effective method for widespread clinical application when compared to current standard of care therapies.

The utilization of acellular grafts have evolved from passive mechanical support to active approaches that truly harness and direct endogenous repair processes. Commercial products based on porcine small intestinal submucosa are now used clinically to augment soft tissue repair, and their mechanism of action is being elucidated and optimized(B. N. Brown, Ratner, Goodman, Amar, & Badylak, 2012). The ultimate goal in the development of an engineered material for urethral reconstruction should be to provide a wide range of products that differ in dimension and shape for adaptation in different indications of urethroplasty (Barbagli & Lazzeri, 2015). The tissue engineered graft should be available at an affordable price to allow for widespread utilization in both developed and developing areas of the world. For many years, oral mucosa represented an amazing source of substitute material for urethral reconstruction, and many patients have been successfully treated. It is now time to change as laboratory-engineered materials are available for our patients and will reduce complications, morbidity, and other risks of transmitted diseases

5.3 Materials and Methods

5.3.1 Preparation of tubular collagen grafts with different density by varying the amount of liquid removed during graft manufacturing.

Tubular collagen grafts were fabricated utilizing liquid type 1 bovine collagen (5mg/ml) provided by Symatese (France). Sterile collagen solution was added to 10x MEM and neutralized with 1M NaOH. This solution was then poured into a 7 cm long tubular steel mold having an outer tube diameter of 1.2 cm. To create the final tubular lumen, a glass mandrel (Verreries de Carouge, CH) was placed inside the tubular mold. The diameter of the glass mandrel was 3 mm. Full collagen gelation was achieved in 15 minutes at RT. The tubular steel mold was opened and the weight of the gelated collagen tube was measured taking into consideration the weight of the glass mandrel. To fabricate the low-density (LD) graft, the gelated collagen tube was manually compressed by rolling it on filter paper being supported by a nylon mesh, followed by an air-drying step. This was done until a liquid content in the graft of 40% w/w is achieved. To fabricate the high-density (HD) graft only air- drying was applied to achieve a desired liquid content of 1% w/w. The liquid loss of the collagen graft after compression and drying steps was calculated by measuring the weight of non-dried and dried grafts with a balance (Mettler Toledo, sensitivity of 0.1 mg). The % of liquid content in grafts (w/w) was calculated by: % of liquid content graft =1- [(weight before drying of graft - weight after drying of graft) / weight before drying of graft]. Both tubular collagen grafts were then separated from the glass mandrel and kept in phosphate buffered saline (PBS pH: 7.2) supplemented with 1% Penicillin/Streptomycin (Gibco, Invitrogen, CH) and 2.5 mg/mL Fungizone (Gibco) in a sterile culture tube (VWR International, USA). The latter was placed into a sterile Falcon® tube to obtain double packaging and was kept at 4ºC. Grafts to be implanted in Kuala Lumpur were shipped at a constant temperature of 4ºC.

5.3.2 *In-vitro* analysis of urothelial and smooth muscle cell behavior on different density

Human primary isolated urothelial and smooth muscle cells were kept at 37 ºC at 95% CO2 throughout experiments. Smooth muscle cells were in alpha-minimum essential medium (Gibco) supplemented with 2mM L-glutamine, 10% fetal bovine serum, and 1% penicillin/streptomycin (100 units/mL). Human urothelial cells were expanded in Primaria-coated flasks (BD Labware) in a keratinocyte serum-free medium supplemented with provider's bovine pituitary extract and epidermal growth factor (Invitrogen/Gibco), and additionally 30 ng/mL cholera toxin (Sigma-Aldrich) was finally added. GFP lenti- virus transduced human urothelial cells were seeded on substrates in a droplet of fibrin gel. Silicone based CytoSoft plates (Advanced Biomatrix, US) with predetermined stiffness values of 0.5 kPa, 8 kPa, and 32 kPa were used. Briefly, 160 µL of fibrin solutions (final concentration of 4 mg/mL of human fibrinogen (plasminogen, fibronectin-depleted; Enzyme Research Laboratories, South Bend, IN, USA), 2 U/mL factor XIIIa (Fibrogammin, CSL Behring, UK), 2 U/mL human thrombin (Sigma Aldrich, Switzerland), and 5 mM Ca2+ in tris-buffered saline (TBS)) were mixed with 40µL of cell solution. 20µL droplets of the cell-fibrin solution were casted on petri dishes and incubated at 37°C for 30min. Urothelial cell-loaded fibrin droplets were placed on specific spots using sterile forceps. Images of urothelial cells were taken with a fluorescent stereomicroscope (Leica, D). Proliferation was assessed by manually counting cells on images taken from each day with Fiji imaging program (ImageJ). 200,000 human smooth muscle cells/mL of collagen solution were seeded within collagen gels made of rat collagen (First link, UK) with concentrations of 1 mg/mL and 2mg/mL, and in two bovine collagen gels with concentrations of 2mg/mL and of 5 mg/mL. In circular disk molds, 500µL of cell-collagen solution was dispensed and gelated. The gels were imaged after gelation, day 7 and at 14 day to observe at gel shrinkage. Immunohistochemistry using human specific collagen type 1 antibodies was performed on rat collagen gels that were fixed after 14 days of cell culture. Images were taken with a LSM 700 confocal laser-scanning microscope (Zeiss, D).

5.3.3 Scanning electron microscopy

To determine the microstructure of the dCGT, scanning electron microscopy (SEM) was performed. 1% tannic acid and 1.25% glutaraldehyde were utilized to fix the samples. This was then washed with 0.1 M cacodylate, and dehydrated in increasing ethanol concentrations prior to critical point drying (CPD). The samples were then coated with gold/palladium and imaged at a voltage of 10 kV using a scanning electron microscope (SEM, XLF30, Philips).

5.3.4 Mechanical evaluation of the fabricated collagen grafts with different density

Burst pressure of the collagen tubes (N = 4 in each group) was measured with an electronic manometer (Extech instruments HD750). Pressure was generated using a syringe pump and applying a flow of 360 mL/ min. All tubes were 1 cm long and had a lumen diameter of 3 mm, the low-density graft had a wall thickness of 1.3 mm (+/- 0.2 mm) whereas the high-density grafts had a wall thickness of 1 mm (±0.1 mm). Pressure changes were directly registered at intervals of one second. The system was first purged of air bubbles and then filled with a mixture of water and methylene blue (1:1) for bettervisualization of the leak after bursting. The burst time-point was determined by the sudden drop of pressure. Instron tensile machine (Norwood, MA, USA) was used to evaluate the collagen tubes' elastic modulus (Young's modulus) and ultimate tensile strength (UTS). The tensile tests were performed with the low- and high-density grafts, respectively. A constant strain rate of 1 mm/min was used in all experiments (N = 4 for each graft). The Young's modulus (E) values, which measures the stiffness of the tube, was obtained from the slope of the linear region just after the initial toe region of the stress-strain curve by means of Hook's law (Stress = E * Strain). UTS values were determined from the maximum tensile stress recorded in the curve.

5.3.5 Surgical testing of grafts with different with density

Four different surgeons had to evaluate graft behavior and score it and to document the results in a score sheet (Table 3). All scores given by the surgeons were added and tabulated for each graft. Tubular collagen grafts with a score of >5 were defined as adequate. Grafts with a score of <5 failed the testing.

Table 5.1: Developed score sheet of collagen grafts for surgeon's subjective evaluation.

Graft appearance	**Uniform (score 2)**	**Non uniform (score 1)**	
Surgical Feel	**Good (score 2)**	**Average (score 1)**	**Poor (score 0)**
Suture application and anastomosis	**Good (Score2)**	**Average (score 1)**	**Poor (score 0)**
Methylene blue test	**No Leak (score 2)**	**Leak (score 1)**	

5.3.6 Sterilization of tubular collagen grafts using X-Ray to examine modification on graft by sterilization for future clinical translation.

The fabricated tubular collagen grafts kept at 4ºC were sent for sterilization to Synergy Health Däniken AG Switzerland. The tubular collagen grafts were sterilized with a minimum dose of 25 kGy. The sterilization of the tubular collagen grafts complied with the following standards:

a) ISO 11137-1:2015 Sterilization of Health Care Products.

b) ISO 9001 Quality Management System

c) ISO 13485 Medical devices /Quality management systems /Requirements for regulatory purposes

d) 21CFR Part 820 (FDA c GMP) Good Manufacturing Practice for Medical Device

5.3.7 Surgical implantation of the graft in the rabbits

Following approval by the Animal Ethics Committees of the Canton of Vaud, Switzerland (Ethical approval number VD2740) and of the Faculty of Medicine of the University of Malaya, Kuala Lumpur (Ethical approval number 2013-09/17/SUR/R/TCR). The experiments were performed on New Zealand white male rabbits (2.5–3.5 kg; Charles River Laboratories France, and Harlan and Bred, Singapore) in Lausanne and Kuala Lumpur. Premedication was done utilizing 1 mg/kg Xylasine (Provet Ag CH-3421 Lyssach) and 10 mg/kg Ketamine (Streuli Pharma CH8730 Uznach) which was administered by intramuscular (I.M). A single-dose of prophylactic antibiotics was given Cefazolin 10 mg/kg (Labatec Pharma S.A. Meyrin) by subcutaneous injection (S.C.). General anesthesia was maintained throughout the surgery with 2% Isofluorane. Surgical disinfection was done with Betadine (Mundipharma). For intra – operative analgesia, Carprofen (Alloga CH-3400 Burgdorf) 4 mg/kg was given by S.C injection after 10 min of surgery and Ketamine was repeated after 45 min. Acellular urethral grafts were implanted using the following surgical method. Prolene-4.0 anchor suture was placed in the glans. A 6F catheter was inserted into the bladder. A 3-cm skin incision was performed just

proximal to the glans. Dissection was done until the urethra within the corpus spongiosum was isolated.5.0-Vicryl stay sutures were placed as stay sutures in the proximal and distal urethra. The middle part of the urethra along with the corpus spongiosum was excised to create a 2 cm long defect, at 0.5 cm proximally from the base of the glans. A 2 cm-long HD/LD graft was then loaded on the catheter. Anastomoses was performed to the native urethra with interrupted sutures (Vicryl-6.0). The anastomoses were further reinforced with the application of 0.1 mL of fibrin glue (Tisseel, Baxter, Volketswil, CH). Finally, the skin was sutured with Vicryl-5.0 interrupted sutures. At the end of the surgery the catheter was removed and a leak test was performed. Post –operative analgesia with Carprofen 4 mg/kg/day was continued for 5 days.

5.3.8 Macroscopic evaluation and cysto-urethrography of rabbits

With the animals under general anesthesia a macroscopic evaluation and 2 voiding cysto-urethrographies (Visipaque 270 mg/mL) were performed. All images were collected using a Philips BV Pulsera. The diameter of the urethra was measured utilizing a scale. Knowing that the graft was sutured at 0.5 cm from the base of the glans and it measured 2 cm in length, the graft's position could be determined on the radioscopic image. It was then possible to estimate the presence of a stricture and their location. As it is a dynamic examination, a stricture was defined as a 50% reduction of the diameter of the urethra at the same location during two repeated examinations.

5.3.9 Participation in the breeding program

Rabbits from the long-term study were enrolled in the in-house breeding program of the Animal Experimental Unit of the Faculty of the Medicine of the University Malaya. Male and female rabbits, which were housed separately were brought together only for breeding. The female rabbit is an induced ovulatory animal, i.e. they can ovulate easily when introduced to a male. A female rabbit (doe) is always placed into a male rabbit's cage in the morning only for a short time for mating. The male rabbit will then mount the doe from behind and proceed to make rapid pelvis thrusts while the doe will raise her hindquarters in response. Mating is confirmed

when the male rabbits pick up their front limbs and throw himself backwards off the doe. The doe is then removed from the male rabbit's cage and the female rabbit is return to her own cage. To increase the conception rate and litter size, re-mating is done approximately 5 to 6 hours after the first mating process. Healthy offspring were delivered after 30 days of gestation period.

5.3.10 Histology and immunohistochemistry

At the determined time of euthanasia, the animals received a lethal intra-venous pentobarbital injection (Esconarkon ad.us VET Streuli). Thereafter, the entire penis was harvested and fixed in 4% Formalin (PFA). For histological and immuno-histochemical work-up, the specimen was embedded in paraffin, and 8µm thick sections were prepared. Antibodies used for immunohistochemistry are summarized below:

Table 5.2: List of antibodies used for immunohistochemistry of LD and HD grafts

Primary Antibodies	**Provider**	**Dilution**
Mouse anti-alpha smooth	Abcam, CH	1:150
Rabbit anti-Collagen type	Abcam, CH	1:250
Goat anti-uroplakin2	Labforce, CH	1:150
Secondary Antibodies	**Provider**	**Dilution**
Donkey anti mouse-	Abcam, CH	1:500
Donkey anti goat-	Abcam, CH	1:500
Donkey anti-rabbit Alexa	Abcam, CH	1:500

Images were taken with a Leica DM5500 microscope (Leica, D) and with a LSM 700 confocal laser-scanning microscope (Zeiss, D). Alpha smooth muscle actin (SMA) expression was quantified in the grafted area with Fiji imaging program (ImageJ). Fluorescent images of only the SMA fluorescent channel were separated from the other used fluorescent channels and were made binary. The SMA positive areas were calculated as percentage of black and white signal.

From N=4 different selected areas for the different time points, a mean and standard deviation was calculated.

5.3.11 Statistical analysis

A two-tailed unpaired Student's t-test was used to analyze if a difference in two data sets of burst pressure, UTS or Young's modulus was statistically significant. A p-value of less than 0.05 was considered significant. Error bars represent the standard deviation (SD) of 4 independent samples.

5.4 Results

5.4.1 The mechanical niche governs urinary tract cell fate

Inspired by the normal rabbit urethral extracellular matrix architecture, spatially controlled collagen density grafts were engineered. Histology of rabbit urethras showed that the closer to the urothelium, the denser collagenous structure was deposited; however, as expected, far less dense collagenous structure was seen in the area of the muscle bundles (Figure 5.1A). From this observation, a decision to analyze the behavior of isolated human urothelial and urinary tract smooth muscle cells in mechanically altered environments in relevant 2D and 3D *in-vitro* cell culture models was done. The rationale for studying urothelial cells in a 2D system was to mimic that urothelial cells grow on top of the extracellular bed *in-vivo*. As density also relates to stiffness, we have investigated different stiffness substrates of various Young's moduli (0.5, 8 and 32 kPa). It was observed that urothelial cells proliferated statistically significantly more on the stiffer matrix (0.5 kPa vs. 8 kPa with $p<0.05$ and 8 kPa vs. 32 kPa with $p<0.01$ at day 7) (Figure 5.1B and 5.1C). Further, evaluation of the interaction of muscle cells within a dense and less dense 3D collagen matrix was evaluated. In low-density rat tail collagen gels (0.5 mg/cm3), it was noted that human smooth muscle cells induce remodeling and degrading of the initial collagen matrix faster as compared to smooth muscle cells in high-density collagen gels when cultured for 7 and 14 days (1 mg/cm3) (Figure 5.1D-5.1F). It was also observed that a similar remodeling/shrinkage pattern with bovine collagen gels seeded with human smooth muscle cells (1 mg/cm3 vs 2.5 mg/cm3) occurred (Figure 5.1D). However, due to a cross-reaction of our antibodies with bovine and human collagen we could not monitor the specific human collagen remodeling. At day 14, the human smooth muscle cells remodels the extracellular matrix of the rat tail collagen gel more pronounced in 0.5 mg/cm3 compared to 1 mg/cm3 (Figure 5.1E and 5.1F).

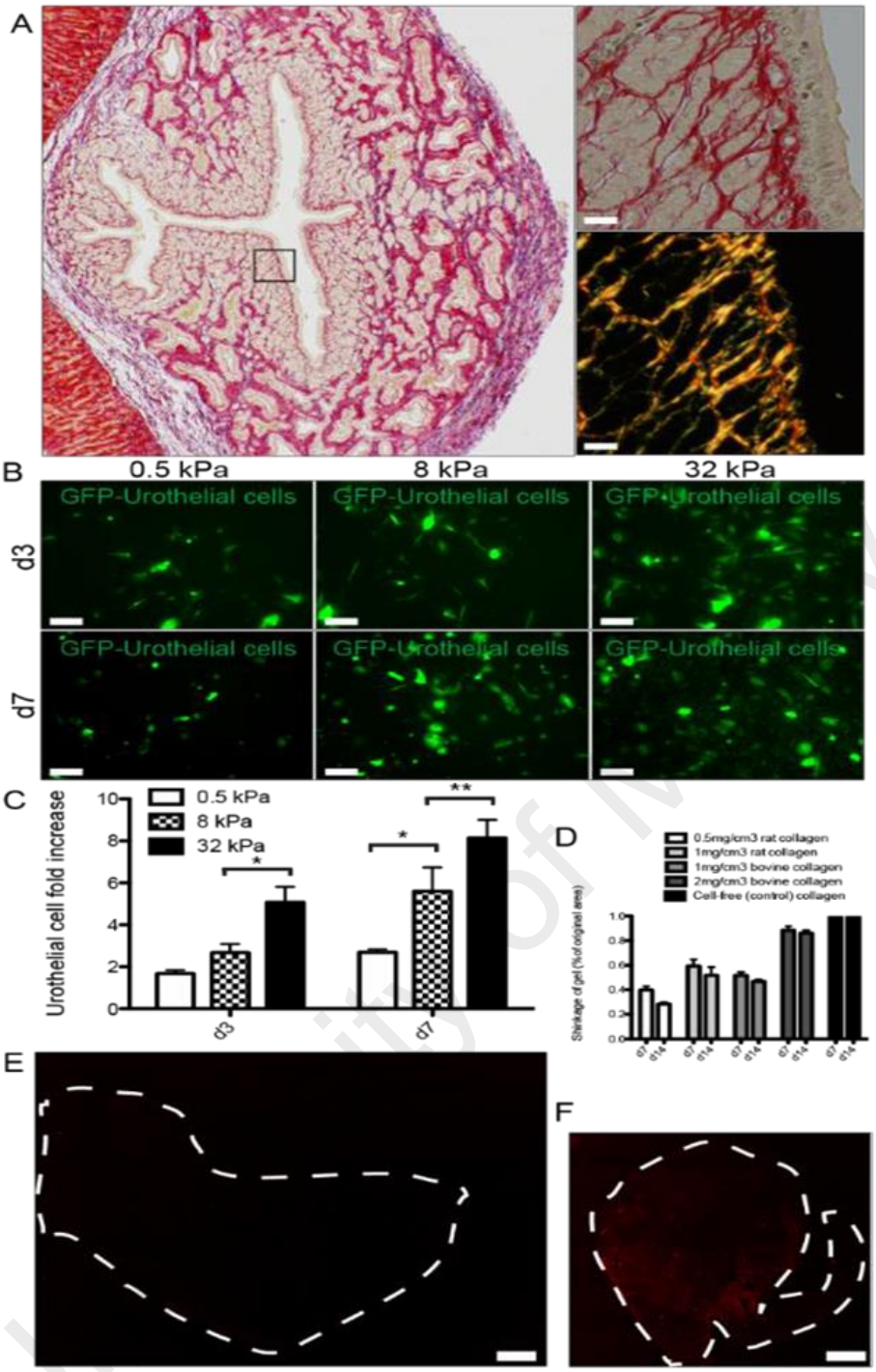

Figure 5.1: Inspiration of the graft design from native urethra histology and in vitro analysis. (A) Sirius red stained native rabbit urethra section (Scale bar 20 µm). (B) Images of GFP-positive human urothelial cells cultured on substrates with pre-determined stiffness of 0.5, 8 and 32 kPa from day 3 and day 7 (Scale bar 100 µm). (C) Urothelial cell proliferation was quantified using manual cell counting of imaged areas and is presented as cell fold increase from day 3 and day 7 (both normalized to day 0), of cells cultured on stiffness substrates of 0.5, 8 and 32 kPa. (D) Collagen graft remodeling/shrinkage analysis of human smooth muscle seeded in collagen grafts with various densities for 7 and 14 days compared to a cell-free control collagen. (E and F) Immunohistochemistry of human collagen type 1 expression in 1 mg/cm3 and 0.5 mg/cm3 rat-tail collagen grafts seeded with human smooth muscle cells at day 14 (Scale bar 500 µm). Error bars represent the standard deviation of four independent samples. *$p < 0.05$, **$p < 0.01$.

5.4.2 Analytical and empirical analysis of collagen grafts

Regenerative materials fabricated for surgical use not only have to fit with the cellular needs but also needs to be compatible with the end-user, the surgeons. Therefore, analytical mechanical testing and empirical assessment of collagen tubes with different liquid content of the collagen grafts was done. Mechanical tensile tests revealed, that the UTS and Young's modulus depended on the liquid content in the grafts (Figure 5.2A and 5.2B). The collagen grafts with higher liquid content had lower mechanical properties while the collagen grafts with lower liquid content had improved mechanical properties. More importantly, the graphs shown in Figure 5.2A and 5.2B revealed that based on the liquid content within the collagen graft, which can be easily controlled during fabrication, one can predict its mechanical behavior.

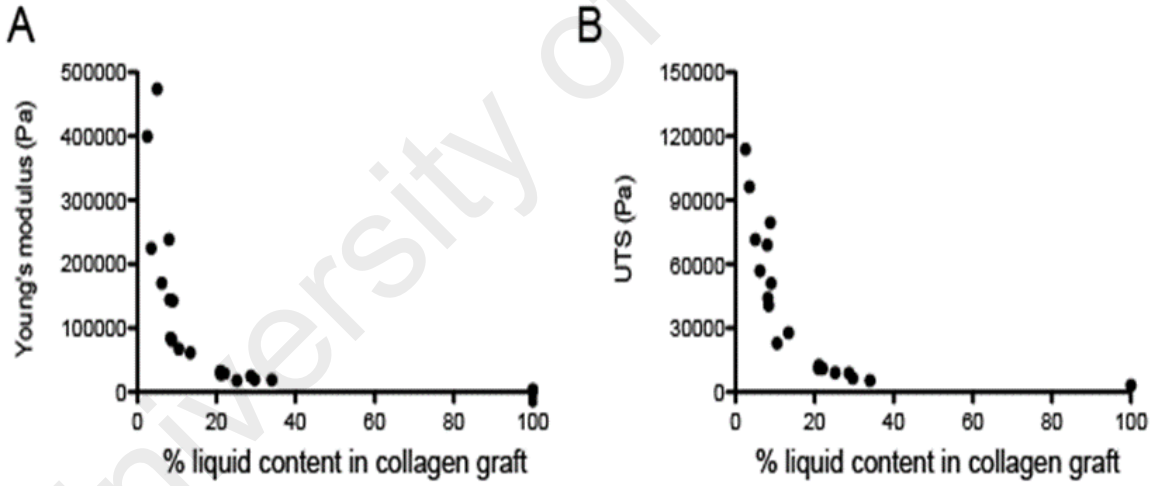

Figure 5.2: Mechanical analysis of collagen grafts with various liquid content. (A and B) Young's modulus and UTS of collagen grafts with various liquid content.

Four surgeons (KP, GV, CRT and PF) subjectively analyzed these different collagen grafts. Their assessment was in relation with the analytical data and the average score is demonstrated in Table 5.3.

Table 5.3: Subjective graft performance according to surgeons` score in relation to the collagen grafts liquid content.

Liquid content in collagen graft (%)	**Score (Passed/Failed surgeon evaluation)**
1-10	8 (Passed)
11-20	7 (Passed)
21-30	7 (Passed)
31-40	6 (Passed)
40-50	6 (Passed)
60-100	0-1(Failed)

5.4.3 Manufacturing technique to yield controlled spatial orientation of collagen grafts

Spatially controlled gradient-based collagen grafts were designed based on the results shown in Figure 5.1, to fit these different cellular regeneration needs of urothelial and smooth muscle cells as shown in the cartoon of Figure 5.3A. Applying a fast graft compression step, resulting in an approximate 50% liquid loss followed by a slow air-drying step, the liquid content of the produced grafts could be controlled (Figure 5.3B and 5.3C). This procedure yields a controlled collagen fiber distribution, with a more dense structure at the compressed surfaces while the internal part of the collagen tubular wall was left with a less dense collagen structure as shown by SEM, immunohistochemistry using collagen type I antibodies and Sirius red staining (Figure 5.3B, 5.3D, 5.3E and 5.3F). This spatial controlled gradient-based collagen graft with a liquid content of 40% after mechanical compression and air-drying, is hereafter referred to as the low-density graft (LD). A high collagen density control graft was also prepared with a liquid content of 1% and displayed a homogeneous collagen distribution by air-drying, as seen in Figure 5.3F. This 1% liquid content collagen graft is hereafter referred to as the high-density (HD) graft. Mechanical assessment of the LD graft revealed a less mechanical strength when compared to the HD graft (Figure 5.3G). However, the LD graft was still considered adequate by the surgeons based on their subjective evaluation using the score sheet assessment developed (Table 5.3).

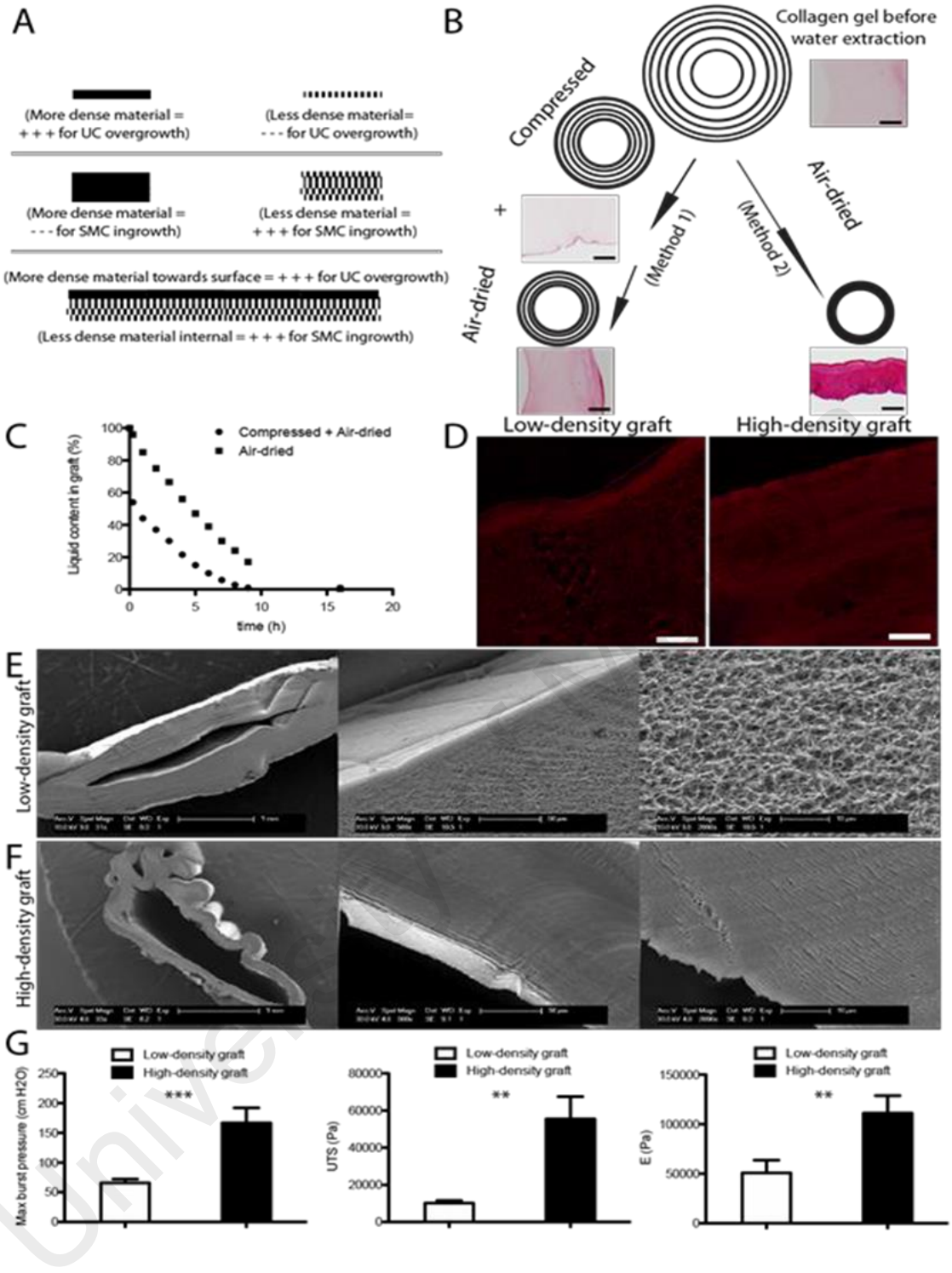

Figure 5.3: Description and characterization of manufactured collagen graft with controlled spatial orientation. (A) Our hypothesis for design principles in order to achieve adequate urothelial and smooth muscle cells growth: smooth muscle cells prefer to infiltrate and proliferate in a less dense matrix while urothelial cells prefer to grow on the surface of a denser matrix. (B) Cartoon of manufacturing process of LD and HD grafts with images of Sirius red staining's (Scale bar 200 µm).(C) Monitoring of weight of collagen graft after liquid content extraction with or without initial fast extraction. (D) Images of collagen type 1 expression by immunohistochemistry of low- and high-density grafts (Scale bar 50 µm). (E and F) SEM images of low- and high- density grafts with three different magnifications. (G) Burst pressures, UTS and Young's Modulus of LD and HD grafts. Error bars represent the standard deviation of four independent samples. $^{**}p < 0.01$, $^{***}p < 0.001$

5.4.4 Short-term *in vivo* evaluation of HD and LD collagen grafts

2 cm long HD and LD grafts were implanted into 22 rabbits for 1, 3 and 6 months. The LD graft had an overall 15.4% complication rate (2 out of 13 rabbits) compared to a 33% complication rate (3 out of 9 rabbits) when using the HD graft (Figure 5.4A). At 1 month, it was noticed that the HD graft still had not been remodeled by the surrounding tissue as shown by the presence of the implanted collagen visualized by Hemotyxlin & Eosin (H&E) and in Masson's Trichrome (MT) staining (Figure 5.4B). The LD graft could be identified in the histological samples at 1 month to a lesser extent (Figure 5.4C). Therefore, it can be concluded that the LD graft was resorbed faster by the surrounding native tissue (Figure 5.4B and 5.4C). The luminal side of both grafts had shown overgrowth of urothelial cells within the first month of implantation (Figure 5.4B and 5.4C). These urothelial cells were somehow disorganized but started to show the typical multilayered stratified urothelium. The ingrowth of smooth muscle cells was still lacking at 1 month, irrespective of the graft type when analyzed with H&E and MT (Figure 5.4B and 5.4C). By the end of 3 months, the presence of collagen graft material could not be seen in any of the histological sections irrespective of graft type (Figure 5.4B and 5.4C). The urothelial cells had covered the grafted region in the HD graft creating a neo-urethra with an organized multilayered urothelial cell distribution (Figure 5.4B). However, even at 3 months, the LD grafts demonstrated less urothelial cell coverage with disorganized stratification (Figure 5.4C). More smooth muscle cell ingrowth from the native tissue into the LD graft samples was seen at 3 months when compared to the HD graft (Figure 5.4B and 5.4C). At 6 months, the urothelium, irrespective of the graft type, showed normal stratification (Figure 5.4B and 5.4C). The LD graft exhibited more ingrowth of smooth muscle cells at 6 months in comparison to the HD graft (Figure 5.4B and 5.4C).

Immunohistochemistry using smooth muscle actin (SMA) antibodies confirmed the H&E and MT results by showing more SMA expression in the LD graft in all months compared to the HD grafts (Figure 5.4D). At 1 month, SMA was expressed in both implanted grafts in vascular structures, clearly present at 1 month, however, not in smooth muscle bundles (Figure 5.4E and 5.4F). At 6 months, there was a statistically significant ($p < 0.01$) higher expression of SMA in the LD grafts compared to the HD grafts (Figure 5.4D-5.4F). Uroplakin-2, a specific antibody for terminal urothelial differentiation, was only seen with sparse expression in the HD graft at 1 month (Figure 5.4G and 5.4H), however at 3 months, uroplakin-2 expression was seen in throughout the region of the HD graft (Figure 5.4H). In comparison, there was only sparse uroplakin-2 expression in the LD graft area (Figure 23G). At 6 months, the LD graft area showed also a complete urothelial lining with uroplakin-2 expression in the superficial cell layers (Figure 5.4G and 5.4H).

A.Low -density graft

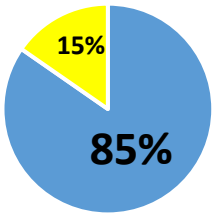

High -density graft

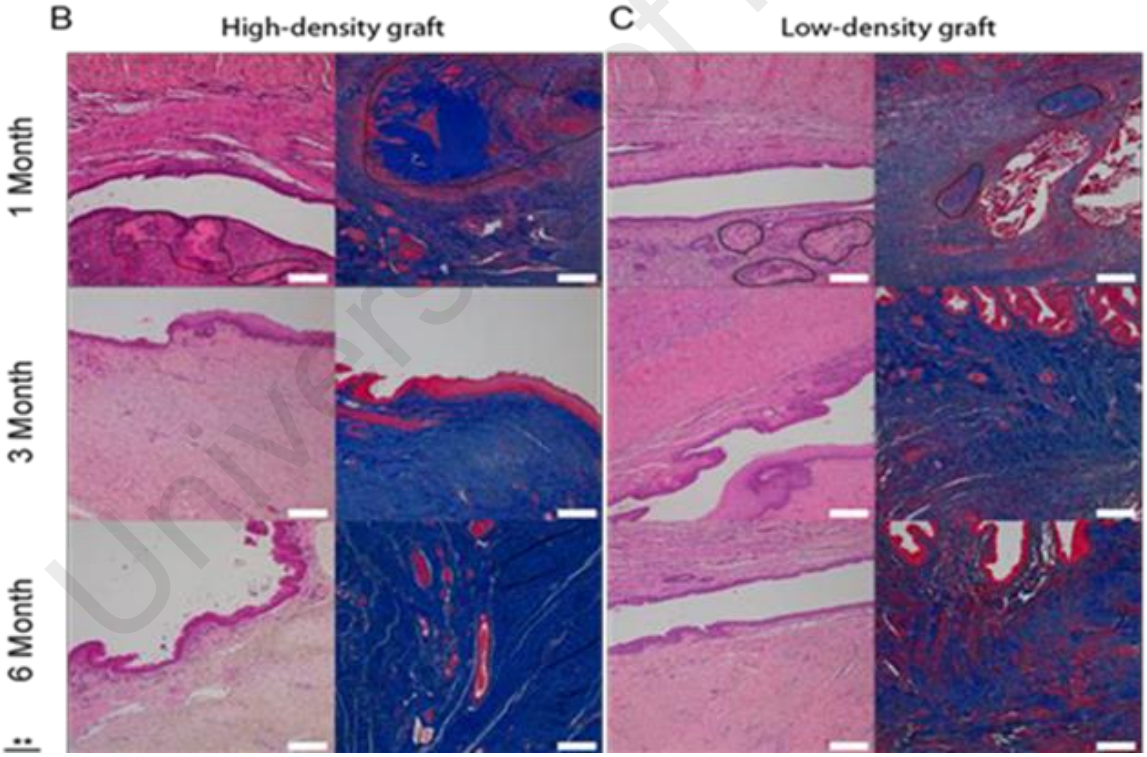

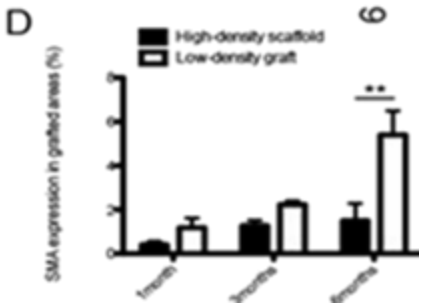

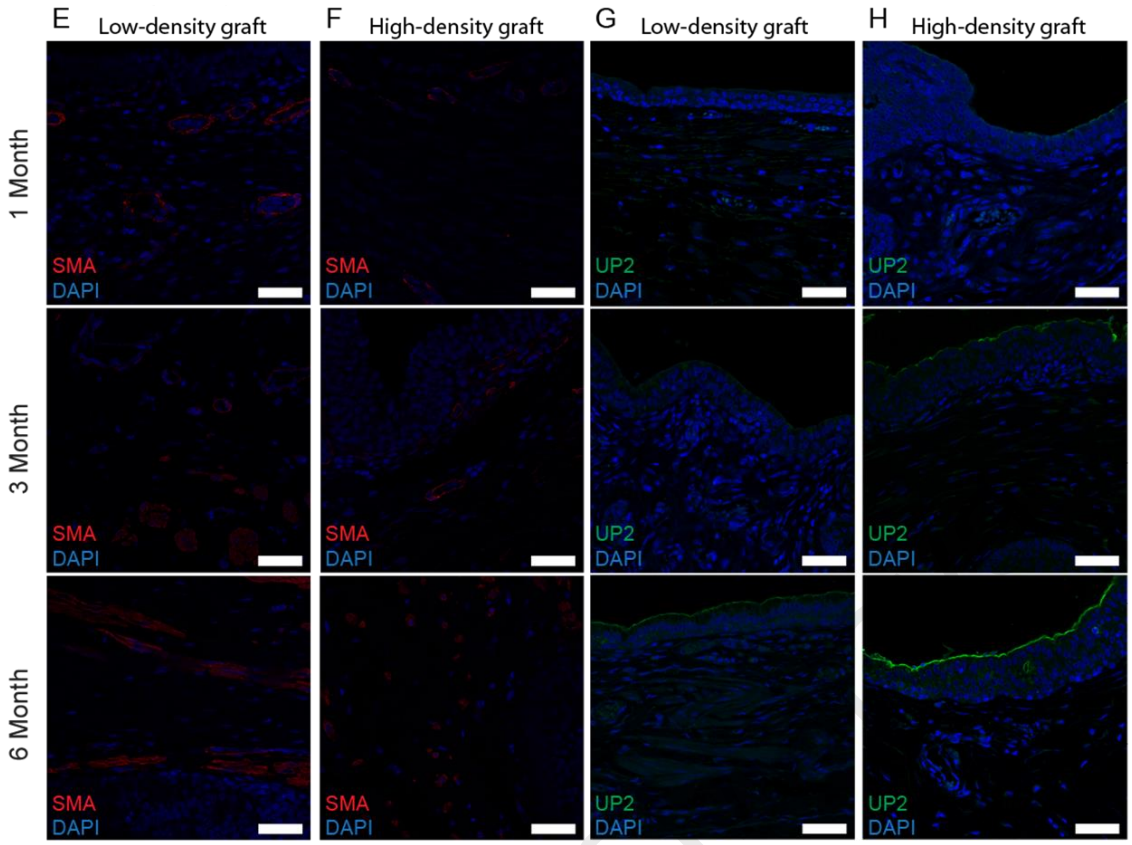

Figure 5.4: Short-term in vivo evaluation of HD and LD collagen grafts in a rabbit urethral defect model. (A) Functional surgical outcome analyzed by micturating cysto-urethrography of rabbit implanted with LD and HD grafts for 1, 3 and 6 months. (B) H&E and MT stained sections of the grafted area of LD graft 1, 3 and 6 months after implantation. (C) H&E and MT stained sections of the grafted area of HD graft 1, 3 and 6 months after implantation. (D) Quantification of SMA expression in grafted areas for rabbits implanted with LD and HD graft after 1, 3, and 6 months. (E) Immunohistochemistry for alpha-SMA of LD graft implanted for 1, 3 and 6 months.(F) Immunohistochemistry for alpha-SMA of HD graft implanted for 1, 3 and 6 months. (G) Immunohistochemistry for Uroplakin- 2 (Up2) of LD graft implanted for 1, 3 and 6 months. (H) Immunohistochemistry for Up2 of HD graft implanted for 1, 3 and 6 months. Note: areas circled in dashed black line indicating the remaining collagen pieces of the grafts after 1 month (Scale bar H&E and MT 250 µm, Scale bar SMA and Up-2 50 µm). Error bars represent the standard deviation of four independent samples. $^{**}p < 0.01$

5.4.5 Long-term *in-vivo* evaluation of LD collagen grafts

Better histological results in smooth muscle ingrowth were shown by the LD grafts compared to the HD graft in the 6 month study (Figure 5.4). This lead to further implantation of the LD graft in 7 rabbits for a long-term evaluation (5 rabbits were euthanized at 9 months and 2 rabbits at 11 months). No complications were noted both macroscopically and on micturating cysto-urethrography for all 7 rabbits (Figure 5.5A). At 9 and 11 months, the urothelial layer appeared comparable to the one of a native rabbit urethra (Figure 5.5B- C, 5.5E-F, and 5.5H-I). There was more ingrowth of smooth muscle cells than in the short-term 6 month experiments. However, the expression of SMA was still not as pronounced as seen in the native rabbit urethras (Figure 5.5D, 5.5G, 5.5J, and 5.5K). Furthermore, all animals in the long-term group were able to mate normally and had produced offspring (Figure 5.5L).

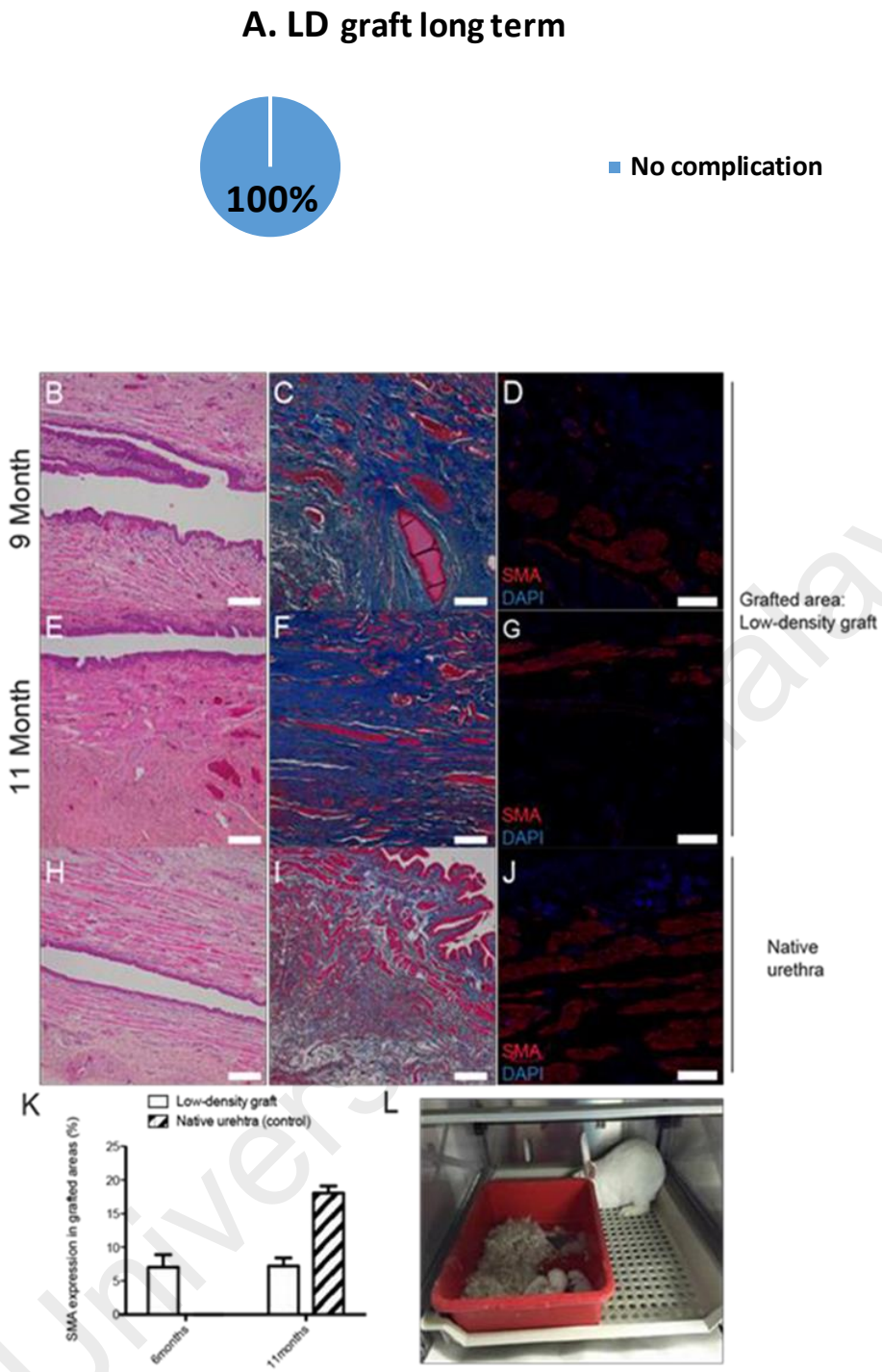

Figure 5.5: Long-term in vivo evaluation of LD collagen grafts in a rabbit urethral defect model. (A) Functional surgical outcome analyzed by micturating cysto- urethrography of rabbits with an artificially created, circumferential urethral defect that was bridged with an LD graft (N=5 rabbits for 9 months, N=2 rabbits for 11 months). (B-C, E-F, and H-I) H&E and MT stained sections of LD graft implanted for 9 and 11 months, and a control native rabbit urethra. (D, G, and J) Immunohistochemistry for SMA of LD graft implanted for 9 and 11 months, and a control native rabbit urethra. (K) Quantification of SMA expression in LD graft compared to a control native rabbit urethra. (L) A photo of rabbit offspring from fathers implanted with a low-density graft. Note: black arrow pointing at offspring (Scale bar H&E and MT 250 µm, Scale bar SMA 50 µm). Error bars represent the standard deviation of four independent samples.

5.4.6 Effects of sterilization on LD graft behavior

X-ray sterilization was applied according to ISO-norms for medical device regulation. Burst pressures, UTS and Young's modulus between non-sterilized and x-ray sterilized grafts did not show a significant difference (Figure 5.6A-C). However, the surgeons reported in the score sheet that the x-ray sterilized graft was more difficult to suture when compared to the non-sterilized one. Rabbits (N=4) implanted with the x-ray sterilized graft did not have any complications when analyzed macroscopically and on micturating cysto-urethrography (Figure 5.6D). At 1 month, the ingrowth of urothelial and smooth muscle cells seen on H&E and MT stained sections were similar to the non- sterilized LD graft (Figure 5.6E-F and 5.4C).

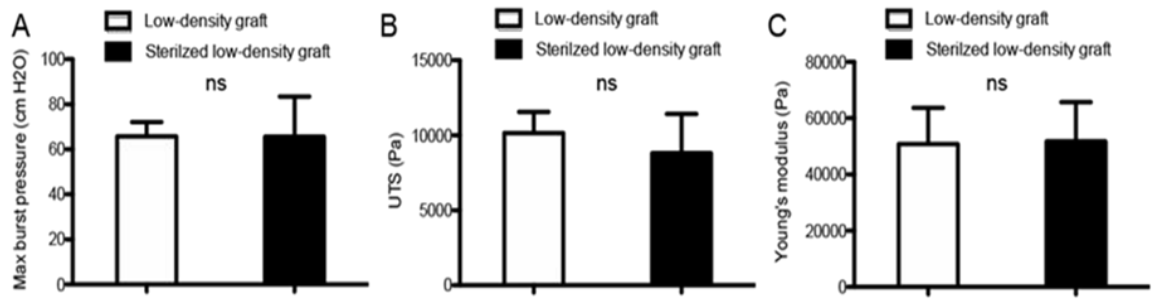

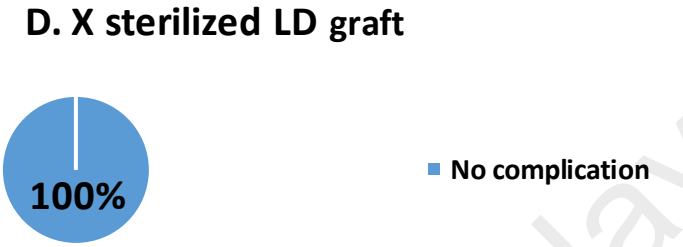

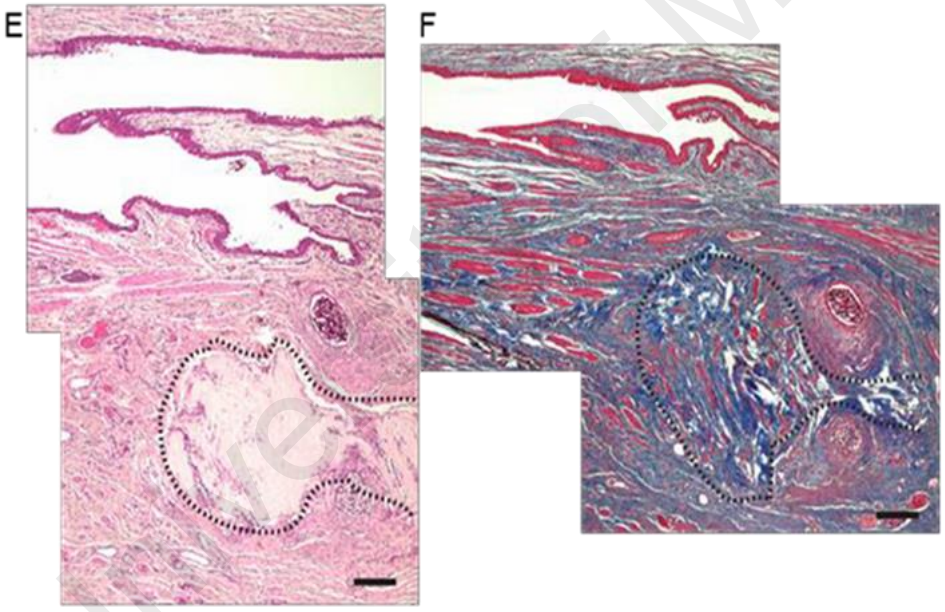

Figure 5.6: Characterization of X-ray sterilized LD collagen grafts. (A, B, and C) Burst pressure, UTS and Young's Modulus of x-ray sterilized LD grafts compared to non-sterilized LD grafts. (D) The functional outcome of the surgery was analyzed by micturating cysto-urethrography and scored as no complication or complication (N=4 rabbits). (E and F) H&E and MT stained sections of the grafted area of implanted sterilized LD graft after 1 month. Note: areas circled in dashed black line indicating the remaining collagen pieces of the graft after 1 month (Scale bar H&E and MT 250 µm). Error bars represent the standard deviation of four independent samples. ns (not significant) $p>0.05$.

5.5 Discussion

Spatially controlled gradient-based collagen grafts were developed for application in urethral reconstructive surgery. The graft design was inspired by the natural extracellular matrix architecture of native urethras and by the *in-vitro* cell fate assessment of urinary tract cells in different mechanical niches. A novel fabrication method was developed to achieve both a surgery compatible material and a cell instructive material mimicking the native urethral architecture. This graft was tested in the same animal model as previous chapters and has demonstrated its potential for clinical use with improved functional and regenerative outcome than previously described grafts in this thesis.

The mechanical analysis of the engineered grafts confirmed the subjective results of the surgical evaluation and demonstrated that the more liquid that was extracted during the fabrication procedure, the easier it was for the surgeon to handle the material. However even the produced grafts with liquid content up to 50% could still be adequately sutured by the surgeons. Although the grafts do not have the same mechanical properties as similar biomaterials for this clinical indication(Ghezzi et al., 2012), they have the advantage of enhanced regenerative potential. Interestingly, the burst pressures of the grafts revealed values well above the maximal burst pressure present within the native human urethra (Müller et al., 2008). Of clinical relevance was the surgeon's feedback that both grafts could be handled easily and allowed adequate suturing. Clearly, the HD graft scored better on the surgeons' score sheets in comparison to the LD graft.

In-vitro assessment of the collagen graft did not show any toxicity for the tested urothelial and smooth muscle cell populations. The urothelial cells demonstrated a better proliferation on a stiffer matrix. To the contrary, one could argue that the smooth muscle cells favor the less stiff and less dense material property, thereby providing a better substrate for regeneration. This is in accordance with the findings of the Discher group: they revealed that different cells respond differently to various stiffness *in-vitro* (Engler, Sen, Sweeney, & Discher, 2006).

In-vivo, the LD graft exhibited a higher ingrowth of muscle cells and formation of muscle bundles due to its softer/less dense structure, whereas the HD graft demonstrated better urothelial regeneration at 3 months thanks to its higher stiffness/density. This faster urothelial lining resulted in earlier Uroplakin-2 expression in areas grafted with the HD graft compared to the one of the LD graft. This concurs with similar histological findings seen by other researchers that stiffer grafts with uniform fiber architecture implanted in animals have good urothelial regeneration but lack muscle regeneration(J. E. Nuininga et al., 2003). The adequate smooth muscle cells infiltration from the surrounding native tissue within the LD graft is a finding that seems not to have been described yet. Early smooth muscle regeneration is no doubt an advantage, as the primary pathology in urethral stricture is fibrosis of the muscular component of the urethra leading to narrowing of the urethral lumen(El Kassaby et al., 2008). By 6 months, the LD graft had statistically significant more expression of SMA when compared to the HD grafts. The LD grafts were then further analyzed for the risk of developing any late complications post implantation, as it is routinely seen in conventional clinical practice when using autologous grafts for urethroplasty (Mundy & Andrich, 2011). Long-term urethral patency could be seen and no complications were recorded up to 11 months. Although smooth muscle regeneration was not complete and not comparable to native rabbits muscle expression even after 11 months. The operated rabbits were still able to micturate normally and successful mating resulting in progeny was observed. These observation prove complete functional urethral regeneration had taken place following graft implantation after urethral excision.

Sterilization is mandatory for all medical devices intended for clinical use. In accordance to ISO 11137-1:2015 (Sterilization of Health Care Products), the best candidate, the LD graft underwent x-ray sterilization with a radiation above 25kGy. This did not influence the maximum burst pressure, but it led to a more brittle tube having a compromising effect on the ability to suture the graft.

It has already been reported that gamma irradiation of collagen material reduces the mechanical properties of collagen due to molecular structural changes(Wiegand et al., 2009). This is the rationale why gamma sterilization was not utilized to sterilize the final collagen grafts in this study. X-ray sterilization however at a high dose did not induce any complications in graft implantation. Histological examinations of these grafts in rabbits at 1 month showed similar tissue architecture when compared to non-sterilized LD grafts for the corresponding time point

This study has several limitations. The rabbit model used had an artificially created urethral defect, with healthy urethral tissue on the edges of the defect. In urethral stricture patients, the underlying problem is ischemia of the corpus spongiosum, leading to pathological tissues. Challenging the regenerative potential of the graft on an unhealthy urethral bed would be ideal. The maximum urethral length that can be replaced in the rabbit in our experience is 2 cm. Therefore; a pilot study in the dog model will be initiated for the replacement of a clinical relevant urethral segment. The graft utilized in this study was a tubular graft and implantation was done onto a totally excised urethral tissue requiring full circumferential replacement. This varies from clinical practice where only partial circumferential replacement is occasionally performed(Mangera, Patterson, & Chapple, 2011; Mundy & Andrich, 2011). The long term study of 11 months only had 2 animals and a larger study with more number of animals should be undertaken. This is to examine for any long term complication from graft implantation.

An off-the-shelf urethral graft that does not require the incorporation of cells and growth factors represents an important advancement over the current cell-seeded option and the classical autologous tissue harvesting for urethral surgery. The urethral graft described here is easy to fabricate in any size, shape and dimension. This graft was able to successfully regenerate a 2 cm long tubular artificially created urethral defect in a rabbit study involving 2 different surgical centers. Urothelial ingrowth as early as 1 month post- implantation and continuous ingrowth of smooth muscle cells into the implanted area was seen rather than healing by fibrosis and scarring over the duration of the study. No complications were observed even 11 months after

implantation in the 2 animals. Sterilization of the graft, mandatory for a medical device is possible and does not induce negative graft behavior *in-vivo*. The LD graft fabricated here shows potential for clinical translation and should be validated in a large animal model on a significant urethral defect.

5.6 Conclusion

This study demonstrated that density modification on the engineered tubular collagen grafts can alter its efficacy when the graft is implanted for urethral regeneration applications. The LD graft exhibited better overall functional results compared to the HD grafts when implanted to regenerate a 2 cm urethral defect in the rabbit model. In histology and immunohistochemistry, the LD graft exhibited a higher ingrowth of smooth muscle cells with formation of muscle bundles. The adequate smooth muscle cells infiltration from the surrounding native tissue within the LD graft due to its softer/less dense structure is a finding that has not been described so far. Early smooth muscle regeneration is no doubt an advantage, as the primary pathology in urethral stricture is fibrosis of the muscular component of the urethra. This graft had also shown to be compatible to x ray sterilization for future clinical translation. This spatially controlled gradient-based collagen graft is cost effective and has the potential for future clinical translation.

CHAPTER 6: A PRECLINICAL PILOT STUDY IN A DOG MODEL USING LOW DENSITY (LD) TUBULAR BOVINE COLLAGEN GRAFT FOR LONG URETHRAL REGENERATION

6.1 Introduction

The journey from bench to bed undertaken for a medical device is often long and full of hurdles. Scientific and functional validations require multiple *in-vitro* and *in-vivo* testing's to prove the efficacy of an engineered medical device for its final intended clinical indication. Compliance to regulatory requirements are also mandatory prior to obtaining clinical trial approval from the relevant authorities. This is all required to ensure safety and to minimize risk of complications when the first in human study is undertaken. Grafts developed for urethral reconstructive surgery similarly undergo this path. The urethral grafts developed in this thesis have demonstrated improved functional outcome in the rabbit model with each subsequent design.

The final LD tubular collagen graft engineered in Chapter 5 demonstrated an overall 90% no complication rate when all implantations were evaluated together both short and long term studies(N=20). Appearance of complications were also not seen even after 11 months post-surgery. The LD graft also underwent X-Ray sterilization in accordance to standard ISO requirements for sterility. Thus complying with an important regulatory requirement prior to clinical trial application. Sterilization did not alter its functional outcome when compared to non-sterilized grafts when implanted in the same animal model. The length of the graft implanted and examined *in-vivo* has been 2 cm for all the different engineered versions in this thesis. This due to the fact that the maximum length that can be surgically placed in a rabbit is only 2cm in our experience. Though representing a subtotal replacement of the urethra for this animal model the average length of urethral stricture seen in clinical practice is however around 4 cm(Alwaal, Blaschko, McAninch, & Breyer, 2014). An *in-vivo* experiment utilizing such a length of graft is important as it validates the data obtained from the previous rabbit implantations and brings us a step closer to the patient. This study should ideally be conducted in an animal model which is as

similar anatomically to humans. The animal model utilized most commonly in literature for studying long urethral defects is the dog. A pilot experiment therefore was undertaken in the dog model, examining the potential to regenerate a completely excised 4 cm urethral defect utilizing the engineered LD tubular collagen graft. This pilot study is an important first step forward in convincing the clinical and scientific community on the potential of this developed cell free biomaterial for future clinical application in urethral surgery.

6.2 Literature Review

Urethral pathologies can be classified as congenital and acquired. Hypospadias represent a congenital anomaly of the urethra. It leads to a functional and cosmetic impairment. The need to correct the penile deviation and rotation, glans cleft and tilt, ectopic and stenotic urethral meatus, hooded prepuce, penoscrotal transposition and penile size can only be undertaken by surgical intervention. Classification is based on the location of the displaced urethral orifice. It is divided as distal hypospadias and proximal hypospadias, with the latter being more severe(Springer, Tekgul, & Subramaniam, 2017). Timing of surgery has been suggested to be at around 6 to 18 months of age (Kass & Kogan, 1996). This recommendation is based on surgical and anesthetic consideration and the physiological development of the child. Surgical techniques that have been developed are in the hundreds. However currently, tubularised incised plate urethroplasty (TIP) repair has become the most popular technique when one is repairing a distal hypospadias(Cook et al., 2005; Springer, Krois, & Horcher, 2011; Steven et al., 2013). Management of proximal hypospadias tend to be more complicated and to date no approach has been shown to be superior over the other(Castagnetti & El-Ghoneimi, 2010). A two stage repair using grafts or flaps is ideal in such complicated cases when there is severe chordee, a small glans and ventral scarring (Bracka, 2008; McNamara et al., 2015). Multiple different types of grafts have been used over the years such as non-hair bearing skin and bladder. Buccal mucosa is currently recognized as the current gold standard (Stein, 2012).

The first use of buccal mucosa as a substitute material in surgery can be traced back to 1873 when Stellwag Von Carion used it in ophthalmologic surgery(Barbagli, Balò, Montorsi, Sansalone, & Lazzeri, 2017). It was highlighted only recently in 2002 that a Ukrainian surgeon by the name of Kiril Sapezhko (1857-1928) is credited as the first surgeon to utilize buccal mucosa in urethral replacement (Korneyev, Ilyin, Schultheiss, & Chapple, 2012). As these pioneering work were developed outside the realm of western medicine, the first report in literature for the utilization of buccal mucosa was credited to Graham Humby from the Hospital for Sick Children in London. However this technique was not described by any other surgeons

following Humby's attempt until 51 years later (Barbagli et al., 2017). In 1992 both Bu¨rger et al and Dessanti et al described the utilization of buccal mucosa in hypospadias surgery (Bürger et al., 1992; Dessanti et al., 1992). Both these papers from pediatric urologist represent landmark articles on the utilization of buccal mucosa in urology. Following this El Kaasaby et al in 1993 reported his experience using this autologous graft for the treatment of urethral stricture(el-Kasaby et al., 1993).

Urethral stricture which is an acquired pathology caused by trauma, inflammatory or iatrogenic causes is divided into anterior urethral strictures and posterior urethral strictures. Treatment is based on the location and length of stricture (Hillary et al., 2014). For short bulbar urethral strictures that are less than 1cm, a direct visual internal urethrotomy (DVIU) is recommended as a first line treatment. However following that any recurrence should be treated with urethroplasty. For strictures longer than 2 cm and which has a high likelihood of recurrence if treated by DVIU, these patients should undergo a primary urethroplasty (Santucci & Eisenberg, 2010; Steenkamp, Heyns, & De Kock, 1997; Wright, Wessells, Nathens, & Hollingworth, 2006). Though DVIU appears to be a simple and easy procedure to treat urethral stricture however its long term efficacy and cost effectiveness is currently in debate. Multiple transurethral procedures have been reported to increase stricture complexity and are potentially counterproductive(Horiguchi et al., 2017). A recent clinical trial conducted in the UK, The OPEN Trial: Open Urethroplasty versus Endoscopic Urethrotomy: Clarifying the management of men with recurrent urethral stricture (ISRCTN98009168 DOI 10.1186/ISRCTN98009168) has just been concluded on 1/2/2017.The objective of the trial was to determine which operation is most clinically-effective and cost-effective. Hopefully the findings of this study will shed some light on this debate. The gold standard for the treatment of short bulbar urethral strictures is excision and primary anastomosis(Barbagli, De Angelis, Romano, & Lazzeri, 2007; Eltahawy EA, Virasoro R, Schlossberg SM, 2007). The ideal length that this method can be safely employed with minimal complication varies between a limit of 1cm or not longer than 2 cm as advised by different experts in the field(Guralnick ML, 2001). Longer or denser strictures of the bulbar or

penile region require an augmented urethroplasty using a flap or graft(Greenwell, Venn, & Mundy, 1999). Buccal mucosa is simple to harvest however is associated with donor site morbidity such as scarring or never injury (Barbagli et al., 2010). Tissue engineering therefor has a role to provide an alternative biomaterial taking into consideration this potential donor site complications and limited autologous tissue availability when long grafts are required for treating lengthy strictures.

An ideal biomaterial should be easy to handle, take well and not undergo rejection or contraction. An "off the shelf" cell free graft could fulfill these requirements and limit the waiting time to surgery compared to cell incorporated grafts. This is important as it has been reported that 16% of patients awaiting urethroplasty experienced a complication at a median of 43 days after a decision for surgery has been undertaken(Hoy, Chapman, Dean, & Rourke, 2017). Though the current gold standard graft for urethral surgery, the buccal mucosa was developed in pediatric urology. Most clinical trials utilizing tissue engineered grafts thus far have been tested on adult urethral stricture patients (Versteegden et al., 2017). The graft developed in this thesis will therefore be first implanted in an adult urethral stricture patient if it shows efficacy in the large animal model experiments and complies with regulatory requirements.

6.3 Materials and Methods

6.3.1 Fabrication of LD tubular bovine collagen grafts for long urethral implantation study

Tubular collagen grafts were fabricated utilizing liquid type 1 bovine collagen (5mg/ml) provided by Symatese (France). Sterile collagen solution was added to 10x MEM and neutralized with 1M NaOH. This solution was then poured into a 7 cm long tubular steel mold having an outer tube diameter of 1.2 cm. To create the final tubular lumen, a glass mandrel (Verreries de Carouge, CH) was placed inside the tubular mold. The diameter of the glass mandrel was 4 mm. Full collagen gelation was achieved in 15 minutes at RT. The tubular steel mold was opened and the weight of the gelated collagen tube was measured taking into consideration the weight of the glass mandrel. The gelated collagen tube was manually compressed by rolling it on filter paper being supported by a nylon mesh, followed by an air-drying step. This was done until a liquid content in the graft of 40% w/w is achieved. The liquid loss of the collagen graft after compression and drying steps was calculated by measuring the weight of non-dried and dried grafts with a balance (Mettler Toledo, sensitivity of 0.1 mg). The % of liquid content in grafts (w/w) was calculated by: % of liquid content graft =1- [(weight before drying of graft - weight after drying of graft) / weight before drying of graft]. The tubular collagen grafts were then separated from the glass mandrel and kept in phosphate buffered saline (PBS pH: 7.2) supplemented with 1% Penicillin/Streptomycin (Gibco, Invitrogen, CH) and 2.5 mg/mL Fungizone (Gibco) in a sterile culture tube (VWR International, USA). The latter was placed into a sterile Falcon® tube to obtain double packaging and was kept at 4ºC. Grafts were shipped to Kuala Lumpur at a constant temperature of 4ºC.

6.3.2 Surgical implantation of the graft in a pilot study in the dog

Implantations were performed in Kuala Lumpur, Malaysia, on weight-matched stray male dogs. The animal experiment was approved by the Animal Ethics Committees of the Faculty of Veterinary Medicine of University Putra Malaysia, Kuala Lumpur (ethical approval number UPM/IACUC/AUP-RO51/2016). Once the dog was under general anesthesia, the perineum and the penis was shaved and prepared with povidone iodine, before sterile draping. Urethral grafts were then implanted using the following surgical procedure: (Figure 6.1):

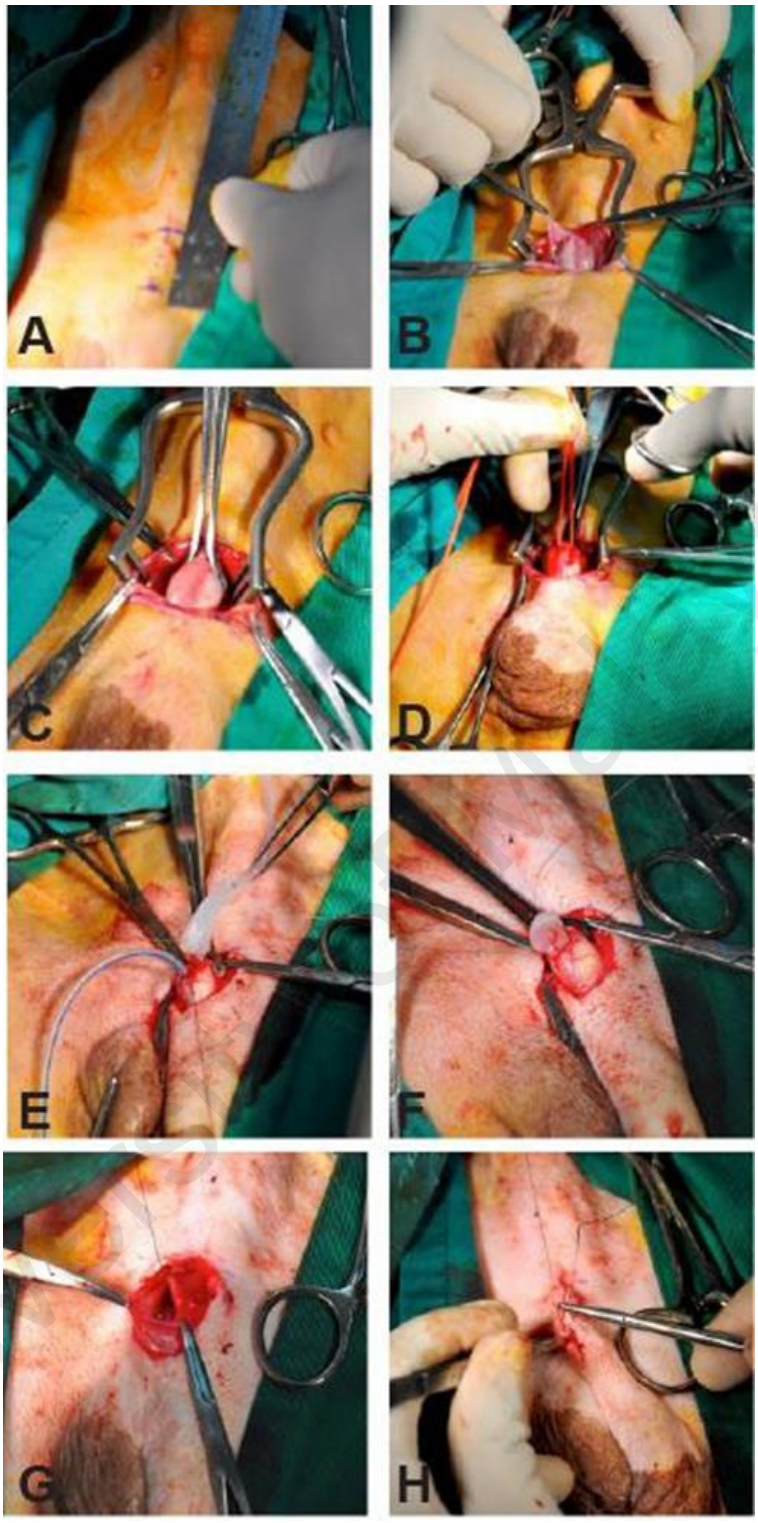

Figure 6.1: Surgical steps in clinical relevant urethral defect length in a dog model. (A) 6 cm long skin incision was done proximal to the os penis. (B) Subcutaneous tissue was dissected. (C) The urethra within the muscular corpora was identified. (D) The urethra was isolated and a 4 cm long urethral segment was resected. (E) Assisted by a catheter, the tubular graft was positioned in the urethral defect. (F) The graft was anastomosed on both ends of the native urethra. (G and H) Closure of the skin.

The glans penis is retracted out of the preputial skin and the covering of the Os penis (baculum). A Prolene® 3.0 holding suture was placed in the glans. After application of lubricating gel, an 8Fr catheter was introduced into the bladder. A skin incision of 6 cm length was performed beginning at the end of the baculum's ending proximal to the glans. Dissection through the subcutaneous planes was continued until the urethra within the corpus spongiosum and the large corpus cavernosum was identified. Fibrous attachments of the corpus cavernosum were released. A surgical loop was applied below the corpus cavernosum once it was released from its fibrous attachment. 6.0 Vicryl ® stay sutures were placed in the proximal and distal urethra and the middle third of the urethra along with the corpus spongiosum was excised from the corpus cavernosum to create a critical- size defect of approximately 4 cm. A graft of 4 cm in length was then loaded on a changed smaller Dog Foley catheter (6Fr) and double end-to-end anastomosis was performed to the native urethra with interrupted sutures (Vicryl 6.0®). In total a minimum of 4 anastomotic sutures between the graft and the native urethra were placed both proximally and distally. Finally, the glans were reduced into the preputial skin, only then the dartos layer was sutured with Vicryl 4.0® interrupted sutures to reinforce the anastomosis. The wound was washed with copious amounts of saline and diluted povidone iodine. The subcutaneous plane was now closed with interrupted Vicryl 4.0® and the skin was adapted with interrupted Vicryl 2.0®. The catheter was anchored on the glans and skin with Vicryl 4.0® sutures. On the tenth postoperative day, the catheter was to be removed under local anesthesia.

6.3.3 Ultrasound and cysto-urethrography examination

The animals were given sedation with Tiletamine HCL/Zolazepam HCI (5mg/kg; Zoletil,Virbac Carros France) and ultrasound was done using a MyLabTM Class C (linear probe, 3-13 MHz) to assess the patency of the urethral lumen at the grafted region compared to the native urethra. Knowing that the graft was sutured at 2 cm proximal to the Os penis/baculum and it measured 4 cm in length, the graft's position could be determined on the ultrasound image. It was then possible to estimate the presence of stricture at the site of the anastomoses. Stricture was defined as a 50% reduction in the diameter of the urethra in comparison to native urethra. For voiding cysto-urethrography (Omnipaque 300mg I/ml) the animal was placed under general anesthesia. All images were collected with an Animage Fidex 3-in-1 scanner. The diameter of the urethra was measured utilizing a scale provided by the imaging software.

6.3.4 Histological analysis

At the determined time of euthanasia, the animals received a lethal intra-venous pentobarbital injection (Esconarkon ad.us VET Streuli). Thereafter, the entire penis was harvested and fixed in 4% Formalin (PFA). For histological work-up, the specimen was embedded in paraffin, and 8µm thick sections were prepared

6.4 Results

6.4.1 Outcome of the pilot study in the dog analyzing the LD tubular collagen graft for long urethral implantation

A 4 cm long LD urethral graft was implanted in a pilot dog study involving 3 animals. The operation of the first dog (dog A) was successful, but was compromised by four post-operative catheter insertions within the 1st week due to dislodgement of the catheter. This caused a urinary leakage at the operative site, followed by scrotal excoriation and cystitis. The animal was started on antibiotic therapy and a decision to have a longer catheter placement was made. However following dislodgement of his catheter on post op day 14 the dog could micturate normally. Subsequently, at post op day 75 the animal was euthanized due to late appearing difficulties of micturation. Macroscopically, the penile region appeared normal and no fistula was seen. During the sample preparation for histology, a narrowing at the distal anastomotic site was revealed (Figure 6.2A). Only a small part of the implanted collagen could be seen in MT close to the distal anastomic site (Figure 6.2E). The native urothelial cells had repopulated the grafted region and exhibited a normal multilayered urothelium appearance (Figure 6.2B-G). There was no apparent ingrowth of smooth muscle cells at the distal anastomotic site and an increased deposition of collagen could be seen (Figure 6.2B and 6.2E). The expression of SMA was linked to vascular structures (Figure 6.2H). In the middle of the grafted area, a patent urethra surrounded by healthy smooth muscle cells could be found similar to native urethra (Figure 6.2C-D, 6.2F-G and 6.2I-J). The post-operative care was optimized for the subsequent operated 2 dogs (dogs B and C). The catheter was kept in place for 10 days in Dog B and recovery was uneventful. In Dog C, one reinsertion of the catheter was necessary on post op day 2, due to the blocking of the catheter, leading to a swelling in the perineal region. By post op day 10, the catheters were removed in both animals and they were able to micturate without any complications. Both dogs B and C underwent a non-invasive ultrasound examination of the grafted urethra at 6 weeks post op to evaluate the urethral patency. No urethral narrowing could be observed with ultrasound imaging (Figure 6.2K and 6.2L). A pilot invasive contrast study was attempted for Dog C at 5 months

post op, though the animal had not demonstrated any clinical signs of distress or difficulty in micturating. The contrast analysis showed patent normal urethra at the grafted site, apart from a mild clinically not relevant narrowing of the urethra at the distal anastomotic site (Figure 6.2M). Both animals from the pilot study are still being observed for potential long-term complications.

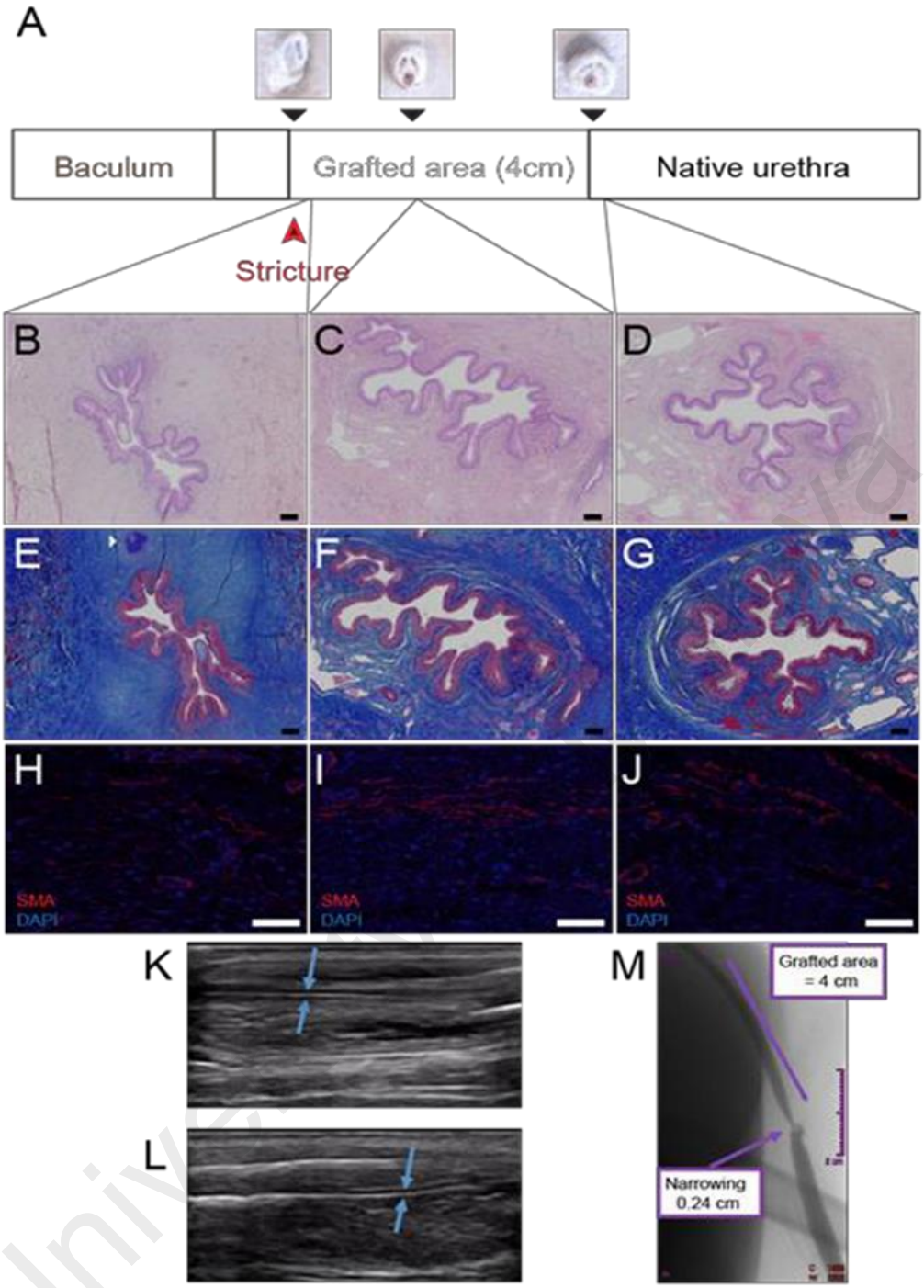

Figure 6.2: Results of a pilot study in a dog model (n=3) to characterize the behavior of a the low- density collagen graft in a clinically relevant urethral defect of 4 cm. (A) Photo showing narrowing of the urethra at the distal anastomotic site of harvest urethra of dog A, with a cartoon showing the locations of the stained sections: distal anastomic site (DAS), middle of graft (MG) and native urethra close to proximal anastomic site (PAS). (B-G) H&E and MT stained section of implanted low-density graft at three different locations (DAS, MG and PAS) in dog urethra after 75 days. (H-J) Immunohistochemistry for -SMA of implanted low-density graft day 75 post-implantation at three different locations (DAS, MG and PAS). (K and L) Ultrasound images of dog B and C 6 weeks post-implantation (Note: blue arrows indicating patent urethra). (M) Micturating cysto-urethrography of dog C (Note: purple arrow indicating narrowing at distal anastomotic site). Note: white arrow in Figure E indicating parts of collagen remaining from the graft (Scale bar H&E and MT 250 µm, Scale bar SMA 50 µm

6.5 Discussion

For clinical translation, the FDA requires the demonstration of safety and efficacy of medical device in at least 2 animal models prior to the translational into humans (M. H. Lee et al., 2010). Certain research groups have utilized the pig model for urethral *in-vivo* implantations, but the long sigmoid shaped fibro-elastic urethra of the male animal makes it impossible for transurethral catheterization as done in clinical practice(Engel et al., 2014). The most utilized large animal model for urethral studies is therefore the dog. In accordance with other reports, a bladder catheter was introduced, but only a transurethral catheter was used and not a supra-pubic bladder catheter as done by other research groups(El-Tabey et al., 2012; Orabi et al., 2013; SHOKEIR et al., 2004; Xie et al., 2014). In clinical practice, the duration of catheterization was reported to vary from 7 to 28 days post-surgery(Al-Qudah, Cavalcanti, & Santucci, 2005). In this study it was opted for 10 days.

Two of three dogs needed re-catheterization leading to minimal urinary extravasation and ultimate infection. Dog A had eventually developed a stricture at post op day 75 and was sacrificed. The urethral histology showed adequate tissue regeneration apart from fibrosis of the distal anastomotic site. It has been described that the center of a cell-free graft is the most difficult site to regenerate. This seems to be due to its distance from a healthy cell population arising from the edges of the native tissue (Dorin et al., 2008). The distal anastomotic stricture seen is most probably due to the dehiscence provoked by early reinsertion of a catheter. Similarly Dog C, who had an early catheter reinsertion, also showed a mild, clinically not relevant narrowing at the distal anastomotic site on contrast cysto-urethrography. A similar occurrence of graft anastomotic site stricture was reported in a clinical trial, where the patients underwent repair using a tissue-engineered urethra. This study suggested leaving the catheter indwelling for up to 4 weeks to maximize the success of the implantation (Raya-Rivera et al., 2011b). This would not be possible in a pre-clinical animal model without causing severe distress to the animal. The remaining 2 dogs still exhibit normal micturition patterns; 10 months post implantation of a 4 cm long cell-free tubular graft. These 2 dogs from the pilot study will be kept for long-term

evaluation for up to 1 year postoperatively. In contrast to the necessity of cellular grafts for successful urethral regeneration described in literature, this thesis could demonstrate for the first time the regenerative potential of a cell-free graft to bridge a 4cm complete urethral defect in the dog. Further implantations will be done to validate the data obtained from this pilot study to have a statistically significant number of animals.

This study had several limitations. One of the challenges in the dog model was the difficulty in maintaining an indwelling catheter for a prolonged period postoperatively, no doubt affecting the outcome of the study. Maintaining a catheter in humans is not a problem. The graft utilized in this study was a tubular graft and implantation was done onto a totally excised urethral tissue requiring full circumferential replacement. This varies from clinical practice where only partial circumferential replacement is performed at times (Mangera, Patterson, & Chapple, 2011; Mundy & Andrich, 2011).As the implantation was done on animals with healthy urethral tissue, challenging the graft in a model with an underlying ischemia of the corpus muscle of the urethra would be ideal. Ideally a sterilized graft should have been utilized for the pilot study. This however was not done as discussions were still ongoing with Synergy Health Däniken AG Switzerland to conduct microbiological lab test (Bioburden Assessment, Recovery, Bacteriostasis, Fungistasis and Product Sterility test) on the graft. These test are undertaken in specific accredited laboratories to determine the minimum dosage required to sterilize the graft to achieve the Sterility Assurance Level SAL 10-6 to comply with standard medical device guidelines.

The urethral graft described here is easy to fabricate in any size, shape and dimension. It was fabricated in Switzerland and shipped to Malaysia and implanted with no adverse effects. The successful pilot study in the dog, where a 4 cm long urethral defect was bridged, showed the graft potential to be utilized in clinical practice. These preliminary data support the potential for clinical translation of this cell-free tubular collagen graft for application in urethral reconstruction surgery.

6.6 Conclusion

A pilot study in the dog was undertaken using the LD graft to bridge a 4cm complete artificially created urethral defect. Three dogs were implanted with the LD tubular bovine collagen graft. Initial difficulty with catheter placement lead to urethral stricture formation in the first dog at post operation day 75. Histological analysis however showed regeneration of urothelial cells at the implanted area and graft remodeling taking place. Post-operative care improvement lead to better outcome in the subsequent 2 implantations. Both dogs are micturating well 10 months post-surgery. The pilot study has shown the potential of the cell free LD to graft to regenerate a 4cm complete urethral defect in a large preclinical animal model. A full study with statically significant number of animals utilizing a certified sterilized graft will have to be conducted to validate this preliminary finding prior to future clinical trial application in patients

CHAPTER 7: CONCLUSION

This research focused on the development of an alternative bioengineered material for urethral reconstruction surgery. Collagen was the foundation biomaterial of choice for the engineering of this envisioned urethral graft as it is a natural biomaterial and the most predominant protein in the human extracellular matrix. The engineered graft had to function independently without the incorporation of cells or bioactive molecules. Cell-free grafts were therefore the main interest of this thesis.

A double-layered tubular collagen graft (dCGT) was initially fabricated in Chapter 3 and implanted in an artificially created 2 cm complete urethral defect in New Zealand White Rabbits (N=20) with a 60% no complication rate. The *in-vivo* data showed a time dependent remodeling of the cell free collagen graft from the surrounding native tissue without the need for incorporation of cells or bioactive compounds.

Subsequent study on a cell modified and decellularized tubular urethral grafts demonstrated improvement in functional outcome with a 75% no complication rate in Chapter 4 in the same animal model (N=12). The development of a differentiated urothelial layer within three months and an increasing smooth muscle bundle formation over time showed the excellent regeneration capacity of this graft for urinary tract tissue engineering applications when compared with the dCGT. However its 4 week fabrication time and the decellularization steps involved to engineer the graft makes it less attractive for clinical translation.

Our study also demonstrated that density modification of the engineered tubular bovine collagen grafts can alter its efficacy. The LD graft in Chapter 5 exhibited an overall 90% no complication rate following implantation in a total of 20 New Zealand White rabbits to regenerate a 2 cm urethral defect when both the short term and long term implantation groups were analyzed together. *In-vivo,* the LD graft exhibited a better ingrowth of smooth muscle cells with formation of muscle bundles. At 6 months post implantation, there was a statistically significant ($p < 0.01$)

higher expression of SMA when compared to the HD grafts. Better urothelial regeneration at 3 months was demonstrated in rabbits implanted with the HD graft as shown by the early expression of Uroplakin-2, a specific antibody for terminal urothelial differentiation. The adequate smooth muscle cells infiltration from the surrounding native tissue within the LD graft due to its softer/less dense structure is a finding that has not been described so far. Early smooth muscle regeneration is no doubt an advantage, as the primary pathology in urethral stricture is fibrosis of the muscular component of the urethra. The LD graft had also shown to be compatible to X-Ray sterilization for future clinical translation.

The pilot study in the dog model in Chapter 6 has shown the potential of the cell free LD graft to regenerate a 4cm complete urethral defect. A full study with statistically significant number of animals will have to be conducted to validate this preliminary finding prior to future clinical trial application in patients.

In summary, this research work has enabled the development of an acellular tubular bovine collagen urethral graft which is now currently in a large pre- clinical animal study. The early involvement and feedback from clinicians from two centers, assisted in the graft engineering. The *in-vitro* and *in-vivo* data has highlighted the preferential graft architecture requirements of both urothelial and smooth muscle cells. Table 7.1 below summarizes the outcome, timing of urothelial and smooth muscle cell in growth for each graft developed in this thesis.

Table 7.1: Comparison between all the grafts developed in the thesis.

Graft Type	No of rabbits implanted	Functional Outcome (No complication)	Timing of Urothelial Cell In growth	Timing of Smooth Muscle Cell In growth
dCGT	20	60%	3 month	6 month
Decellularized	12	75%	1 month	3 month
HD	9	67%	1 month	6 month
LD	20	90%	3 month	3 month

Early ingrowth of smooth muscle cells appears to be far more relevant for an improved functional outcome. The final graft has been fabricated fulfilling a balance between the requirements of the surgeon, ease of translation, urothelial and smooth muscle cells preference. The ultimate objective of this study is to ensure an overall better outcome for the patient using this graft.

Future Outlook

The data generated from the full dog study will be utilized for submission for a future clinical trial in urethral stricture patients. The understanding on urinary tract cell preference obtained from this study has also lead to concurrent experiments in bladder regeneration utilizing the similar material. A paper comparing the different animal models utilized in this research is in preparation in collaboration with the veterinarians who assisted in the study.

REFERENCES

Abdul Manan, M. M., & Várhelyi, A. (2012). Motorcycle fatalities in Malaysia. *IATSS Research*, *36*(1), 30–39.

Abou Neel, E. A., Cheema, U., Knowles, J. C., Brown, R. A., & Nazhat, S. N. (2006). Use of multiple unconfined compression for control of collagen gel scaffold density and mechanical properties. *Soft Matter*, *2*(11), 986.

Al-Qudah, H. S., Cavalcanti, A. G., & Santucci, R. A. (2005). Early catheter removal after anterior anastomotic (3 days) and ventral buccal mucosal onlay (7 days) urethroplasty. *International Braz J Urol*, *31*(5), 459–464.

Allen, R. A., Seltz, L. M., Jiang, H., Kasick, R. T., Sellaro, T. L., Badylak, S. F., & Ogilvie, J. B. (2010). Adrenal Extracellular Matrix Scaffolds Support Adrenocortical Cell Proliferation and Function *In Vitro*. *Tissue Engineering Part A*, *16*(11), 3363–3374.

Almine, J. F., Bax, D. V., Mithieux, S. M., Nivison-Smith, L., Rnjak, J., Waterhouse, A., … Weiss, A. S. (2010). Elastin-based materials. *Chemical Society Reviews*.

Alwaal, A., Blaschko, S. D., McAninch, J. W., & Breyer, B. N. (2014). Epidemiology of urethral strictures. *Translational Andrology and Urology*, *3*(2), 209–13.

Andrich, D. E., & Mundy, a R. (2001). Substitution urethroplasty with buccal mucosal-free grafts. *The Journal of Urology*, *165*(4), 1131-1133; discussion 1133-1134.

Atala, A. (2004). Tissue engineering for the replacement of organ function in the genitourinary system. *American Journal of Transplantation*, *4 Suppl 6*, 58–73. https://doi.org/346 [pii]

Atala, A., Bauer, S. B., Soker, S., Yoo, J. J., & Retik, A. B. (2006). Tissue-engineered autologous bladders for patients needing cystoplasty. *Lancet*, *367*(9518), 1241–1246.

Atala, A., Guzman, L., & Retik, A. B. (1999). A novel inert collagen matrix for hypospadias repair. In *Journal of Urology* (Vol. 162, pp. 1148–1151).

B.L. Seala, T.C. Oterob, A. Panitch, Seal, B. L., Otero, T. C., & Panitch, A. (2001). Polymeric biomaterials for tissue and organ regeneration. *Materials Science and Engineering: R: Reports*.

Babu, R. P., O'Connor, K., & Seeram, R. (2013). Current progress on bio-based polymers and their future trends. *Progress in Biomaterials*.

Badylak, S. F., Freytes, D. O., & Gilbert, T. W. (2015). Reprint of: Extracellular matrix as a biological scaffold material: Structure and function. *Acta Biomaterialia*.

Barbagli, G., Balò, S., Montorsi, F., Sansalone, S., & Lazzeri, M. (2017). History and evolution of the use of oral mucosa for urethral reconstruction. *Asian Journal of Urology*, *4*(2), 96–

Barbagli, G., De Angelis, M., Romano, G., & Lazzeri, M. (2007). Long-Term Followup of Bulbar End-to-End Anastomosis: A Retrospective Analysis of 153 Patients in a Single Center Experience. *Journal of Urology*, *178*(6), 2470–2473.

Barbagli, G., & Lazzeri, M. (2015). Reply to Nadir I. Osman, Christopher R. Chapple, Sheila MacNeil's letter to the editor re: Guido Barbagli, Massimo Lazzeri. Clinical experience with urethral reconstruction using tissue-engineered oral mucosa: A quiet revolution. Eur Urol. in press. http: *European Urology*, *68*(5), e101–e102.

Barbagli, G., Vallasciani, S., Romano, G., Fabbri, F., Guazzoni, G., & Lazzeri, M. (2010). Morbidity of Oral Mucosa Graft Harvesting from a Single Cheek. *European Urology*, *58*(1), 33–41.

Barkan, D., Green, J. E., & Chambers, A. F. (2010). Extracellular matrix: A gatekeeper in the transition from dormancy to metastatic growth. *European Journal of Cancer*, *46*(7), 1181–1188.

Baskin, L. S. (2000). Hypospadias and urethral development. *The Journal of Urology*, *163*(3), 951–956. https://doi.org/10.1097/00005392-200003000-00076

Bhargava, S., Patterson, J. M., Inman, R. D., MacNeil, S., & Chapple, C. R. (2008). Tissue-Engineered Buccal Mucosa Urethroplasty-Clinical Outcomes. *European Urology*, *53*(6), 1263–1271.

Bickler, S. W., & Rode, H. (2002). Surgical services for children in developing countries. *Bulletin of the World Health Organization*.

Birder, L. A., & de Groat, W. C. (2007). Mechanisms of disease: involvement of the urothelium in bladder dysfunction. *Nature Clinical Practice. Urology*, *4*(1), 46–54.

Bornstein, P., & Sage, E. H. (2002). Matricellular proteins: Extracellular modulators of cell function. *Current Opinion in Cell Biology*.

Bracka, A. (2008). The role of two-stage repair in modern hypospadiology. *Indian Journal of Urology : IJU : Journal of the Urological Society of India*, *24*(2), 210–8.

Brown, B. N., Ratner, B. D., Goodman, S. B., Amar, S., & Badylak, S. F. (2012). Macrophage polarization: An opportunity for improved outcomes in biomaterials and regenerative medicine. *Biomaterials*, *33*(15), 3792–3802.

Brown, R. A., Wiseman, M., Chuo, C. B., Cheema, U., & Nazhat, S. N. (2005). Ultrarapid engineering of biomimetic materials and tissues: Fabrication of nano- and microstructures by plastic compression. *Advanced Functional Materials*, *15*(11), 1762–1770.

Bullers, S. J., Baker, S. C., Ingham, E., & Southgate, J. (2014). The Human Tissue–Biomaterial Interface: A Role for PPARγ-Dependent Glucocorticoid Receptor Activation in Regulating the CD163\n +\n M2 Macrophage Phenotype. *Tissue Engineering Part A*, *20*(17–18), 2390–2401.

Bürger, R. A., Müller, S. C., el-Damanhoury, H., Tschakaloff, A., Riedmiller, H., & Hohenfellner, R. (1992). The buccal mucosal graft for urethral reconstruction: a preliminary report. *The Journal of Urology*.

Caldamone, A. A., Edstrom, L. E., Koyle, M. A., Rabinowitz, R., & Hulbert, W. C. (1998). Buccal mucosal grafts for urethral reconstruction. *Urology*, *51*(5 SUPPL. A), 15–19.

Castagnetti, M., & El-Ghoneimi, A. (2010). Surgical management of primary severe hypospadias in children: Systematic 20-year review. *Journal of Urology*, *184*(4), 1469–1474.

Chapple, C., Barbagli, G., Jordan, G., Mundy, A. R., Rodrigues-Netto, N., Pansadoro, V., & McAninch, J. W. (2004). Consensus statement on urethral trauma. *BJU International*.

Chapple, C., Osman, N., & MacNeil, S. (2013). Developing tissue-engineered solutions for the treatment of extensive urethral strictures. *European Urology*, *63*(3), 539–541.

Charriere, G., Bejot, M., Schnitzler, L., Ville, G., & Hartmann, D. J. (1989). Reactions to a bovine collagen implant: Clinical and immunologic study in 705 patients. *Journal of the American Academy of Dermatology*, *21*(6), 1203–1208. https://doi.org/10.1016/S0190-9622(89)70330-3

Chen, F., Yoo, J. J., & Atala, A. (1999). Acellular collagen matrix as a possible "off the shelf" biomaterial for urethral repair. *Urology*, *54*(3), 407–410.

Cheng, N.-C., Estes, B. T., Awad, H. A., & Guilak, F. (2009). Chondrogenic Differentiation of Adipose-Derived Adult Stem Cells by a Porous Scaffold Derived from Native Articular Cartilage Extracellular Matrix. *Tissue Engineering Part A*, *15*(2), 231–241.

Chirdan, L. B., Ameh, E. A., Abantanga, F. A., Sidler, D., & Elhalaby, E. A. (2010). Challenges of training and delivery of pediatric surgical services in Africa. *Journal of Pediatric Surgery*.

Cook, A., Khoury, A. E., Neville, C., Bagli, D. J., Farhat, W. a, & Pippi Salle, J. L. (2005). A multicenter evaluation of technical preferences for primary hypospadias repair. *The Journal of Urology*, *174*(6), 2354–2357, discussion 2357.

Cortiella, J., Niles, J., Cantu, A., Brettler, A., Pham, A., Vargas, G., … Nichols, J. E. (2010). Influence of Acellular Natural Lung Matrix on Murine Embryonic Stem Cell Differentiation and Tissue Formation. *Tissue Engineering Part A*, *16*(8), 2565–2580.

Crookes, W. J., Ding, L. L., Huang, Q. L., Kimbell, J. R., Horwitz, J., & HcFall-Ngai, M. J. (2004). Reflectins: The Unusual Proteins of Squid Reflective Tissues. *Science*.

Daher, A., de Boer, W. I., El-Marjou, A., van der Kwast, T., Abbou, C. C., Thiery, J.-P., … Chopin, D. K. (2003). Epidermal growth factor receptor regulates normal urothelial regeneration. *Laboratory Investigation; a Journal of Technical Methods and Pathology*, *83*(9), 1333–41.

Dahl, S. L. M., Kypson, A. P., Lawson, J. H., Blum, J. L., Strader, J. T., Li, Y., … Niklason, L. E. (2011). Readily Available Tissue-Engineered Vascular Grafts. *Science Translational Medicine*, *3*(68), 68ra9-68ra9.

De Santis, E., Lang, N. P., Scala, A., Vigan??, P., Salata, L. A., & Botticelli, D. (2012). Healing outcomes at implants installed in grafted sites: An experimental study in dogs. *Clinical Oral Implants Research*, *23*(3), 340–350.

Derwin, K. a, Baker, A. R., Spragg, R. K., Leigh, D. R., & Iannotti, J. P. (2006). Commercial extracellular matrix scaffolds for rotator cuff tendon repair. Biomechanical, biochemical, and cellular properties. *The Journal of Bone and Joint Surgery. American Volume*, *88*(12), 2665–72.

Dessanti, A., Rigamonti, W., Merulla, V., Falchetti, D., & Caccia, G. (1992). Autologous buccal mucosa graft for hypospadias repair: an initial report. *The Journal of Urology*, *147*(4), 1081–1084.

Dorin, R. P., Pohl, H. G., De Filippo, R. E., Yoo, J. J., & Atala, A. (2008). Tubularized urethral replacement with unseeded matrices: What is the maximum distance for normal tissue regeneration? *World Journal of Urology*, *26*(4), 323–326.

Ehrlich, R. M., Reda, E. F., Koyle, M. A., Kogan, S. J., & Levitt, S. B. (1989). Complications of bladder mucosal graft. *J Urol*, *142*(2 Pt 2), 626–7; discussion 631.

el-Kasaby, A. W., Fath-Alla, M., Noweir, A. M., el-Halaby, M. R., Zakaria, W., & el-Beialy, M. H. (1993). The use of buccal mucosa patch graft in the management of anterior urethral strictures. *The Journal of Urology*, *149*(2), 276–278.

El-Tabey, N., Shokeir, A., Barakat, N., El-Refaie, H., El-Hamid, M. A., & Gabr, M. (2012). Cell-seeded tubular acellular matrix for replacing a long circumferential urethral defect in a canine model: Is it clinically applicable? *Arab Journal of Urology*, *10*(2), 192–198.

El Kassaby, A., AbouShwareb, T., & Atala, A. (2008). Randomized Comparative Study Between Buccal Mucosal and Acellular Bladder Matrix Grafts in Complex Anterior Urethral Strictures. *Journal of Urology*, *179*(4), 1432–1436.

Eltahawy EA, Virasoro R, Schlossberg SM, et al. (2007). Long term follow up for excision and primary anastomosis for anterior urethral strictures. *J Urol*, (177), 1803–1806.

Elvin, C. M., Carr, A. G., Huson, M. G., Maxwell, J. M., Pearson, R. D., Vuocolo, T., … Dixon, N. E. (2005). Synthesis and properties of crosslinked recombinant pro-resilin. *Nature*.

Engel, O., de Petriconi, R., Volkmer, B. G., Gust, K. M., Mani, J., Haferkamp, A., … Bartsch, G. (2014). The feasibility of ureteral tissue engineering using autologous veins: an orthotopic animal model with long term results. *Journal of Negative Results in BioMedicine*, *13*(1), 17.

Engelhardt, E. M., Micol, L. A., Houis, S., Wurm, F. M., Hilborn, J., Hubbell, J. A., & Frey, P. (2011). A collagen-poly(lactic acid-co-e{open}-caprolactone) hybrid scaffold for bladder tissue regeneration. *Biomaterials*, *32*(16), 3969–3976.

Engler, A. J., Sen, S., Sweeney, H. L., & Discher, D. E. (2006). Matrix Elasticity Directs Stem Cell Lineage Specification. *Cell*, *126*(4), 677–689.

Feng, C., Xu, Y. M., Zhu, W. D., Cui, L., & Chen, J. (2011). Biocompatibility and mechanical properties of naturally derived and synthetic scaffolds for urethral reconstruction. *Journal of Clinical Rehabilitative Tissue Engineering Research*, *15*(2), 409–412.

Fenton, A. S., Morey, A. F., Aviles, R., & Garcia, C. R. (2005). Anterior urethral strictures: Etiology and characteristics. *Urology*, *65*(6), 1055–1058.

Fiala, R., Vidlar, A., Vrtal, R., Belej, K., & Student, V. (2007). Porcine Small Intestinal Submucosa Graft for Repair of Anterior Urethral Strictures. *European Urology*, *51*(6), 1702–1708.

Fossati, N., Barbagli, G., Larcher, A., Dell'Oglio, P., Sansalone, S., Lughezzani, G., … Lazzeri, M. (2016). The surgical learning curve for one-stage anterior urethroplasty: A prospective single-surgeon study. *European Urology*, *69*(4), 686–690.

Fossum, M., Svensson, J., Kratz, G., & Nordenskjöld, A. (2007). Autologous in vitro cultured urothelium in hypospadias repair{star, open}. *Journal of Pediatric Urology*, *3*(1), 10–18.

Fu, Q., & Cao, Y. L. (2012). Tissue engineering and stem cell application of urethroplasty: From bench to bedside. *Urology*, *79*(2), 246–253.

Fu, Q., Deng, C. L., Liu, W., & Cao, Y. L. (2007). Urethral replacement using epidermal cell-seeded tubular acellular bladder collagen matrix. *BJU International*, *99*(5), 1162–1165.

Gebbink, M. F. B. G., Claessen, D., Bouma, B., Dijkhuizen, L., & Wösten, H. A. B. (2005). Amyloids - A functional coat for microorganisms. *Nature Reviews Microbiology*.

Ghezzi, C. E., Marelli, B., Muja, N., & Nazhat, S. N. (2012). Immediate production of a tubular dense collagen construct with bioinspired mechanical properties. *Acta Biomaterialia*, *8*(5), 1813–1825.

Greenwell, T. J., Venn, S. N., & Mundy, A. R. (1999). Changing practice in anterior urethroplasty. *BJU International*, *83*(6), 631–635.

Gu, G. L., Xia, S. J., Zhang, J., Liu, G. H., Yan, L., Xu, Z. H., & Zhu, Y. J. (2012). Tubularized urethral replacement using tissue-engineered peritoneum-like tissue in a rabbit model. *Urologia Internationalis*, *89*(3), 358–364.

Guralnick ML, W. G. (2001). The augmented anastomotic urethroplasty. indications and outcome in 29 patients. *J Urol*, (165), 1496–501.

Hauser, S., Bastian, P. J., Fechner, G., & Müller, S. C. (2006). Small intestine submucosa in urethral stricture repair in a consecutive series. *Urology*, *68*(2), 263–266.

Heyns, C. F., & Marais, D. C. (2002). Prospective evaluation of the American Urological Association symptom index and peak urinary flow rate for the followup of men with known urethral stricture disease. *The Journal of Urology*, *168*(5), 2051–2054.

Hillary, C. J., Osman, N. I., & Chapple, C. R. (2014). Current trends in urethral stricture management. *Asian Journal of Urology*, *1*(1), 46–54.

Horiguchi, A., Shinchi, M., Masunaga, A., Ito, K., Asano, T., & Azuma, R. (2017). Do Transurethral Treatments Increase the Complexity of Urethral Strictures? *The Journal of Urology*, (October), 1–7.

Hoy, N. Y., Chapman, D. W., Dean, N., & Rourke, K. F. (2017). Incidence and predictors of complications due to urethral stricture in patients awaiting urethroplasty. *The Journal of Urology*.

Hu, X., Cebe, P., Weiss, A. S., Omenetto, F., & Kaplan, D. L. (2012). Protein-based composite materials. *Materials Today*.

Hu, X., Shmelev, K., Sun, L., Gil, E. S., Park, S. H., Cebe, P., & Kaplan, D. L. (2011). Regulation of silk material structure by temperature-controlled water vapor annealing. *Biomacromolecules*.

Huynh, T., Abraham, G., Murray, J., Brockbank, K., Hagen, P.-O., & Sullivan, S. (1999). Remodeling of an acellular collagen graft into a physiologically responsive neovessel. *Nature Biotechnology*, *17*(11), 1083–1086.

Iqbal, H. M. N., Kyazze, G., Locke, I. C., Tron, T., & Keshavarz, T. (2015). Development of bio-composites with novel characteristics: Evaluation of phenol-induced antibacterial, biocompatible and biodegradable behaviours. *Carbohydrate Polymers*.

Iqbal, H. M. N., Kyazze, G., Tron, T., & Keshavarz, T. (2014a). A preliminary study on the development and characterisation of enzymatically grafted P(3HB)-ethyl cellulose based novel composites. *Cellulose*.

Iqbal, H. M. N., Kyazze, G., Tron, T., & Keshavarz, T. (2014b). "One-pot" synthesis and characterisation of novel P(3HB)-ethyl cellulose based graft composites through lipase catalysed esterification. *Polymer Chemistry*.

Jang, T. L., Erickson, B., Medendorp, A., & Gonzalez, C. M. (2005). Comparison of donor site intraoral morbidity after mucosal graft harvesting for urethral reconstruction. *Urology*, *66*(4), 716–720.

Jin, H. J., & Kaplan, D. L. (2003). Mechanism of silk processing in insects and spiders. *Nature*.

Jordan, G. H., Eltahawy, E. A., & Virasoro, R. (2007). The Technique of Vessel Sparing Excision and Primary Anastomosis for Proximal Bulbous Urethral Reconstruction. *Journal of Urology*, *177*(5), 1799–1802.

Källén, B. (1988). Case-control study of hypospadias, based on registry informations. *Teratology*, *38*(1), 45–50.

Kass, E., & Kogan, S. (1996). Timing of elective surgery on the genitalia of male children with particular reference to the risks, benefits, and psychological effects of surgery and anesthesia. *Pediatrics*, *97*(4), 590–4. Retrieved from

Kero, K., Rautava, J., Syrjänen, K., Grenman, S., & Syrjänen, S. (2012). Oral mucosa as a reservoir of human papillomavirus: Point prevalence, genotype distribution, and incident infections among males in a 7-year prospective study. *European Urology*, *62*(6), 1063–1070.

Khandelwal, P., Abraham, S. N., & Apodaca, G. (2009). Cell biology and physiology of the uroepithelium. *American Journal of Physiology. Renal Physiology*, *297*(6), F1477-501.

Kim, B. S., Choi, J. S., Kim, J. D., Yoon, H. I., Choi, Y. C., & Cho, Y. W. (2012). Human collagen isolated from adipose tissue. *Biotechnology Progress*, *28*(4), 973–980.

Korneyev, I., Ilyin, D., Schultheiss, D., & Chapple, C. (2012). The first oral mucosal graft urethroplasty was carried out in the 19th century: The pioneering experience of Kirill Sapezhko (1857-1928). *European Urology*.

Koyle, M. A., & Ehrlich, R. M. (1987). The bladder mucosal graft for urethral reconstruction. *The Journal of Urology*, *138*(4 Pt 2), 1093–1095.

Kramer, R. M., Crookes-Goodson, W. J., & Naik, R. R. (2007). The self-organizing properties of squid reflectin protein. *Nature Materials*.

Kropp, B. P., Ludlow, J. K., Spicer, D., Rippy, M. K., Badylak, S. F., Adams, M. C., … Thor, K. B. (1998). Rabbit urethral regeneration using small intestinal submucosa onlay grafts. *Urology*, *52*(1), 138–142.

Kuraitis, D., Giordano, C., Ruel, M., Musarò, A., & Suuronen, E. J. (2012). Exploiting extracellular matrix-stem cell interactions: A review of natural materials for therapeutic muscle regeneration. *Biomaterials*.

Lee, M. H., Arcidiacono, J. a, Bilek, A. M., Wille, J. J., Hamill, C. a, Wonnacott, K. M., … Oh, S. S. (2010). Considerations for tissue-engineered and regenerative medicine product development prior to clinical trials in the United States. *Tissue Engineering. Part B, Reviews*, *16*(1), 41–54.

Lee, Y. J., & Kim, S. W. (2013). Current management of urethral stricture. *Korean Journal of Urology*.

Li, Z., Yang, J., & Loh, X. J. (2016). Polyhydroxyalkanoates: Opening doors for a sustainable future. *NPG Asia Materials*.

Lim, M. L., Jungebluth, P., Ajalloueian, F., Friedrich, L. H., Gilevich, I., Grinnemo, K. H., … Macchiarini, P. (2013). Whole organ and tissue reconstruction in thoracic regenerative surgery. *Mayo Clinic Proceedings*, *88*(10), 1151–1166.

Loo, D. D. F., & Diamond, J. M. (1985). Crystal accumulation and very high short-circuit currents in rabbit urinary bladder. *American Journal of Physiology - Renal Fluid and Electrolyte Physiology*, *17*(1), F70–F77.

Lu, L., Peter, S. J., D. Lyman, M., Lai, H. L., Leite, S. M., Tamada, J. A., … Mikos, A. G. (2000). In vitro and in vivo degradation of porous poly(DL-lactic-co-glycolic acid) foams. *Biomaterials*.

Lumen, N., Hoebeke, P., Willemsen, P., De Troyer, B., Pieters, R., & Oosterlinck, W. (2009). Etiology of Urethral Stricture Disease in the 21st Century. *Journal of Urology*, *182*(3), 983–987.

Lumen, N., Vierstraete-Verlinde, S., Oosterlinck, W., Hoebeke, P., Palminteri, E., Goes, C., … Spinoit, A. F. (2016). Buccal Versus Lingual Mucosa Graft in Anterior Urethroplasty: A Prospective Comparison of Surgical Outcome and Donor Site Morbidity. *Journal of Urology*, *195*(1), 112–117.

Lutolf, M. P., & Hubbell, J. A. (2005). Synthetic biomaterials as instructive extracellular microenvironments for morphogenesis in tissue engineering. *Nature Biotechnology*.

Mangera, A., & Chapple, C. R. (2012). Tissue engineering in urethral reconstruction—an update. *Asian Journal of Andrology*, (October 2012), 89–92.

Mangera, A., & Chapple, C. R. (2014). Urethral stricture disease. *Surgery (United Kingdom)*, *32*(6), 304–309.

Mangera, A., Patterson, J. M., & Chapple, C. R. (2011). A systematic review of graft augmentation urethroplasty techniques for the treatment of anterior urethral strictures. *European Urology*.

Mantovani, F., Tondelli, E., Cozzi, G., Abed El Rahman, D., Spinelli, M. G., Oliva, I., … Rocco, F. (2011). [Reconstructive urethroplasty using porcine acellular matrix (SIS): evolution of the grafting technique and results of 10-year experience]. *Urologia*, *78*(2), 92–97.

Mantovani, F., Trinchieri, A., Castelnuovo, C., Romanò, A. L., & Pisani, E. (2003). Reconstructive Urethroplasty Using Porcine Acellular Matrix. *European Urology*, *44*(5), 600–602.

Markiewicz, M. R., Margarone, J. E., Barbagli, G., & Scannapieco, F. A. (2007). Oral Mucosa Harvest: An Overview of Anatomic and Biologic Considerations{A figure is presented}. *EAU-EBU Update Series*.

Mathur, R., Aggarwal, G., Satsangi, B., Khan, F., & Odiya, S. (2011). Prognosis of urethral strictures following pelvic fracture urethral distraction defects-A single centre study. *International Journal of Surgery*, *9*(1), 68–71.

McNamara, E. R., Schaeffer, A. J., Logvinenko, T., Seager, C., Rosoklija, I., Nelson, C. P., … Cendron, M. (2015). Management of proximal hypospadias with 2-stage repair: 20-year experience. *Journal of Urology*, *194*(4), 1080–1085.

Micol, L. A., Arenas da Silva, L. F., Geutjes, P. J., Oosterwijk, E., Hubbell, J. A., Feitz, W. F. J., & Frey, P. (2012a). In-vivo performance of high-density collagen gel tubes for urethral regeneration in a rabbit model. *Biomaterials*, *33*(30), 7447–7455.

Micol, L. A., Arenas da Silva, L. F., Geutjes, P. J., Oosterwijk, E., Hubbell, J. A., Feitz, W. F. J., & Frey, P. (2012b). In-vivo performance of high-density collagen gel tubes for urethral regeneration in a rabbit model. *Biomaterials*, *33*(30), 7447–7455.

Morey, A. F., McAninch, J. W., Duckett, C. P., & Rogers, R. S. (1998). American urological association symptom index in the assessment of urethroplasty outcomes. *Journal of Urology*, *159*(4), 1192–1194.

Müller, B., Ratia Garcia, J., Marti, F., & Leippold, T. (2008). Mechanical Properties of Urethral Tissue. *Journal of Biomechanics*, *41*(July), S61.

Mundy, A. R., & Andrich, D. E. (2011). Urethral strictures. *BJU International*.

Nagase, H., Visse, R., & Murphy, G. (2006). Structure and function of matrix metalloproteinases and TIMPs. *Cardiovascular Research*.

Nagata, S., Hanayama, R., & Kawane, K. (2010). Autoimmunity and the Clearance of Dead Cells. *Cell*.

Nelson, C. M., & Bissell, M. J. (2006). Of Extracellular Matrix, Scaffolds, and Signaling: Tissue Architecture Regulates Development, Homeostasis, and Cancer. *Annual Review of Cell and Developmental Biology*, *22*(1), 287–309.

Niklason, L. E. (1999). Functional Arteries Grown in Vitro. *Science*, *284*(5413), 489–493.

Nillesen, S. T. M., Geutjes, P. J., Wismans, R., Schalkwijk, J., Daamen, W. F., & van Kuppevelt, T. H. (2007). Increased angiogenesis and blood vessel maturation in acellular collagen-heparin scaffolds containing both FGF2 and VEGF. *Biomaterials*, *28*(6), 1123–1131.

Nuininga, J. E., Koens, M. J. W., Tiemessen, D. M., Oosterwijk, E., Daamen, W. F., Geutjes, P. J., … Feitz, W. F. J. (2010). Urethral Reconstruction of Critical Defects in Rabbits Using Molecularly Defined Tubular Type I Collagen Biomatrices: Key Issues in Growth Factor Addition. *Tissue Engineering Part A*, *16*(11), 3319–3328.

Nuininga, J. E., Van Moerkerk, H., Hanssen, A., Hulsbergen, C. A., Oosterwijk-Wakka, J., Oosterwijk, E., … Feitz, W. F. J. (2003). Rabbit urethra replacement with a defined biomatrix or Small Intestinal Submucosa. *European Urology*, *44*(2), 266–271.

Okamoto, M., & John, B. (2013). Synthetic biopolymer nanocomposites for tissue engineering scaffolds. *Progress in Polymer Science*.

Olsen, D., Yang, C., Bodo, M., Chang, R., Leigh, S., Baez, J., … Polarek, J. (2003). Recombinant collagen and gelatin for drug delivery. *Advanced Drug Delivery Reviews*, *55*(12), 1547–1567.

Omenetto, F. G., & Kaplan, D. L. (2010). New opportunities for an ancient material. *Science*.

Orabi, H., Aboushwareb, T., Zhang, Y., Yoo, J. J., & Atala, A. (2013). Cell-seeded tubularized scaffolds for reconstruction of long urethral defects: A preclinical study. *European Urology*, *63*(3), 531–538.

Osman, N. I., & Chapple, C. R. (2016). Re: Guido Barbagli, Massimo Lazzeri. Clinical experience with urethral reconstruction using tissue-engineered oral mucosa: A quiet revolution. Eur Urol 2015;68:917-918. *European Urology*, *69*(4), e78–e79.

Ozdil, D., & Aydin, H. M. (2014). Polymers for medical and tissue engineering applications. *Journal of Chemical Technology and Biotechnology*.

Palminteri, E., Berdondini, E., Colombo, F., & Austoni, E. (2007). Small Intestinal Submucosa (SIS) Graft Urethroplasty: Short-term Results. *European Urology*, *51*(6), 1695–1701.

Palminteri, E., Berdondini, E., Fusco, F., De Nunzio, C., & Salonia, A. (2012). Long-term results of small intestinal submucosa graft in bulbar urethral reconstruction. *Urology*, *79*(3), 695–701.

Pan, Z., & Ding, J. (2012). Poly(lactide-co-glycolide) porous scaffolds for tissue engineering and regenerative medicine. *Interface Focus*.

Parekh, A., Mantle, B., Banks, J., Swarts, J. D., Badylak, S. F., Dohar, J. E., & Hebda, P. A. (2009). Repair of the tympanic membrane with urinary bladder matrix. *Laryngoscope*, *119*(6), 1206–1213.

Parnigotto, P. P., Conconi, M. T., Gamba, P. G., & Midrio, P. (2000). Experimental defect in rabbit urethra repaired with acellular aortic matrix. *Urological Research*, *28*(1), 46–51.

Pascual, G., García-Honduvilla, N., Rodríguez, M., Turégano, F., Bujan, J., & Bellón, J. M. (2001). Effect of the thawing process on cryopreserved arteries. *Annals of Vascular Surgery*, *15*(6), 619–627.

Paulozzi, L. J., Erickson, J. D., Jackson, R. J., Angerpointer, T., Källén, B., Bertolini, E., … Culp, O. (1997). Hypospadias trends in two US surveillance systems. *Pediatrics*, *100*(5), 831–4.

Pawar, S. N., & Edgar, K. J. (2012). Alginate derivatization: A review of chemistry, properties and applications. *Biomaterials*.

Pierik, F. H., Burdorf, A., Nijman, J. M. R., de Muinck Keizer-Schrama, S. M. P. F., Juttmann, R. E., & Weber, R. F. a. (2002). A high hypospadias rate in the Netherlands. *Human Reproduction (Oxford, England)*, *17*(4), 1112–1115.

Prockop, D. J., & Kivirikko, K. I. (1995). Collagens: Molecular Biology, Diseases, and Potentials for Therapy. *Annual Review of Biochemistry*, *64*(1), 403–434.

Qin, G., Lapidot, S., Numata, K., Hu, X., Meirovitch, S., Dekel, M., … Kaplan, D. L. (2009). Expression, cross-linking, and characterization of recombinant chitin binding resilin. *Biomacromolecules*.

Ram-Liebig, G., Barbagli, G., Heidenreich, A., Fahlenkamp, D., Romano, G., Rebmann, U., … Knispel, H. (2017). Results of Use of Tissue-Engineered Autologous Oral Mucosa Graft for Urethral Reconstruction: A Multicenter, Prospective, Observational Trial. *EBioMedicine*.

Ram-Liebig, G., Bednarz, J., Stuerzebecher, B., Fahlenkamp, D., Barbagli, G., Romano, G., … Knispel, H. (2015). Regulatory challenges for autologous tissue engineered products on their way from bench to bedside in Europe. *Advanced Drug Delivery Reviews*.

Ram-Liebig, G., Engel, O., Schwaiger, B., Reiss, P., Pfalzgraf, D., Dahlem, R., & Fisch, M. (2012). 621 Tissue-engineered buccal mucosa urethroplasty. Outcome of our first 10 patients. *European Urology Supplements*, *11*(1), e621–e621a.

Raya-Rivera, A., Esquiliano, D. R., Yoo, J. J., Lopez-Bayghen, E., Soker, S., & Atala, A. (2011a). Tissue-engineered autologous urethras for patients who need reconstruction: An observational study. *The Lancet*, *377*(9772), 1175–1182.

Raya-Rivera, A., Esquiliano, D. R., Yoo, J. J., Lopez-Bayghen, E., Soker, S., & Atala, A. (2011b). Tissue-engineered autologous urethras for patients who need reconstruction: An observational study. *The Lancet*, *377*(9772), 1175–1182.

Reichl, S. (2009). Films based on human hair keratin as substrates for cell culture and tissue engineering. *Biomaterials*.

Ribeiro-Filho, L. A., & Sievert, K. D. (2015). Acellular matrix in urethral reconstruction. *Advanced Drug Delivery Reviews*.

Ross, E. A., Williams, M. J., Hamazaki, T., Terada, N., Clapp, W. L., Adin, C., … Batich, C. D. (2009). Embryonic Stem Cells Proliferate and Differentiate when Seeded into Kidney Scaffolds. *Journal of the American Society of Nephrology*, *20*(11), 2338–2347.

Rouse, J. G., & Van Dyke, M. E. (2010). A review of keratin-based biomaterials for biomedical applications. *Materials*.

Sandovici, M., Deelman, L. E., Benigni, A., & Henning, R. H. (2010). Towards graft-specific immune suppression: Gene therapy of the transplanted kidney. *Advanced Drug Delivery Reviews*, *62*(14), 1358–1368.

Santucci, R., & Eisenberg, L. (2010). Urethrotomy Has a Much Lower Success Rate Than Previously Reported. *Journal of Urology*, *183*(5), 1859–1862.

Schultz, J. R., Klykylo, W. M., & Wacksman, J. (1983). Timing of elective hypospadias repair in children. *Pediatrics*, *71*(3), 342–351.

Sellaro, T. L., Ranade, A., Faulk, D. M., McCabe, G. P., Dorko, K., Badylak, S. F., & Strom, S. C. (2010). Maintenance of human hepatocyte function in vitro by liver-derived extracellular matrix gels. *Tissue Engineering. Part A*, *16*(3), 1075–82.

Shanmugasundaram, N., Ravichandran, P., Neelakanta Reddy, P., Ramamurty, N., Pal, S., & Panduranga Rao, K. (2001). Collagen-chitosan polymeric scaffolds for the in vitro culture of human epidermoid carcinoma cells. *Biomaterials*.

Shokeir, A., Osman, Y., El-Sherbiny, M., Gabr, M., Mohsen, T., & El-Baz, M. (2003). Comparison of Partial Urethral Replacement with Acellular Matrix versus Spontaneous Urethral Regeneration in a Canine Model. *European Urology*, *44*(5), 603–609.

SHOKEIR, A., OSMAN, Y., GABR, M., MOHSEN, T., DAWABA, M., & EL-BAZ, M. (2004). Acellular Matrix Tube for Canine Urethral Replacement:: is It Fact or Fiction? *The Journal of Urology*, *171*(1), 453–456.

Shorter, J., & Lindquist, S. (2004). Hsp104 catalyzes formation and elimination of self-replicating Sup35 prion conformers. *Science*.

Sievert, K. D. (2017). Tissue Engineering of the Urethra: Solid Basic Research and Farsighted Planning are Required for Clinical Application. *European Urology*.

Sievert, K. D., & Tanagho, E. a. (2000). Organ-specific acellular matrix for reconstruction of the urinary tract. *World Journal of Urology*, *18*(1), 19–25.

Snodgrass, W., MacEdo, A., Hoebeke, P., & Mouriquand, P. D. E. (2011). Hypospadias dilemmas: A round table. *Journal of Pediatric Urology*, *7*(2), 145–157.

Snodgrass, W. T., & Lorenzo, A. (2002). Tubularized incised-plate urethroplasty for hypospadias reoperation. *BJU International*, *89*(1), 98–100.

Soave, A., Dahlem, R., Pinnschmidt, H. O., Rink, M., Langetepe, J., Engel, O., … Fisch, M. (2017). Substitution Urethroplasty with Closure Versus Nonclosure of the Buccal Mucosa Graft Harvest Site: A Randomized Controlled Trial with a Detailed Analysis of Oral Pain and Morbidity. *European Urology*.

Springer, A., Krois, W., & Horcher, E. (2011). Trends in hypospadias surgery: Results of a worldwide survey. *European Urology*, *60*(6), 1184–1189.

Springer, A., Tekgul, S., & Subramaniam, R. (2017). An Update of Current Practice in Hypospadias Surgery. *European Urology, Supplements*, *16*(1), 8–15.

Steenkamp, J. W., Heyns, C. F., & De Kock, M. L. S. (1997). Internal urethrotomy versus dilation as treatment for male urethral strictures: A prospective, randomized comparison. *Journal of Urology*, *157*(1), 98–101.

Stein, R. (2012). Hypospadias. *European Urology, Supplements*, *11*(2), 33–45.

Steven, L., Cherian, A., Yankovic, F., Mathur, A., Kulkarni, M., & Cuckow, P. (2013). Current practice in paediatric hypospadias surgery; A specialist survey. *Journal of Pediatric Urology*, *9*(6 PART B), 1126–1130.

Taylor, K. R. (2006). Glycosaminoglycans and their proteoglycans: host-associated molecular patterns for initiation and modulation of inflammation. *The FASEB Journal*, *20*(1), 9–22.

Teixeira, J., Maheswaran, S., & Donahoe, P. K. (2001). Müllerian inhibiting substance: An instructive developmental hormone with diagnostic and possible therapeutic applications. *Endocrine Reviews*.

Thambi Dorai, C. R., Boucaut, H. A., & Dewan, P. A. (1993). Urethral injuries in girls with pelvic trauma. *Eur Urol*, *24*(3), 371–374.

Vacanti, N. M., Cheng, H., Hill, P. S., Guerreiro, J. D. T., Dang, T. T., Ma, M., … Anderson, D. G. (2012). Localized delivery of dexamethasone from electrospun fibers reduces the foreign body response. *Biomacromolecules*.

Valentin, J. E., Turner, N. J., Gilbert, T. W., & Badylak, S. F. (2010). Functional skeletal muscle formation with a biologic scaffold. *Biomaterials*, *31*(29), 7475–7484.

van der Rest, M., & Garrone, R. (1991). Collagen family of proteins. *FASEB Journal : Official Publication of the Federation of American Societies for Experimental Biology*, *5*(13), 2814–23.

Vardar, E., Larsson, H. M., Engelhardt, E. M., Pinnagoda, K., Briquez, P. S., Hubbell, J. A., & Frey, P. (2016). IGF-1-containing multi-layered collagen-fibrin hybrid scaffolds for bladder tissue engineering. *Acta Biomaterialia*, *41*, 75–85.

Venkatesan, J., Bhatnagar, I., Manivasagan, P., Kang, K., & Kim, S. (2014). Alginate composites for bone tissue engineering: A review. *International Journal of Biological Macromolecules*.

Versteegden, L. R. M., de Jonge, P. K. J. D., IntHout, J., van Kuppevelt, T. H., Oosterwijk, E., Feitz, W. F. J., … Daamen, W. F. (2017). Tissue Engineering of the Urethra: A Systematic Review and Meta-analysis of Preclinical and Clinical Studies. *European Urology*, 1–13

Vorotnikova, E., McIntosh, D., Dewilde, A., Zhang, J., Reing, J. E., Zhang, L., … Braunhut, S. J. (2010). Extracellular matrix-derived products modulate endothelial and progenitor cell migration and proliferation in vitro and stimulate regenerative healing in vivo. *Matrix Biology*, *29*(8), 690–700. 7

Werner, S., & Grose, R. (2003). Regulation of wound healing by growth factors and cytokines. *Physiological Reviews*, *83*(3), 835–870.

Wiegand, C., Abel, M., Ruth, P., Wilhelms, T., Schulze, D., Norgauer, J., & Hipler, U. C. (2009). Effect of the sterilization method on the performance of collagen type I on chronic wound parameters in vitro. *Journal of Biomedical Materials Research - Part B Applied Biomaterials*, *90 B*(2), 710–719.

Wright, J. L., Wessells, H., Nathens, A. B., & Hollingworth, W. (2006). What is the most cost-effective treatment for 1 to 2-cm bulbar urethral strictures: Societal approach using decision analysis. *Urology*, *67*(5), 889–893.

Wu, X.-R., Kong, X.-P., Pellicer, A., Kreibich, G., & Sun, T.-T. (2009). Uroplakins in urothelial biology, function, and disease. *Kidney International*, *75*(11), 1153–1165.

Xie, M., Xu, Y., Song, L., Wang, J., Lv, X., & Zhang, Y. (2014). Tissue-engineered buccal mucosa using silk fibroin matrices for urethral reconstruction in a canine model. *Journal of Surgical Research*, *188*(1), 1–7.

Yang, Y., Ritchie, A. C., & Everitt, N. M. (2017). Comparison of glutaraldehyde and procyanidin cross-linked scaffolds for soft tissue engineering. *Materials Science and Engineering C*, *80*, 263–273.

Zheng, M. H., Chen, J., Kirilak, Y., Willers, C., Xu, J., & Wood, D. (2005). Porcine small intestine submucosa (SIS) is not an acellular collagenous matrix and contains porcine DNA: Possible implications in human implantation. *Journal of Biomedical Materials Research - Part B Applied Biomaterials*, *73*(1), 61–67.

LIST OF PUBLICATIONS AND PAPERS PRESENTED

PUBLICATIONS AND PATENTS

K Pinnagoda, HM Larsson, **G.Vythilingam**, E.Vardar, EM Engelhardt, R.C Thambidorai, JA Hubbell, P Frey. Engineered acellular collagen scaffold for endogenous cell guidance, a novel approach in urethral regeneration. 2016. Acta Biomaterialia Oct 1; 43:208-17.

G. Vythilingam, H.M. Larsson, K. Pinnagoda, E. Vardar, E.-M. Balet, R. Thambidorai, T. Kamarul, J. Hubbell, P. Frey Off the shelf tissue-engineered material for urethral reconstruction European Urology Supplements March 2017 Volume 16, Issue 3, Pages e1787-e1788

G. Vythilingam, H.M. Larsson, K. Pinnagoda, E. Vardar, E.-M. Balet,S.Sothilingam, R. Thambidorai, T. Kamarul, J. Hubbell, P. Frey Tissue-engineered graft for urethral reconstruction BJUI Supplements Volume 120, Supplement 4, November 2017

H. M. Larsson, **G.Vythilingam**, K. Pinnagoda, E.Vardar, E. M. Engelhardt, S. Sothilingam, R. C.Thambidorai, T. Kamarul, J.A. Hubbell P. Frey. Fiber density of collagen grafts impacts rabbit urethral regeneration.2018 SCIENTIFIC RePortS 8:10057

"POLYMERIC SCAFFOLDS AND METHODS FOR PRODUCING THERE OF" International Patent Application n° PCT/IB2016/052096 filed April 2016.

PAPERS PRESENTED

1. Oral presentation, Off-the shelf scaffolds: the future of urethroplasty ,European Chapter Meeting of the Tissue Engineering and Regenerative Medicine International Society 2016 28 June - 1 July, 2016 Uppsala, Sweden

2. Standard presentation with poster and oral, European Association of Urology Congress 2017, 24-28 March 2017 London United Kingdom. **(Best Poster Award)**- Off the shelf tissue-engineered material for urethral reconstruction

3. Oral presentation, 26th Malaysian Urological Conference ,24th -26th November 2017 **(Best Oral Presentation)**-Tissue engineered graft for urethral reconstruction